CANADIAN THESES ON MICROFICHE

I.S.B.N.

THESES CANADIENNES SUR MICROFICHE

National Library of Canada
Collections Development Branch

Canadian Theses on
Microfiche Service

Ottawa, Canada
K1A 0N4

Bibliothèque nationale du Canada
Direction du développement des collections

Service des thèses canadiennes
sur microfiche

NOTICE

The quality of this microfiche is heavily dependent upon the quality of the original thesis submitted for microfilming. Every effort has been made to ensure the highest quality of reproduction possible.

If pages are missing, contact the university which granted the degree.

Some pages may have indistinct print especially if the original pages were typed with a poor typewriter ribbon or if the university sent us a poor photocopy.

Previously copyrighted materials (journal articles, published tests, etc.) are not filmed.

Reproduction in full or in part of this film is governed by the Canadian Copyright Act, R.S.C. 1970, c. C-30. Please read the authorization forms which accompany this thesis.

THIS DISSERTATION
HAS BEEN MICROFILMED
EXACTLY AS RECEIVED

AVIS

La qualité de cette microfiche dépend grandement de la qualité de la thèse soumise au microfilmage. Nous avons tout fait pour assurer une qualité supérieure de reproduction.

S'il manque des pages, veuillez communiquer avec l'université qui a conféré le grade.

La qualité d'impression de certaines pages peut laisser à désirer, surtout si les pages originales ont été dactylographiées à l'aide d'un ruban usé ou si l'université nous a fait parvenir une photocopie de mauvaise qualité.

Les documents qui font déjà l'objet d'un droit d'auteur (articles de revue, examens publiés, etc.) ne sont pas microfilmés.

La reproduction, même partielle, de ce microfilm est soumise à la Loi canadienne sur le droit d'auteur, SRC 1970, c. C-30. Veuillez prendre connaissance des formules d'autorisation qui accompagnent cette thèse.

LA THÈSE A ÉTÉ
MICROFILMÉE TELLE QUE
NOUS L'AVONS REÇUE

NL-339 (r. 82/08)

Canada

0-315-08994-X

National Library of Canada
Canadian Theses Division
Ottawa, Canada
K1A 0N4

Bibliothèque nationale du Canada
Division des thèses canadiennes

56811

PERMISSION TO MICROFILM — AUTORISATION DE MICROFILMER

• Please print or type — Écrire en lettres moulées ou dactylographier

Full Name of Author — Nom complet de l'auteur

Hans Josef Gros

Date of Birth — Date de naissance

02. 12. 1954

Country of Birth — Lieu de naissance

West Germany

Permanent Address — Résidence fixe

Holzstrasse 24
6228 Eltville /Rhein
West Germany

Title of Thesis — Titre de la thèse

Computerized Analysis of the Pole Vault Utilizing Biomechanics Cinematography and Direct Force Measurements.

University — Université

University of Alberta

Degree for which thesis was presented — Grade pour lequel cette thèse fut présentée

PhD

Year this degree conferred — Année d'obtention de ce grade

1981.

Name of Supervisor — Nom du directeur de thèse

Dr. Juris Terauds

Permission is hereby granted to the NATIONAL LIBRARY OF CANADA to microfilm this thesis and to lend or sell copies of the film.

The author reserves other publication rights, and neither the thesis nor extensive extracts from it may be printed or otherwise reproduced without the author's written permission.

L'autorisation est, par la présente, accordée à la BIBLIOTHÈQUE NATIONALE DU CANADA de microfilmer cette thèse et de prêter ou de vendre des exemplaires du film.

L'auteur se réserve les autres droits de publication; ni la thèse ni de longs extraits de celle-ci ne doivent être imprimés ou autrement reproduits sans l'autorisation écrite de l'auteur.

Date

March 22, 1981

Signature

H. J. Gros

NL-91 (4/77)

THE UNIVERSITY OF ALBERTA

COMPUTERIZED ANALYSIS OF THE POLE VAULT UTILIZING BIOMECHANICS CINEMATOGRAPHY AND DIRECT FORCE MEASUREMENTS

by

© HANS JOSEF GROS

A THESIS

SUBMITTED TO THE FACULTY OF GRADUATE STUDIES AND RESEARCH

IN PARTIAL FULFILMENT OF THE REQUIREMENT FOR THE DEGREE

OF DOCTOR OF PHILOSOPHY

DEPARTMENT OF PHYSICAL EDUCATION

EDMONTON, ALBERTA

SPRING, 1982

THE UNIVERSITY OF ALBERTA

RELEASE FORM

NAME OF AUTHOR . . .Hans Josef Gros. . . . . .

TITLE OF THESIS. . .Computerized Analysis.of the Pole.Vault. . . . . .

. . .Utilizing.Biomechanics Cinematography. . . . . .

. . .and.Direct Force Measurements. . . . . .

DEGREE FOR WHICH THESIS WAS PRESENTED. . . Ph.D. . . . . .

YEAR THIS DEGREE GRANTED . . . .1982 . . . . . .

Permission is hereby granted to THE UNIVERSITY OF ALBERTA LIBRARY to reproduce single copies of this thesis and to lend or sell such copies for private, scholarly or scientific research purposes only.

The author reserves other publication rights, and neither the thesis nor extensive extracts from it may be printed or otherwise reproduced without the author's written permission.

. . . H. J. Gros . . . . . .

PERMANENT ADDRESS:

Holzstrasse 24

6228 Eltville

West Germany

DATED . . . . . March 1982

THE UNIVERSITY OF ALBERTA

FACULTY OF GRADUATE STUDIES AND RESEARCH

The undersigned certify that they have read, and recommend to the Faculty of Graduate Studies and Research, for acceptance, a thesis entitled "Computerized Analysis of the Pole Vault Utilizing Biomechanics Cinematography and Direct Force Measurements" submitted by Hans Josef Gros in partial fulfilment of the requirements for the degree of Doctor of Philosophy in Physical Education.

Supervisor

External Examiner

Date April 5, 1982

To my parents

ABSTRACT

The purpose of this study was to investigate the relationship between kinematic and kinetic parameters of the pole vault event determined from biomechanics cinematography procedures and direct measurements of horizontal and vertical force components in the vaulting box. Cinematographic records of a side view of the performance and simultaneous analog force data were obtained from two phase-locked Photosonics 1PL cameras. The data films were analyzed to yield kinematic data, the translational, rotational and gravitational potential energy,,angular and linear momentum, and horizontal as well as vertical forces throughout the vault. The force-time data was numerically integrated. The impulses were compared to the changes in momentum obtained through biomechanics cinematography procedures. The results indicate good agreement between the data computed from the cinematographic record of the vaulting performance and the concomitant forces and impulses measured in the vaulting box.

ACKNOWLEDGEMENTS

The author wishes to express his sincere gratitude to Dr. Juris Terauds for truly invaluable support and assistance throughout the course of this study. The "Thank You" is extended to Dr. E.W. Bedingfield, the committee members Dr. D.G. Bellow, Dr. S. Mendryk, Prof. G. Simonyi, Dr. Mohan Singh and the external examiner, Dr. M. Adrian.

The support of Photo Sonics Inc. and Instrumentation Marketing Corporation during the data collection phase is gratefully acknowledged.

TABLE OF CONTENTS

CHAPTER		PAGE
I	STATEMENT OF THE PROBLEM.	1
	Introduction.	1
	Purpose	1
	Limitations	2
	Delimitations	3
	Definition of Terms	3
II	REVIEW OF LITERATURE.	6
III	METHOD AND PROCEDURES	10
	Data Collection	11
	Cinematographic Procedures.	11
	Force Measurements.	13
	Analytical Procedures	16
	Subject Film Analysis	16
	Force Data Analysis	25
	Comparison of Cinematographic Data to Direct Force Measurements.	26
	Measurement Error	27
IV	RESULTS AND DISCUSSION.	32
	Phase Structure of the Pole Vault	32
	Kinematic Parameters.	34
	Energy.	36
	Force Measurements.	39
	Angular Momentum.	43
	Comparison of Cinematographic Data to Criterion Direct Force Measurements	46
	Measurement Error	52
	Discussion.	56
V	SUMMARY AND RECOMMENDATIONS	63
BIBLIOGRAPHY.		65

CHAPTER PAGE

APPENDICES 70

Appendix A. Kinematic Data. 71
Appendix B. Translational/Rotational Kinetic and Gravitational Potential Energy. 90
Appendix C. Momentum. 103
Appendix D. Force and Impulse 118

LIST OF TABLES

TABLE	DESCRIPTION	PAGE
1	MIT Humanscale: Relative Masses of the Body Segments	20
2	Moments of Inertia About the Transverse Axis through the Segmental CM	21
3	Comparison of Horizontal Impulse as Computed from Criterion Force Measurements and Biomechanics Cinematography.	47
4	Comparison of Vertical Impulse Measured with Biomechanics Cinematography and Force Transducer	53
5	Comparison of Repeated Measurements and Resulting X,Y Coordinates of the CM (m).	57
6	Comparison of Integrated Horizontal and Vertical Velocities of the CM and Raw Data X,Y Displacements of the CM over the Entire Performance.	58
7	Comparison of Integrated Horizontal Velocities and Raw Displacement Data of the CM over 2 Frame Intervals.	59

LIST OF FIGURES

FIGURE		PAGE
1	Schematic Diagram of Experimental Setup	12
2	Standard Measurement Chain for Dynamic Forces	14
3	Schematic Diagram of Measurement Chain Designed to Measure Horizontal and Vertical Forces in the Vaulting Box.	15
4	Assembly Drawing of the Force Summing Device.	17
5	MIT Humanscale Data for Relative Positions of the Segmental Centers of Mass	19
6	Stickfigure Plot of Selected Phases of the Pole Vault.	33
7	Linear Velocity of the Vaulter's Center of Mass and Its Horizontal (Vx) and Vertical (Vy) Components.	35
8	Kinetic Energy (T(K)), Gravitational Potential Energy (T(g)) and Total Energy (T).	38
9	Horizontal Force Measured in the Vaulting Box	40
10	Vertical Force Measured in the Vaulting Box	41
11	Resultant Force Measured in the Vaulting Box.	42
12	Angular Momentum (HCM) About the Center of Mass . . .	44
13	Moment of Inertia (ICM) and Angular Velocity (ωCM) About the Center of Mass.	45
14	Comparison of the Change in Horizontal Momentum Obtained from Biomechanics Cinematography and Horizontal Impulse Measured in the Vaulting Box . . .	49
15	Influence of the Rotational Component on the Predicted Change in Momentum.	50
16	Absolute Difference of Changes in Momentum Obtained from Biomechanics Cinematography and Horizontal Impulse Measured in the Vaulting Box . . .	51

FIGURE		PAGE
17	Relative Difference of Changes in Momentum Obtained from Biomechanics Cinematography and Horizontal Impulse Measured in the Vaulting Box. . . .	51
18	Comparison of the Change in Vertical Momentum Obtained from Biomechanics Cinematography and Vertical Impulse Measured in the Vaulting Box (Iv) . .	54
19	Absolute and Relative Difference between Force Plate Measured Vertical Impulse and Change in Vertical Momentum Obtained from Biomechanics Cinematography	54
A1	Horizontal (Vx), Vertical (Vy) and Linear (VCM) Velocities of the CM (Raw Data).	76
A2	Velocities of CM Obtained from First Differences Smoothing.	82
D1	Horizontal Impulse	122
D2	Vertical Impulse	126
D3	Vertical Force Adjusted to 0=Body Weight	128

CHAPTER I

STATEMENT OF THE PROBLEM

Introduction

Experimental biomechanics research of the pole vault event, has, in the past, relied primarily on biomechanics cinematography analysis. Although potential problems associated with this method were recognized, reliability of the derived data was largely assumed. To date only one study reported direct force and impulse measurements from the vaulting box (Barlow, 1973). However, only designated phases of the vault were involved. No comparison of results obtained from biomechanics cinematography with simultaneous direct force measurements throughout the vault have been made. The present study was undertaken to compare data derived from biomechanics cinematography to criterion data obtained from piezoelectric force transducers.

Purpose

The purpose of the present study was to compare data derived from a two dimensional cinematographical analysis of the pole vault event to direct measurements of the horizontal and vertical force components acting on the tip of the pole throughout the vault. Furthermore, selected variables contributing to the overall

performance were computed and interpreted.

Limitations

The results of the study were presented and interpreted in light of the following limitations:

(1) The limitations inherent to cinematographic data collection and analysis, more specifically the possibility of perspective errors, film graininess and distortions through the optical elements of the recording and/or projection devices. The location of proximal and distal end points of temporarily hidden segments had to be carefully estimated.

(2) No correction was attempted for 'out of the plane' motion and rotation about any other but the transverse axis through the sagittal plane.

(3) Use of the force summing device embedded into the pole vaulting box and the laminated foam insert designed to guide the pole tip to the exact measuring area altered the shape of the vaulting box and could have caused a loading error.

(4) The sampling frequency of 100 frames per second for the force data did not allow accurate determination of the duration of the striking impulse.

(5) The force transducers were designed to measure transient phenomena. However only static and quasistatic calibration were performed. The assumption was made that the calibration would apply to dynamic phenomena.

Delimitations

The present study was delimited in the following ways:

(1) Data were collected on a single vault of one subject, a nationally ranked pole vaulter with a personal best of 5.50m.

(2) A two dimensional analysis based on a cinematographical record of movements in the sagittal plane was performed.

(3) Force measurements were taken in the horizontal and vertical directions.

(4) Only parameters listed under "Methods and Procedures" were considered.

(5) A sampling rate of 20 frames per second for the analysis of the film showing the vaulting performance was chosen.

Definition of Terms

Adjusted predicted height (H_{ap}). The predicted vertical rise of the center of mass based on the initial and final kinetic energy of the vaulter.

Bendix Platen. The proper name of the digitizing board employed in the present study.

Chord. An imaginary line through the tip and the end of the pole.

Chordlength. A measure of the deflection or amount of bending of the pole calculated from the distance of the tip of the pole to the end of the pole.

CM. The center of mass of the body or body segment.

Conversion factor. A dimensionless number converting the projected image size to real life size measure.

High Point (HP). The time or position at which the center of mass reached its maximum elevation with respect to ground level.

Impact. The time instant at which the tip of the pole contacts the vaulting box.

Maximum Pole Bend (MPB). The time instant at which the measured chordlength reaches a minimum for a particular vault.

Measured impulse. Impulse obtained from numerical integration of force-time data recorded in the vaulting box.

Peak Vertical Extension Force (PVEF). The maximum vertical force acting on the tip of the pole recorded during the pole uncoiling phase and the associated time.

Phase-lock. A special electronics circuit ensuring frame by frame synchronization of several cameras.

Pole release. The time or position the vaulter releases the pole.

Pole Straight (PS). The instant or position when the pole is straight.

Predicted height. Predicted vertical rise of the vaulter's CM based on the initial energy of the system at impact as calculated from biomechanics cinematography data.

Predicted impulse. An impulse value obtained from changes of momentum as measured through biomechanics cinematography procedures.

Push-off angle. The angle with respect to the horizontal of a line through the CM and the vaulter's top hand at the instant

when the pole is released.

Striking force. The magnitude and direction of the force recorded when the pole first contacts the force summing device.

Striking impulse. The area under the force-time curve for the duration of the initial force peak at impact.

t(s). A specified time based on the occurrence of impact at t = 0.0 s.

CHAPTER II

REVIEW OF LITERATURE

The pole vaulting event has been the subject of many coaching and research oriented publications. However, comparatively few articles attempt a biomechanical analysis of the event and even fewer report quantitative data. From a methodological point of view three approaches are seen as being prevalent:

1. Investigators trying to isolate independent variables and estimate their empiric-statistic performance relevance based on a criterion such as the maximum vertical displacement of the vaulter's center of mass. Primary kinematic data are usually obtained from a cinematographical analysis of the event.

WOZNIK (et al)(1980) presented a non-deterministic model designed to identify variables with a statistically significant influence on the dependent variable (performance criterion). A similar approach was chosen by STEBEN (1970) who used multiple regression techniques to determine the influence of selected variables such as: run-up velocity and take-off velocity on the performance. HAY (1967) analyzed factors that do influence the pole bend. Angle of take-off, horizontal take-off velocity and the horizontal distance between the top hand and the take-off foot were statistically significant.

2. Several researchers have reported kinematic and/or kinetic data. DILLMAN(et al)(1968) determined relative changes in kinetic and potential energies occurring during the vault. A nine segment model was used to compute the vaulter's center of mass. Kinetic energy was estimated from:

$$T = \frac{1}{2} m (V_x^2 + V_y^2) = \frac{m V^2}{2}$$

where m equals the mass of the vaulter and V_x, V_y are the horizontal and vertical velocities of the center of mass, respectively. The authors identified the efficient use of initially available energy as being crucial. Predicted height (the height the vaulter would attain if the initial kinetic energy was transformed completely into potential energy) and adjusted predicted height (the predicted vertical displacement after subtracting the final from the initial kinetic energy), in comparison to each other, and the actual maximum height of the center of mass provided a valuable tool to estimate the vaulter's ability to effectively use the available energy. HAY (1968) presented a "preliminary analysis of mechanical energy changes" throughout the vault. Translational and rotational kinetic energy as well as gravitational potential energy were computed for two vaults. Translational kinetic energy was calculated from mean linear CM velocities. Rotational kinetic energy was estimated by summing the contributions of fourteen body segments:

$$T_{(R)} = \Sigma (\frac{1}{2} I \omega^2)$$

where I represents the moment of inertia of the segmental center of mass about the body CM and ω is the corresponding angular velocity. Results

were discussed and presented in graphical form. HAY suggested that a large rotational kinetic energy in the early swing phases of the vault and a large translational kinetic energy in the pole uncoiling phase produce better results provided that the ratio between kinetic and potential energy at bar clearance is favourable. Based on the available literature the most comprehensive experimental study of the fibreglass pole vault was performed by BARLOW (1973). BARLOW analyzed selected kinematic and kinetic parameters using cinematography, a force plate under the take-off area and a strain gage instrumented vaulting box. Individual and statistically treated data for performance oriented groups and the total sample were reported. A brief summary of BARLOW's main findings was published (BARLOW, 1979).

3. Several authors discuss mechanical factors influencing the pole vault performance or selected phases thereof. These publications, in general, do not present quantitative data but are concerned with theoretical discussions of mechanically sound approaches to the analysis of the event.

BERGEMANN (1979) discussed mechanical factors of relevance to the pole vault performance with respect to the traditional phases, Hang-Swing, Swing-Tuck, Extension, Pull-up and Push-off. WALKER (et al) (1973) and VERNON (1974) attempted to computer-model the pole vault in order to isolate the influence of selected independent on the dependent variable (performance). VERNON's model was used to derive charts and equations designed to help the vaulter select the appropriate pole for his size and speed. Furthermore, an estimate of the potential performance, assuming perfect execution of the vault and the use of the proper pole, was obtained. STEPP (1977) presented an equation for the

'energy budget of the pole vault' considering the following terms:

- initial potential energy,
- kinetic energy of translation at take-off,
- potential energy added by the take-off action,
- energy dissipated through internal friction,
- energy added due to the work done by the vaulter,
- final kinetic energy at the peak of the vault.

CHAPTER III

METHOD AND PROCEDURES

The primary purpose of the present study was to determine the validity of Biomechanics Cinematography data collection and analysis procedures. Validation was sought because cinematography is a non-invasive technique widely used as a source of data in situations where measurements that do influence the athlete or his environment cannot be obtained. This typically includes competitive situations.

The validation of cinematographic procedures required a criterion measure to provide a basis for the comparison of results. In the present study direct force measurements in the vaulting box were performed. The vaulting box is the only surface providing ground reaction force to the pole and the vaulter after take-off.

The experimental and analytical methods and procedures employed in the present study are described and discussed under the following headings: (1) Data Collection; (1.1) Cinematographic Procedures; (1.2) Force Measurements; (2) Analytical Procedures; (2.1) Subject Film Analysis; (2.2) Force Data Analysis; (2.3) Comparison of Cinematographic Data to Direct Force Measurements; and (3) Measurement Error.

Data Collection

Cinematographic and force data were collected at Point Loma College, San Diego, California. The outdoor facility was equipped with a tartan runup and standard vaulting box and landing pits. The subject, a United States Olympic team member (1980) with a personal best of 5.5 m, was 22 years old, weighed 820 N and was 1.84 m tall. A Skypole 16-175-B Flex 7.1 was used for the analysed vault.

The vaulter was given a sufficient number of trials for warm-up and to familiarize himself with the experimental procedure and the modified vaulting box. No markings or any restrictive equipment were placed on the vaulter.

Cinematographic Procedures

Two Photo-Sonics 1PL pin registered and phase-locked 16 mm cameras were used for the cinematographic data collection (Figure 1). Camera one recorded the side view of the entire performance. It was set 40 m from and perpendicular to the plane of motion. The optical axis intersected the plane 2.5 m from the end of the vaulting box closest to the pit. The camera was levelled 2.0m above ground level.

The frame rate of 100 frames per second and a shutter angle of 15^{o} produced an exposure time of 1/2400 s. The Angenieux 12 - 120 zoom lens was set at 35 mm which gave a field of view encompassing the penultimate runup stride and the entire vault. A 3.0 m segment of the uprights was used as a reference for the conversion of image to life size coordinates.

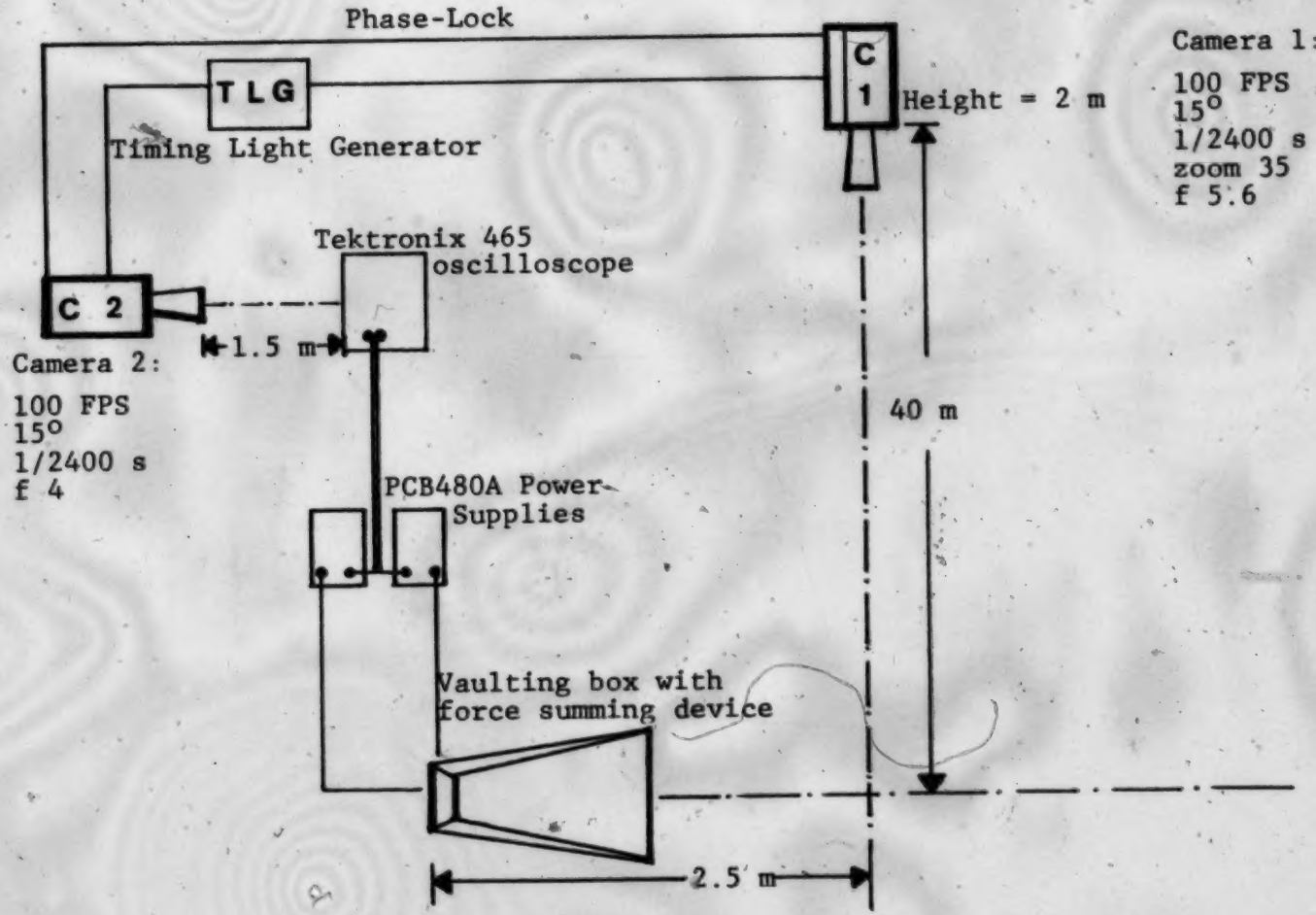

FIGURE 1

SCHEMATIC DIAGRAM OF EXPERIMENTAL SETUP

Camera #1 recorded the analog force transducer output displayed on a Tektronix 465 oscilloscope. The exposure time was 1/2400 s (15^{o} at 100 frames per second), the oscilloscope - camera distance was 1.5 m.

Cameras #1 and #2 were connected through a phase-lock system that ensured frame by frame synchronization. Furthermore, one timing light generator produced light marks on the edges of both films. These marks were used for precise frame rate determination and event matching. The flash frequency was set at 10 Hz and switched to 100 Hz for 0.1 second after the cameras had reached operating speed. This procedure allowed the determination of a common frame for each camera and performance. Both cameras used Ektachrome 7239 colour film rated at 160 ASA. Light measurements were taken with a Pentax 1^{o} Spotmeter V.

Force Measurements

Horizontal and vertical force components in the vaulting box were measured throughout the vault using two PCB 208A04 piezoelectric force transducers. Compressive stresses on the quartz element produced a positive output voltage, Δ V, directly proportional to the input measurand. Built-in miniature amplifiers yielded low impedance, high level output (Figure 2). The transducers were driven by two PCB 480A DC power supplies through shielded coaxial cables (Figures 2 and 3). The sensitivity of the transducer measuring the horizontal force component was given by the manufacturer as T.1758 mV/N. The corresponding value for the vertical force transducer was 1.2455 mV/N. A special force summing device that fit into a standard pole vaulting box was designed

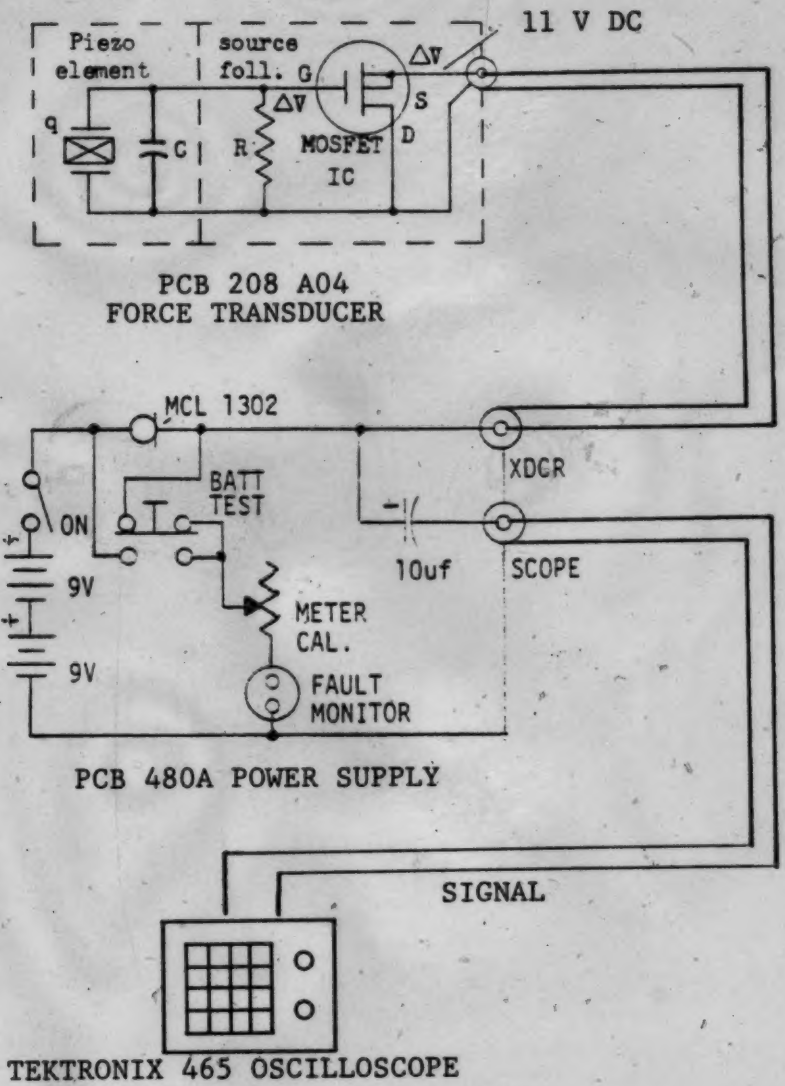

FIGURE 2

STANDARD MEASUREMENT CHAIN FOR DYNAMIC FORCES

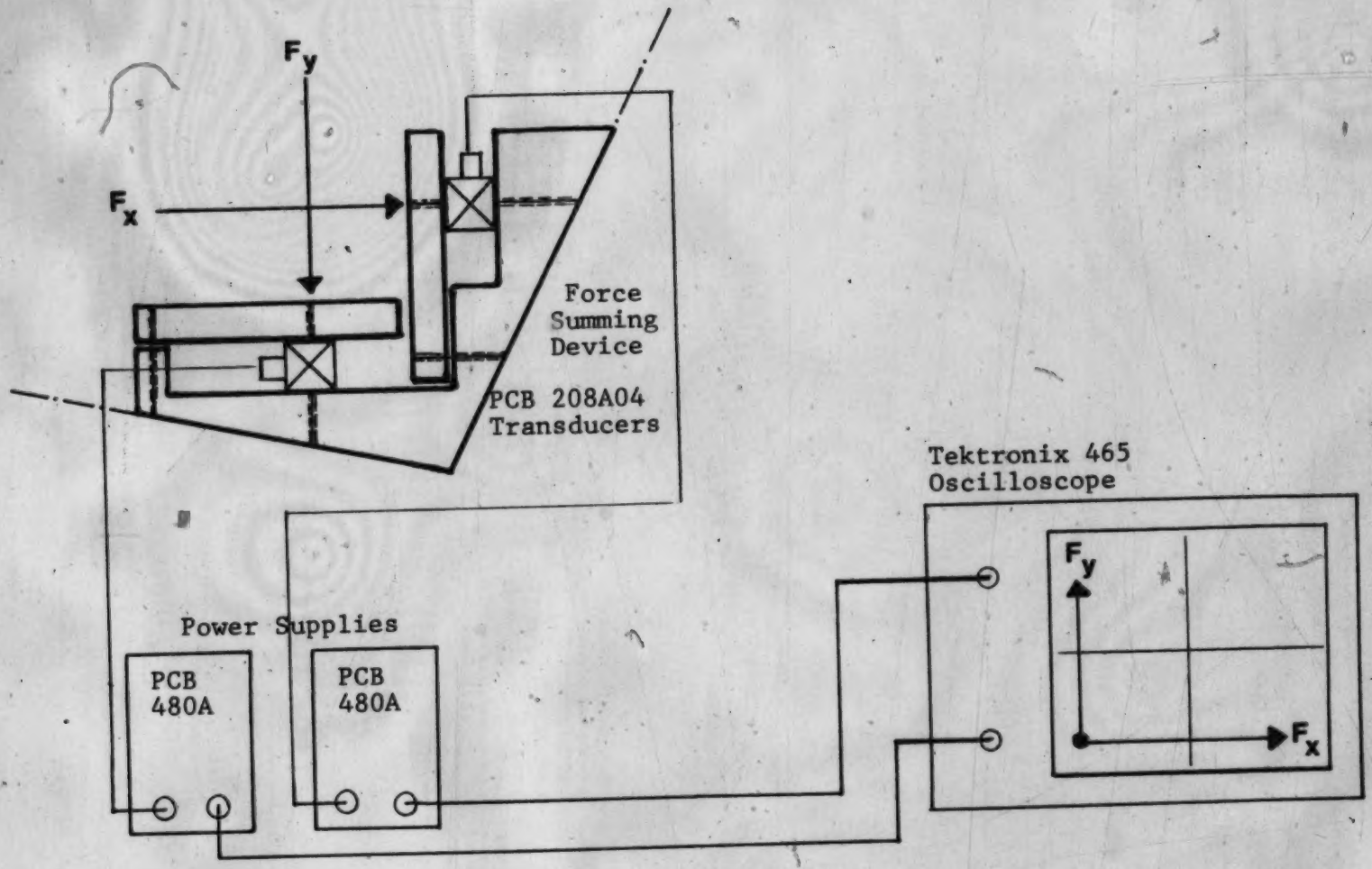

FIGURE 3

SCHEMATIC DIAGRAM OF MEASUREMENT CHAIN DESIGNED TO MEASURE HORIZONTAL AND VERTICAL FORCES IN THE VAULTING BOX

and machined to the mounting specifications of the transducer manufacturer (Figure 4).

The analog force signal was fed directly into a Tektronix 465 oscilloscope operating in X-Y display mode. Scope sensitivity was set at 0.5 volts per division. For the force measurements throughout the vault, the force summing device was secured into the vaulting box. A high density foam insert was shaped and laminated to guide the pole tip to the exact measuring area.

Analytical Procedures

The data films were edited and matched such that frame X in the subject film corresponded to frame X in the oscilloscope film. The image was projected onto a Bendix Platen using a TRIAD VR/100 pin registered film analyser. The Bendix Platen was interfaced to a HP9825B desk top computer via a HP9864A digitizer. The primary accuracy of this system as reported by the manufacturer allowed determination of cartesian coordinates accurate to 0.036 cm. The projected image was aligned with the internal axis of the Bendix Platen.

The precise frame rate was determined using the light marks produced by the timing light generator on the edge of the films at 0.1 second intervals. Both cameras operated at precisely 100 frames per second in phase-lock mode.

Subject Film Analysis

A 3.0 m section of the uprights was used to compute the

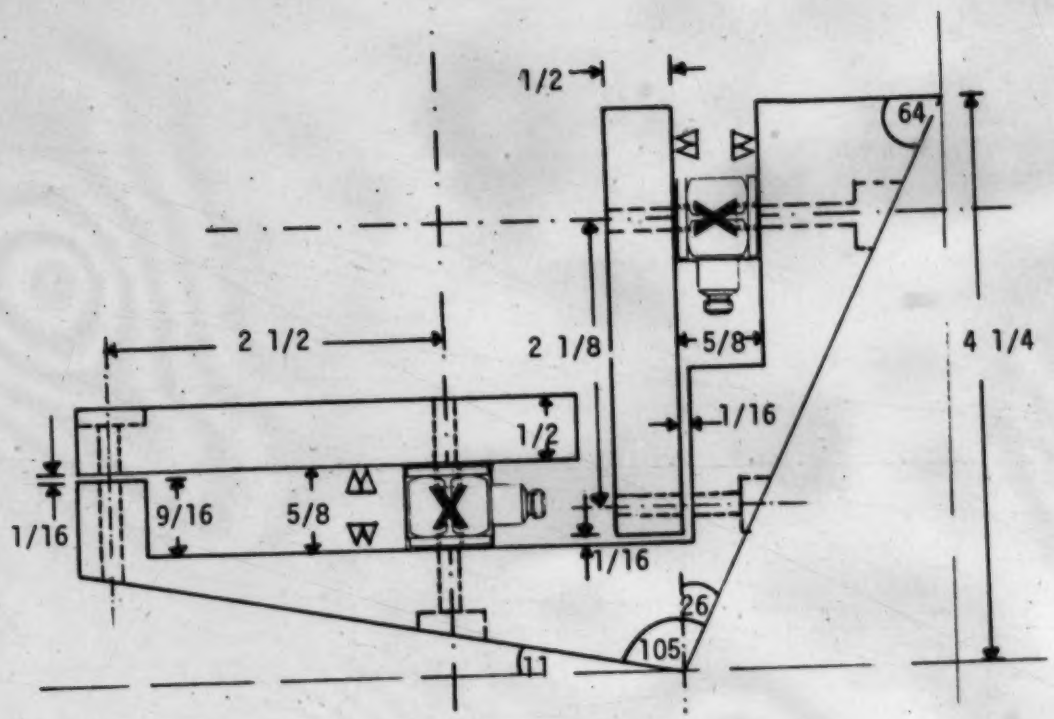

LEGEND:

All measures are given in inches and degrees.

▽▽ : These surfaces are flat to within 0.001 TIR 125 µinch surface finish.

X : PCB 208A04 piezoelectric force transducers.

FIGURE 4

ASSEMBLY DRAWING OF THE FORCE SUMMING DEVICE

correction factor from projected image size to real life size. The entire performance from the penultimate stride to post bar clearance was digitized at five frame intervals. Each frame required input of the proximal and distal X and Y coordinates for the following body segments: head and neck, trunk, as well as right and left upper arm, lower arm, hand, thigh, leg and foot. In addition five points along the pole (end of the pole, top hand, bottom hand, mid-pole and box) and the location of the cross bar were digitized. The data digitizing and storage program was set to store all raw data points on magnetic tape for subsequent analysis.

Massachusetts Institute of Technology 'Humanscale' data (Figure 5)(Table I) for the location of the segmental CM relative to the proximal end point and the percent mass of the segment were used to compute the segmental and total CM (Diffrient, 1974). Moments of Inertia for the segments about a transverse axis through their CM were taken from Dapena (1978)(Table II).

Analysis of the subject film entailed quantification of the following parameters:

(1) Horizontal, vertical and linear velocities (m/s) of the segmental and body CM's between frames x and x+1

$$\bar{V} = \frac{\sqrt{((X_{x+1} - X_x)^2 + (Y_{x+1} - Y_x)^2)}\ (C)}{\Delta t}$$

Where:

$\bar{V}$ = average velocity of a point between adjacent frames;

X,Y = cartesian coordinates of a point in frames x and x+1;

C = conversion factor converting displacement to life size units.

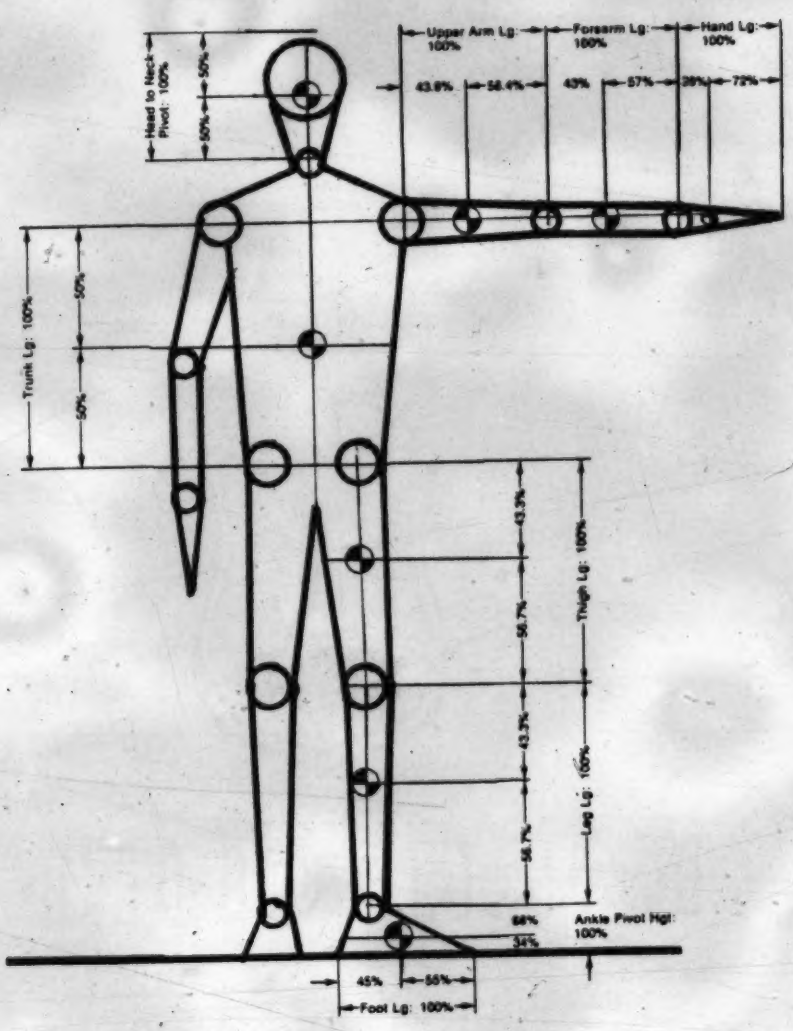

FIGURE 5

MIT HUMANSCALE DATA FOR RELATIVE POSITIONS OF THE SEGMENTAL CENTERS OF MASS

TABLE I

MIT HUMANSCALE: RELATIVE MASSES OF THE BODY SEGMENTS

Head	7.1
Neck	2.5
Trunk	45.8
Upper Arms	6.6
Forearms	3.8
Hands	1.3
Thighs	21.0
Legs	9.0
Feet	2.9
	100 %

TABLE II

MOMENTS OF INERTIA ABOUT THE TRANSVERSE AXIS

THROUGH THE SEGMENTAL CM

(Dapena, 1978)

Segment	I (kg m^2)
Head	0.0248
Upper Arm	0.0213
Forearm	0.0076
Hand	0.0005
Trunk	1.3080
Thigh	0.1052
Lower Leg	0.0505
Foot	0.0038

(2) Horizontal, vertical and linear momentum (Ns) of the vaulter

$$M = (m_V)\ \bar{V}_{CM}$$

where:

M = momentum;

m_V = mass of the Vaulter;

$\bar{V}_{CM}$ = velocity of the center of mass.

(3) Angular displacement (rad) and velocity (rad/s) of each segment

$$\omega_i = \frac{\tan^{-1}\left(\frac{m_2 - m_1}{1+m_1 m_2}\right)}{\Delta t}$$

where:

ω_i = angular velocity of segment i;

m_1, m_2 = slope of the line through proximal and distal joint centers of segment i in frames x and x+1 obtained from:

$$m = \frac{(P_y - D_y)}{(P_x - D_x)}$$

where:

m = slope of the line through proximal and distal segmental endpoints;

P_y, D_y, P_x, D_x are the proximal and distal x and y coordinates of the segment.

(4) Translational kinetic energy (Joule) of the vaulter

$$T_{(T)} = \sum_{i=1}^{14} \left[\frac{1}{2} m_i\ (\bar{V}_{x_i}{}^2 + \bar{V}_{y_i}{}^2)\right]$$

where:

$T_{(T)}$ = translational kinetic energy;

m_i = mass of the ith segment;

$\bar{V}_{x_i}$, $\bar{V}_{y_i}$ are the horizontal and vertical velocities of the segmental CM between frames x and x+1.

(5) Rotational kinetic energy (Joule)

$$T_{(R)} = \sum_{i=1}^{14} \left[\frac{1}{2} I_i \bar{\omega}_i^2\right]$$

where:

$T_{(R)}$ = rotational kinetic energy;

I_i = moment of inertia of segment i about the transverse axis through the segmental CM;

$\bar{\omega}_i$ = angular velocity of segment i between frames x and x+1.

(6) The total kinetic energy of the vaulter (Joule)

$$T = \sum_{i=1}^{14} \left[\frac{1}{2} m_i (\bar{V}_{x_i}^2 + \bar{V}_{y_i}^2) + \frac{1}{2} I_i \bar{\omega}_i^2\right]$$

where:

T = total kinetic energy comprised of translational and rotational components.

(7) Gravitational potential energy (Joule)

$$T_{(g)} = m_V gh$$

where:

$T_{(g)}$ = gravitational potential energy;

m_V = mass of the vaulter;

g = acceleration due to gravity;

h = height of the vaulter's CM above ground level.

(8) Total angular momentum (Kg m^2/s) of the vaulter

$$\bar{H}_{T_{x \to x+1}} = \sum_{i=1}^{14} \left[I_i \, \bar{\omega}_i + m_i \, \bar{r}_i^{\,2} \, \bar{\omega}_{i/A} \right]$$

where:

$\bar{H}_T$ = average total angular momentum of the body between frames x and x+1;

I_i = moment of inertia of segment i about the transverse axis through its CM;

$\bar{\omega}_i$ = average angular velocity of segment i between frames x and x+1 about its CM;

m_i = mass of the ith segment;

$\bar{r}$ = distance between the axis of rotation and the CM of segment i between frames x and x+1;

$\bar{\omega}_{i/A}$ = average angular velocity of the CM of segment i about the axis of rotation between frames x and x+1.

$I_i \, \bar{\omega}_i$ is the local angular momentum of segment i, $m_i \bar{r}_i^{\,2} \bar{\omega}_{i/A}$ is the transfer term or remote angular momentum about the axis of rotation.

The cinematographic raw data were smoothed using the finite differences method, a local approximation technique providing formulae to compute first and second derivatives of functions (Miller/Nelson, 1973). Furthermore a cubic spline function was employed. A third degree polynomial was fitted through user defined points. The curve was integrated for each interval $(x_i - x_{i+1})$, differentiated for each $y = f(x)$ and interpolated.

Force Data Analysis

The film obtained from camera two was used as data source for the forces acting on the tip of the pole in X and Y directions throughout the vault. The analysis program first aligned the oscilloscope grid with the internal X and Y axis of the digitizing board. A correction-factor based on the projected image size was computed. The X,Y coordinates of the input point representing the instantaneous X,Y force components were digitized at one frame intervals and converted to force values in Newtons adjusted for the different sensitivities of the transducers. Numerical output and graphs of the horizontal, vertical and resultant force were provided. Temporal and quantitative data were taken from the raw data which were subsequently processed through the cubic spline program. The following parameters were determined:

(1) Duration of application of horizontal and vertical forces (s);

(2) The time at which the maximum vertical extension force occurred (s);

(3) The peak horizontal force (N);

(4) The peak vertical extension force (N);

(5) The horizontal striking impulse was computed by assuming a triangular peak over a period of 0.01 second;

(6) The horizontal and vertical impulses for the entire vault and specified phases thereof were obtained through numerical integration of the force-time data:

$$\text{Impulse} = \int_{t1}^{t2} F\,(dt)$$

(7) Numerical and graphical output of the force-time history of the entire performance was provided.

Comparison of Cinematographic Data to Direct Force Measurements

The comparison of data derived from biomechanics cinematography procedures to data obtained through bi-axial force measurements in the vaulting box was performed using the following procedures:

(1) The total momentum (Ns) of the vaulter, accounting for the rotational component was computed as:

$$M_{(T)} = (m_V)\overline{V}_{CM} + \sum_{i=1}^{14} \left[m_i \, \overline{r}_{i/CM} \, \overline{\omega}_{i/CM} \right]$$

where:

$M_{(T)}$ = total momentum;

m_V = mass of the vaulter;

$\overline{V}_{CM}$ = average velocity of the CM between frames x and x+1;

m_i = mass of the ith segment;

$\overline{r}_{i/CM}$ = average distance of the segmental CM to the body CM;

$\overline{\omega}_{i/CM}$ = angular velocity of the segmental CM about the body CM between frames x and x+1.

(2) The change in momentum was obtained from:

$$\Delta M_{(T)} = M_{(T)_{t_2}} - M_{(T)_{t_1}}$$

where:

$\Delta M_{(T)}$ = change in momentum;

t_1, t_2 = two distinct times limiting the interval over which the change in momentum was computed.

(3) The difference between the impulse measured in the vaulting box and the resulting change in momentum was computed by subtracting the

change in momentum determined from the cinematographical analysis from the impulse obtained from the direct force measurements:

$$E_a = \int_{t1}^{t2} F\,(dt) - \left(M_{(T)t_2} - M_{(T)t_1} \right)$$

where:

E_a = absolute error of the changes in momentum as obtained from biomechanics cinematography procedures with respect to the criterion force measurements.

Measurement Error

The magnitude and impact of random and systematic errors depend upon the method and procedures employed in any specific study and the parameters to be quantified and derived. In the following section potential sources of errors are identified, discussed and, in some cases, operationally defined. The actual absolute and relative errors incurred in this study are reported in Chapter IV.

An assessment of the performance characteristics of the measurement chain employed to record and digitize the horizontal and vertical force components in the vaulting box was made to estimate the error associated with the criterion force measurements. The PCB 208A04 piezoelectric force transducers were calibrated by the manufacturer: linearity was tested in a range from 0.0 to 4.5 kN and was reported to be better than 1%. Hysteresis was less than 1%.

The operator precision in digitizing the analog force signal was assessed from repeated measures. Each digital force value was ob-

tained by digitizing the analog force signal which was displayed as a point on the oscilloscope. This point represented the magnitude and direction of the resulting force vector. Each measurement had an absolute uncertainty caused by the size of the displayed point and/or its positional change during the exposure time of the film. This uncertainty was independent of the magnitude of the horizontal and vertical force components and was referred to as resolution limit of the force data analysis.

The two basic sources of error inherent in cinematographical analysis are time error and displacement error. Time error is caused by inconsistent or incorrectly determined frame rates and results in systematic or random errors when derivatives with respect to time are computed from the displacement data. Displacement error is caused by incorrect determination of the X,Y coordinates of a point in successive frames. Factors that aggravate displacement error include: poor film quality, distortion through the optical elements of the camera and projection systems, incorrect determination of the conversion factor and the fact that coordinates of temporarily obscured segments have to be estimated based on the segment's location in adjacent frames. Furthermore, the anatomical input data for the location of the segmental CM's with respect to the proximal endpoint, the percent body mass of each segment and the data for moments of inertia of each segment about the transverse axis through the segmental center of mass are derived from statistical analysis and cadaver studies; they do not necessarily reflect the individual characteristics of the subject.

In the present study, operator error was operationally defined as the researcher's ability to precisely determine the proximal and

distal coordinates of any body segment. The precision of the researcher was estimated from repeated digitization of all input points from frames #20 and #39 of the subject film. The average mean error was obtained from:

$$E_D = \pm \frac{\sum_{i=1}^{n} \left[\sqrt{(X_{1_i} - \bar{X}_i)^2 + (X_{2_i} - \bar{X}_i)^2} \right]}{n}$$

where:

E_D = average mean absolute error;

$\bar{X}_i$ = mean measurement at time i;

n = number of measurements;

X_{1_i}, X_{2_i} are the first and second measurement taken at time i.

The effect of the error in reproducing a number of single input points on the computed location of the total body CM was assessed through comparison of the resulting X and Y coordinates of the center of mass.

The influence of smoothing the raw displacement data on the subsequent computation of the first derivative was determined by integrating smoothed velocity-time data and comparing the results to the raw displacement data. The discrepancy was mathematically defined as:

$$D = \int_{t1}^{t2} \tilde{V}\,(dt) - ds$$

where:

D = discrepancy between the displacement obtained from smoothed and integrated velocity-time curves and the raw displacement data;

$\int_{t1}^{t2} \tilde{V}(dt)$ = area under the smoothed velocity-time graph;

ds = raw displacement data for the time interval t2 - t1.

The data derived from the cinematographical analysis should ideally match the criterion force and impulse measures obtained from the force summing device in the vaulting box. The difference between the measures, plus or minus the error of the criterion force data, was defined as the total absolute or relative error of the cinematographic analysis. The relative error was computed for each measurement based on the criterion force (impulse) measure:

$$E_r = \frac{I - \Delta M_{(T)}}{I} \quad 100$$

where:

E_r = relative error;

I = impulse measured in the vaulting box;

$\Delta M_{(T)}$ = change in momentum as determined from biomechanics cinematography.

The mean relative error was obtained from:

$$\bar{E}_r = \frac{\sum_{i=1}^{n} (E_r)}{n}$$

where:

$\bar{E}_r$ = mean relative error;

n = number of measurements.

Similarly, the absolute error was defined as:

$$E_a = I - \Delta M_{(T)}$$

where:

E_a = absolute error of the changes in momentum computed from cinematographic data.

The mean absolute error was computed from:

$$\bar{E}_a = \frac{\sum_{i=1}^{n} (| E_a |)}{n}$$

where:

$\bar{E}_a$ = mean absolute error.

CHAPTER IV

RESULTS AND DISCUSSION

The results obtained from the present study are reported in graphical and tabular form. All raw data are contained in the respective appendices. This chapter is subdivided into the following sections: (1) Phase Structure of the Pole Vault; (2) Kinematic Parameters; (3) Energy; (4) Force Measurements; (5) Angular Momentum; (6) Comparison of Data Derived from Biomechanics Cinematography to the Criterion Direct Force Measurements in the Vaulting Box; and (7) Measurement Error.

Phase Structure of the Pole Vault

The following phases of the performance were identified to provide an unambiguous temporal frame of reference, based on kinematic and kinetic parameters, for the presentation and the discussion of the results (Figure 6):

(1) Impact (t=0.0s). The instant at which the pole makes contact with the force summing divice in the vaulting box. All times and time intervals are measured from impact.

(2) Take-off (t=0.03s). The last visible foot contact with the ground.

(3) Maximum Pole Bend (MPB) (t=0.55s). The time at which the pole reaches its maximum deflection as measured from a reduction in chord length.

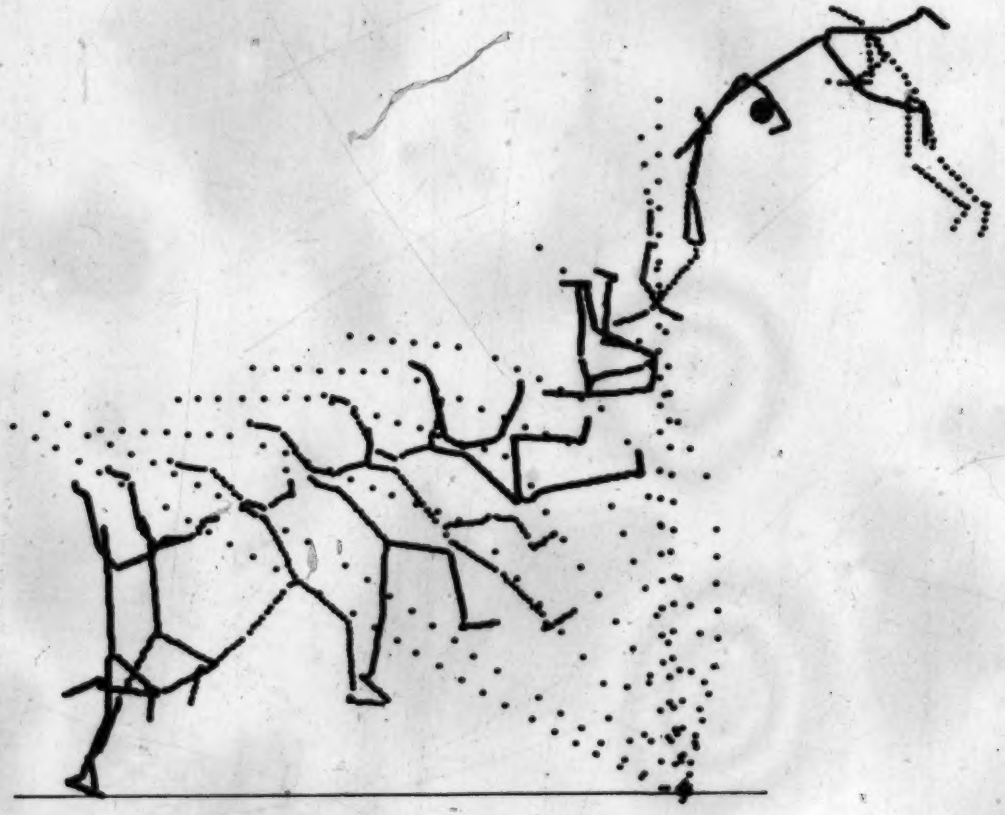

FIGURE 6

STICKFIGURE PLOT OF SELECTED PHASES OF THE POLE VAULT

(4) Peak Vertical Extension Force (PVEF) (t=0.78s). The instant at which the maximum vertical force component is measured during the pole uncoiling phase.

(5) Pole Straight (PS) (t=1.01s).The time at which the pole is fully uncoiled.

(6) Pole Release (PR) (t=1.31s). The instant at which the last contact between the pole and the vaulter is observed. Force application ceases.

(7) High Point (HP) (t=1.47s). The time or position where the vaulter's CM has reached its maximum height above ground level.

Kinematic Parameters

A graphical representation of the velocity-time curves of the CM for the horizontal velocity, the vertical velocity and the linear velocity is presented in Figure 7. The following main trends were observed: The horizontal velocity reached a peak value of 8.02 m/s at the end of the positively accelerating phase of the last stride. During amortization and until take-off the linear velocity decreased to 6.8 m/s. At the same time the vertical velocity increased, due to the active take-off, to 2.5 m/s (t=0.03s). The maximum vertical acceleration in this phase was 23 m/s^2. After take-off the horizontal CM velocity decreased at a rate of -8.9 m/s^2. At maximum pole bend the horizontal acceleration was -5 m/s^2 and continued to decrease reaching values close to zero at approximately 0.83 seconds. Throughout the remainder of the vault the horizontal velocity varied from 1.7 m/s to 2.2 m/s (mean: 1.85 m/s). The vertical velocity after take-off dropped to 1.7 m/s (t=0.33s). At t = 0.6 seconds, the vertical CM velocity exceeded the horizontal velo-

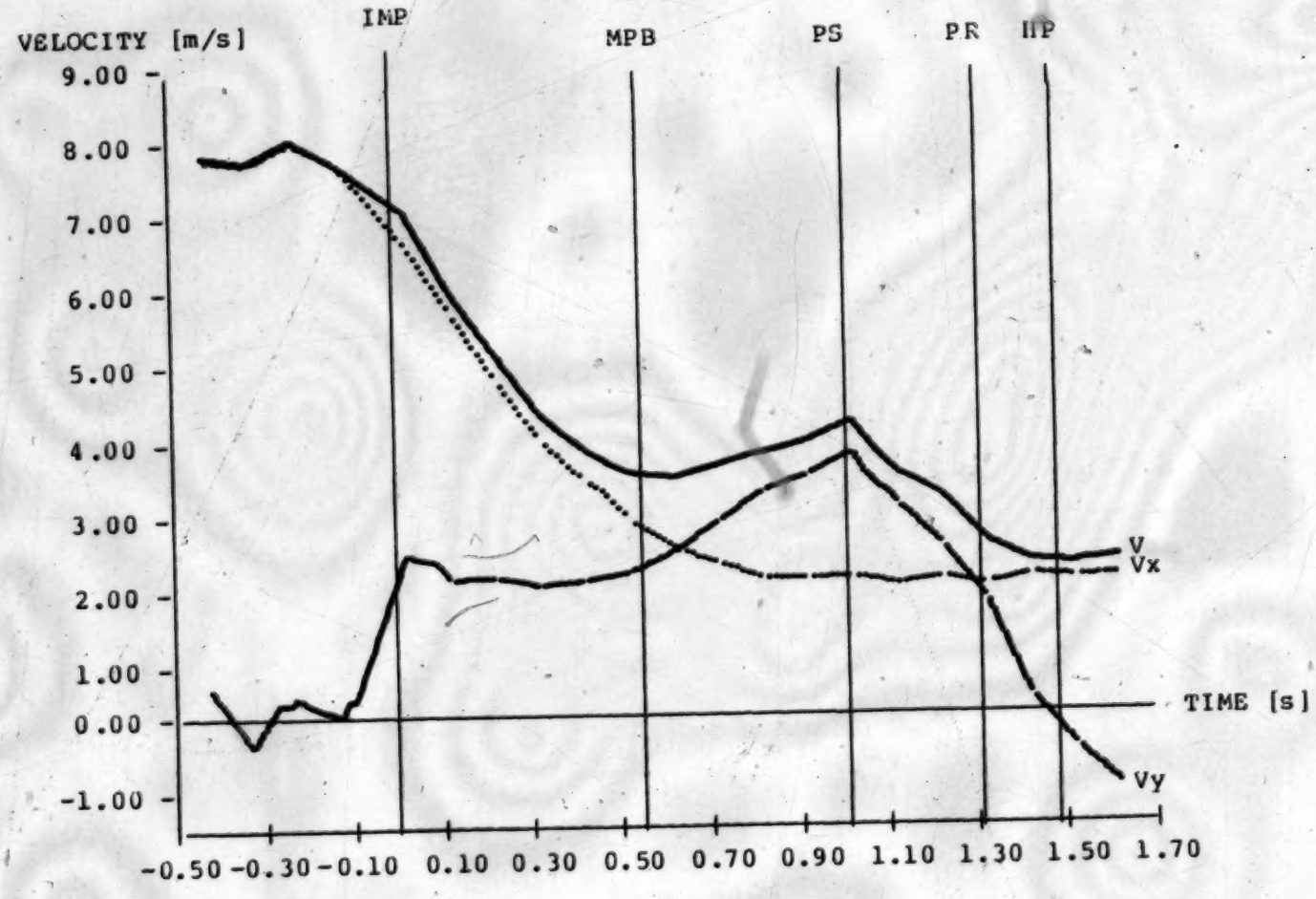

FIGURE 7

LINEAR VELOCITY OF THE VAULTER'S CENTER OF MASS AND ITS HORIZONTAL (V_x) AND VERTICAL (V_y) COMPONENTS

city: The center of mass moved at an angle greater than 45^{o} to the horizontal. The vertical CM velocity reached a peak of 3.8 m/s at the instant when the pole was fully uncoiled (t=1.01s). After the pole was straight and until the vaulter released the pole the average vertical acceleration was determined as $-7.5\ m/s^2$. The vertical acceleration after the vaulter broke contact with the pole was $-8.6\ m/s^2$. The error of the mean, compared to the acceleration due to gravity, was 12.3%. The vertical velocity at the instant when the pole was released was 1.74 m/s. The theoretical vertical displacement after release obtained from:

$$\Delta y = \frac{V_y^2}{2g}$$

where:

Δy = theoretical vertical displacement;

V_y = measured vertical velocity;

g = acceleration due to gravity

was 0.17 m. The measured vertical displacement in this phase was 0.115 m. The difference between the theoretical and actual vertical displacement was 0.015 m (8.8%). The linear velocity reached relative minima at t = 0.58 seconds (3.3 m/s) and t = 1.5 seconds (2.0 m/s) corresponding to the maximum pole bend and the time when the CM reached the peak of its flight curve. A relative maximum of 4.2 m/s was observed at the instant when the pole was straight.

ENERGY

Translational and rotational kinetic energy as well as gravitational potential energy and the total energy of the vaulter through-

out the performance are plotted versus time in Figure 8. At impact the kinetic energy of the system was 2444 J. Added to the initial gravitational potential energy this yielded a total kinetic energy of 3419 J. Assuming complete conversion to potential energy, the predicted vertical rise of the center of mass was:

$$H_p = \frac{T_{(K)i} + T_{(g)i}}{mg} = 4.15 \text{ m}$$

where:

H_p = predicted vertical CM displacement;

$T_{(K)i}$ = initial kinetic energy;

$T_{(g)i}$ = initial gravitational potential energy;

mg = weight of the vaulter.

Accounting for the final kinetic energy, defined as the amount of kinetic energy at the instant when the potential energy reached its maximum value, the adjusted predicted height was written as:

$$H_{ap} = \frac{T_{(K)i} - T_{(K)f} + T_{(g)i}}{mg} = 3.88 \text{ m}$$

where:

H_{ap} = adjusted predicted height;

$T_{(K)f}$ = final kinetic energy.

The difference between adjusted predicted height and predicted height was 0.27 m. The difference between the actually achieved height of 4.66 m and the adjusted predicted height was 0.78 m. This is a measure for the net work done by the vaulter where the net work is defined as the total work done by the vaulter minus the energy converted to non-usable forms.

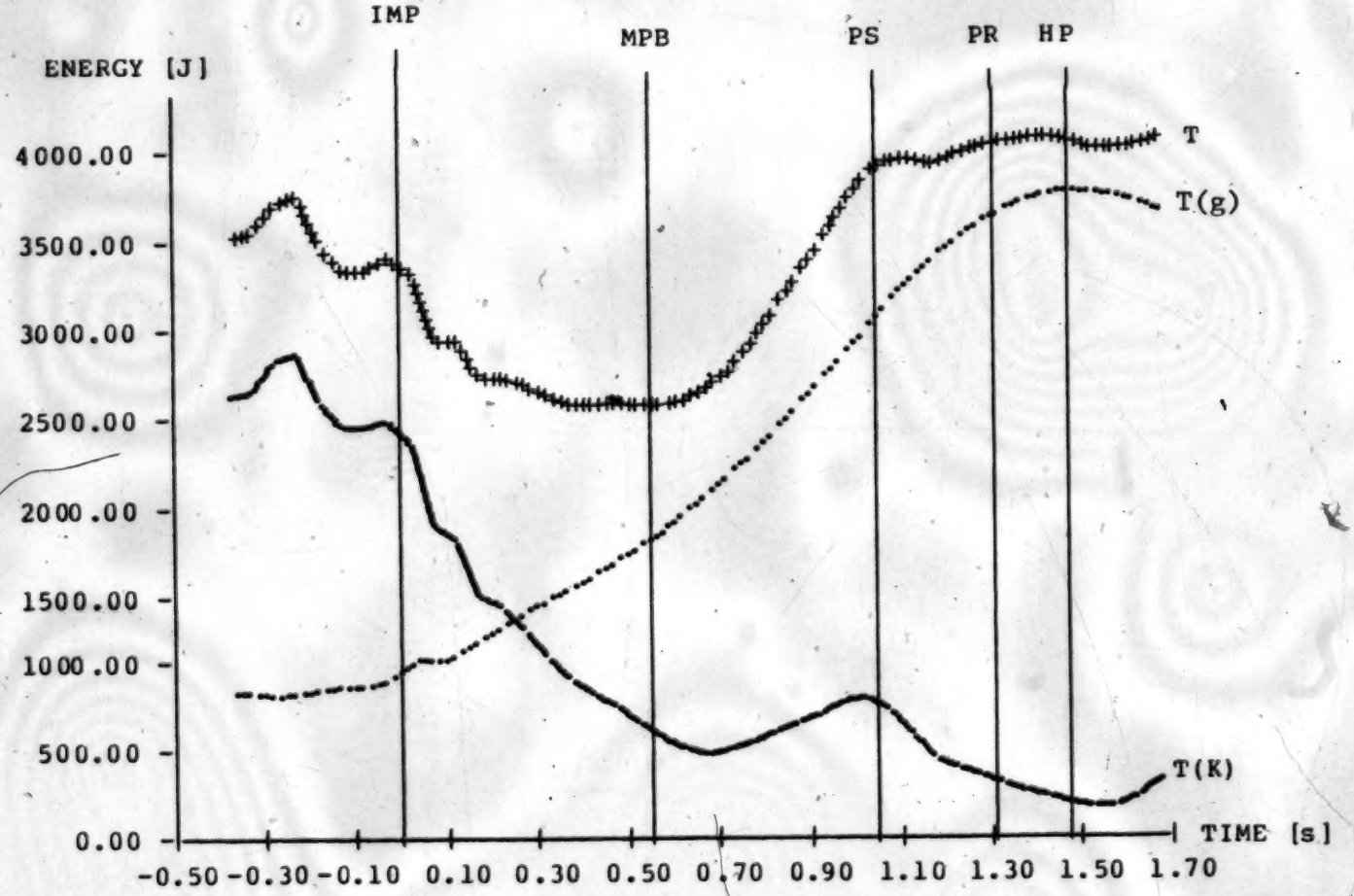

FIGURE 8

KINETIC ENERGY ($T_{(K)}$), GRAVITATIONAL POTENTIAL ENERGY ($T_{(g)}$) AND TOTAL ENERGY (T)

Hence:

$$W = T_f - T_i = 621 \text{ J}$$

where:

W = net work done by the vaulter;

T_f = total final energy of the system;

T_i = total initial energy of the system.

Conversely, the work done by the vaulter is equal to the energy equivalent of the difference between actually achieved height and the adjusted predicted height:

$$\frac{W}{mg} = H - H_{ap} = 0.76 \text{ m}$$

where:

mg = weight of the vaulter;

H = actually achieved height of the center of mass.

The rotational kinetic energy calculated from the rotation of each segment about the transverse axis through its CM was found to have absolute values varying between 2.0 and 32.0 J throughout the vault.

Force Measurements

The force summing device in the vaulting box in conjunction with the display and recording devices allowed measurement of horizontal and vertical force components throughout the vault at 0.01 second intervals. Graphical representations of the horizontal force, the vertical force and the resultant force are given in Figures 9,10 and 11 respectively. The peak horizontal striking force, measured when the pole tip made contact with the force plate, was 3734 N. The horizontal force

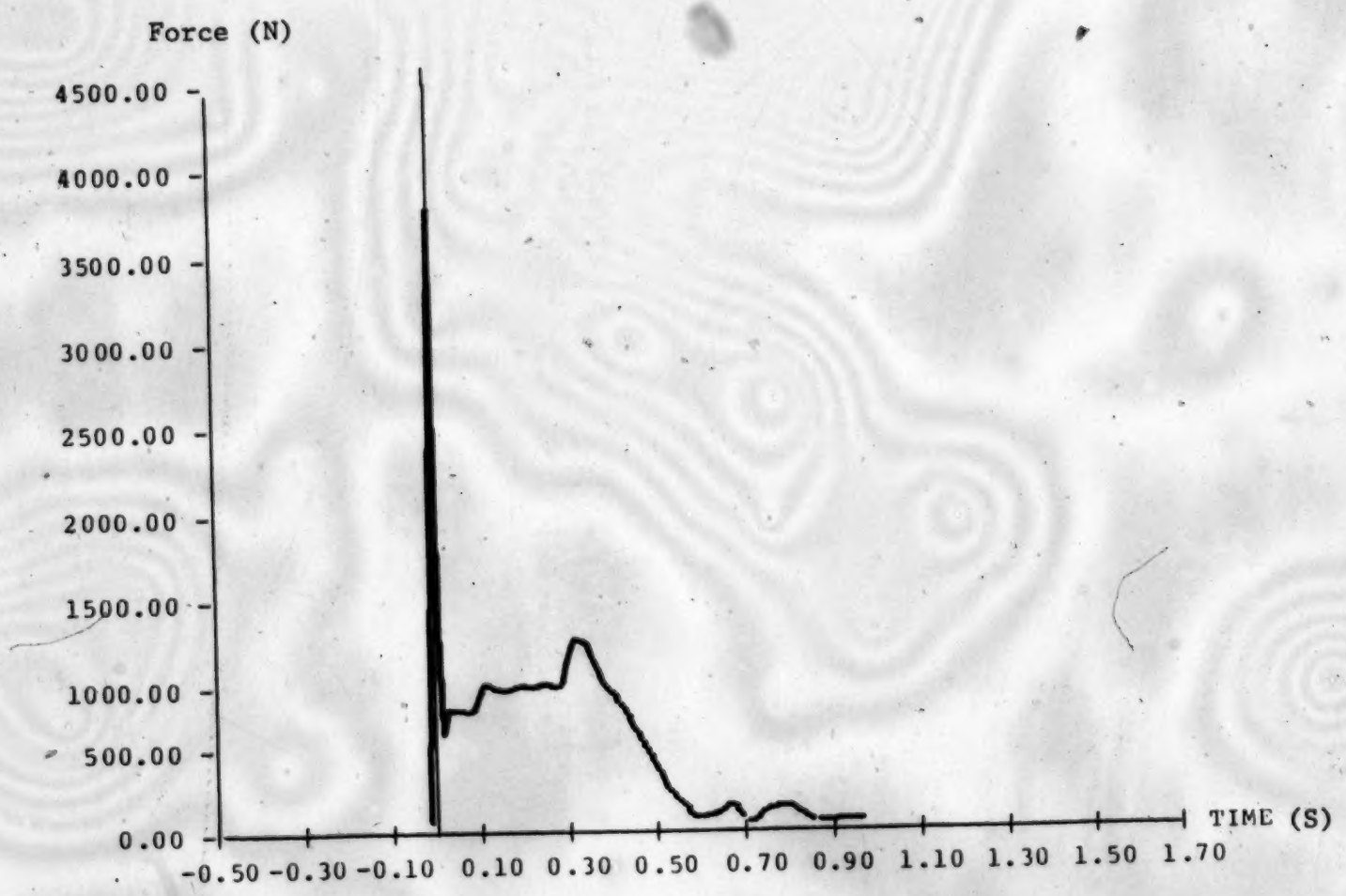

FIGURE 9

HORIZONTAL FORCE MEASURED IN THE VAULTING BOX

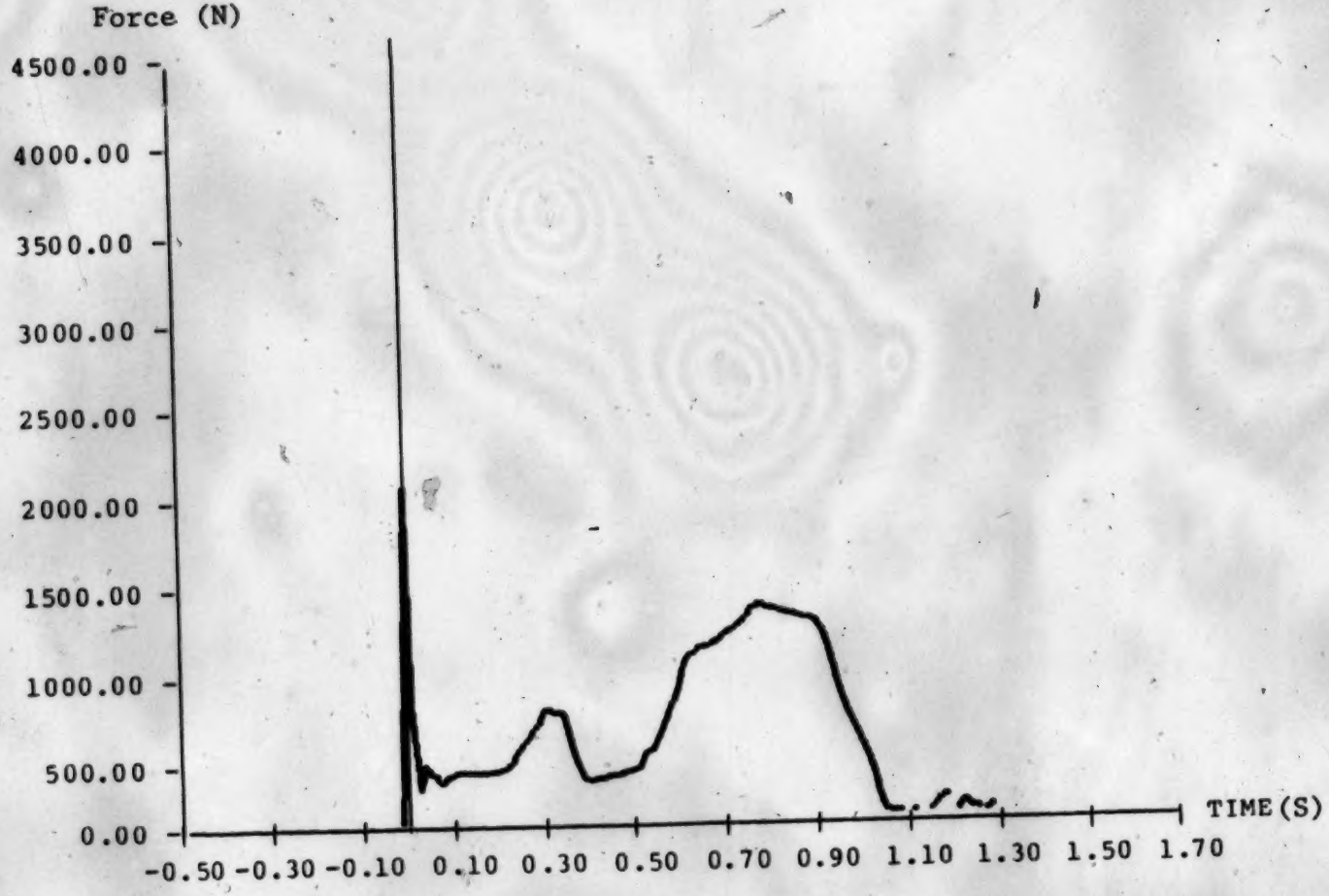

FIGURE 10

VERTICAL FORCE MEASURED IN THE VAULTING BOX

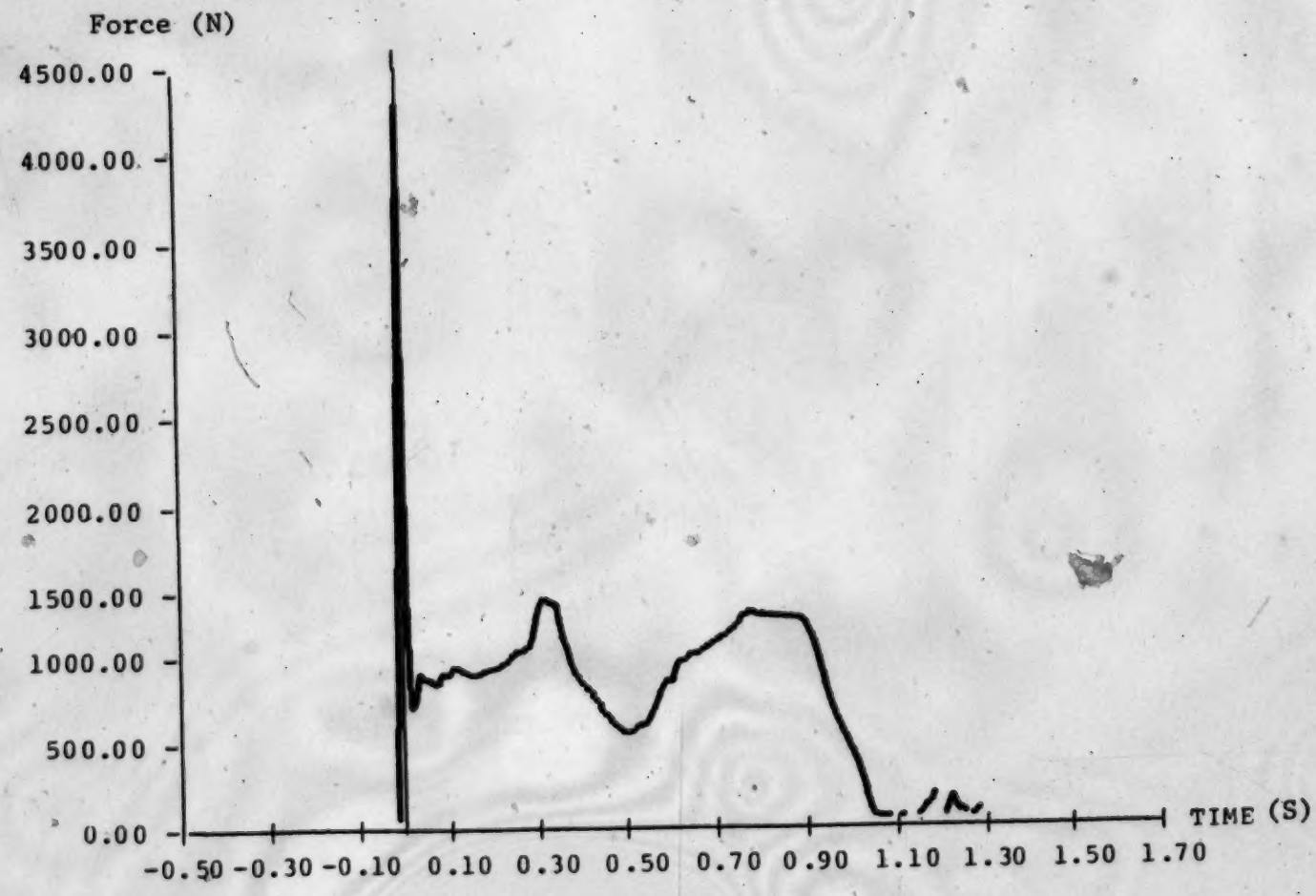

FIGURE 11

RESULTANT FORCE MEASURED IN THE VAULTING BOX

varied in a range from 700 N to 900 N from t = 0.04 seconds to t = 0.29 seconds. A relative maximum was observed at t = 0.32 seconds followed by a constant drop to 33 N at t = 0.6 seconds. After maximum pole bend the horizontal force remained below 130 N. Application of force in the horizontal direction ceased at t = 0.98 seconds, three onehundredths of a second before the pole was straight at 89.5 degrees to the horizontal. At impact the vertical force component was 2021 N. The recorded vertical force varied between 160 and 350 N before reaching a first relative maximum of 762 N at t = 0.31 seconds. Between t = 0.37 and 0.49 seconds the vertical force decreased to 200 to 350 N. A fast increase (t=0.62s) was followed by a moderate rise to the peak vertical extension force of 1322 N (t=0.78s). Over the interval t = 0.6 to 0.95 seconds the vertical force recorded exceeded the body weight of the vaulter. After the pole reached the initial unbent position and until the vaulter broke contact with the pole the force reading fluctuated between 0.0 and 150 N.

Angular Momentum

The angular momentum of the vaulter about the transverse axis through the center of mass is plotted versus time in Figure 12. The components, namely moment of inertia and angular velocity are graphically represented in Figure 13. During the final stride prior to take-off, moments of inertia of 10 to 12 Kgm^2 were measured. After impact and until t = 0.275 seconds the moment of inertia increased to a maximum of 13.3 Kgm^2. In the following phase of the vault the athlete decreased the moment of inertia in order to facilitate the transition from the hang to the inverted hang position. The rock-back phase was completed,

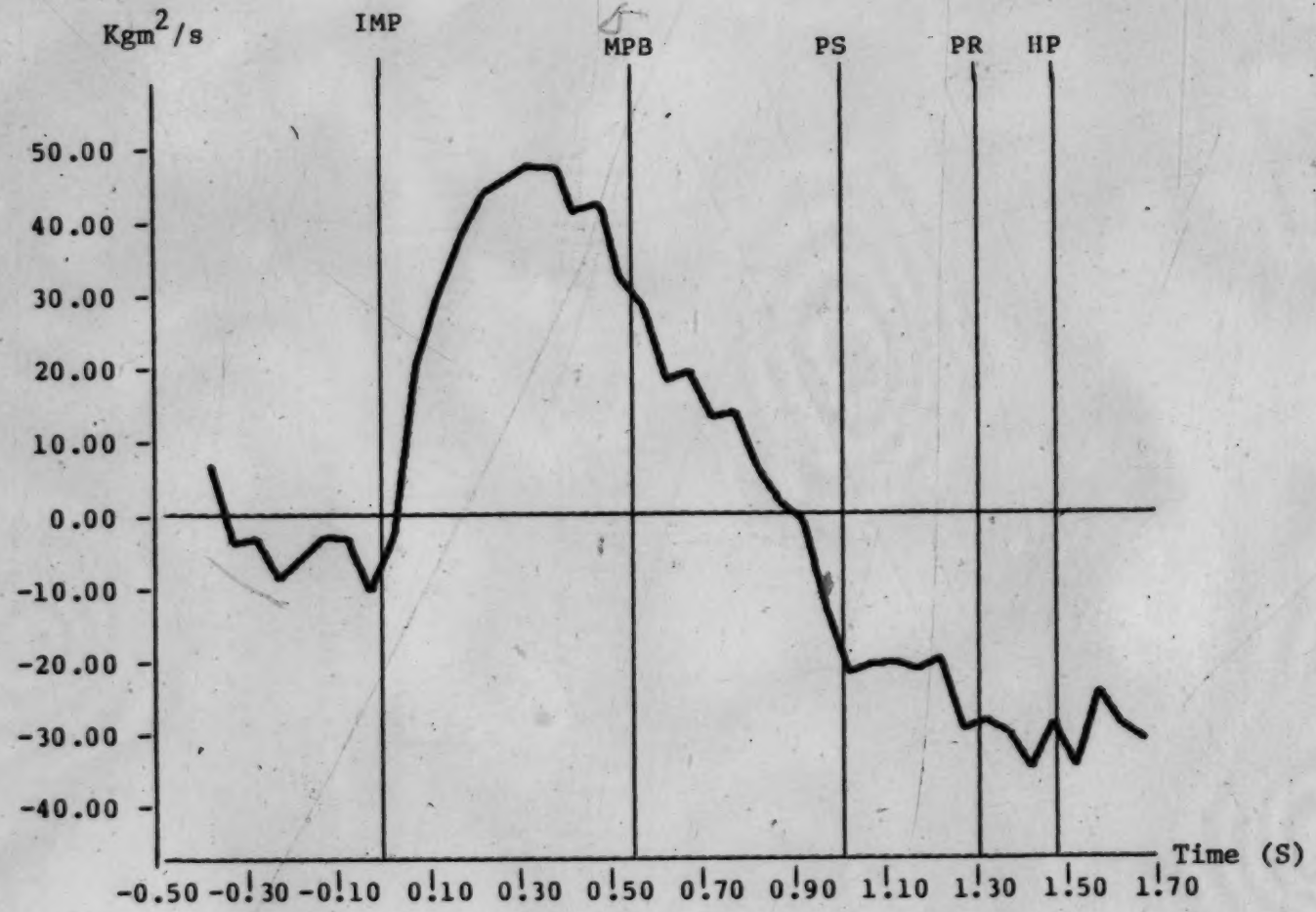

FIGURE 12

ANGULAR MOMENTUM (H_{CM}) ABOUT THE CENTER OF MASS

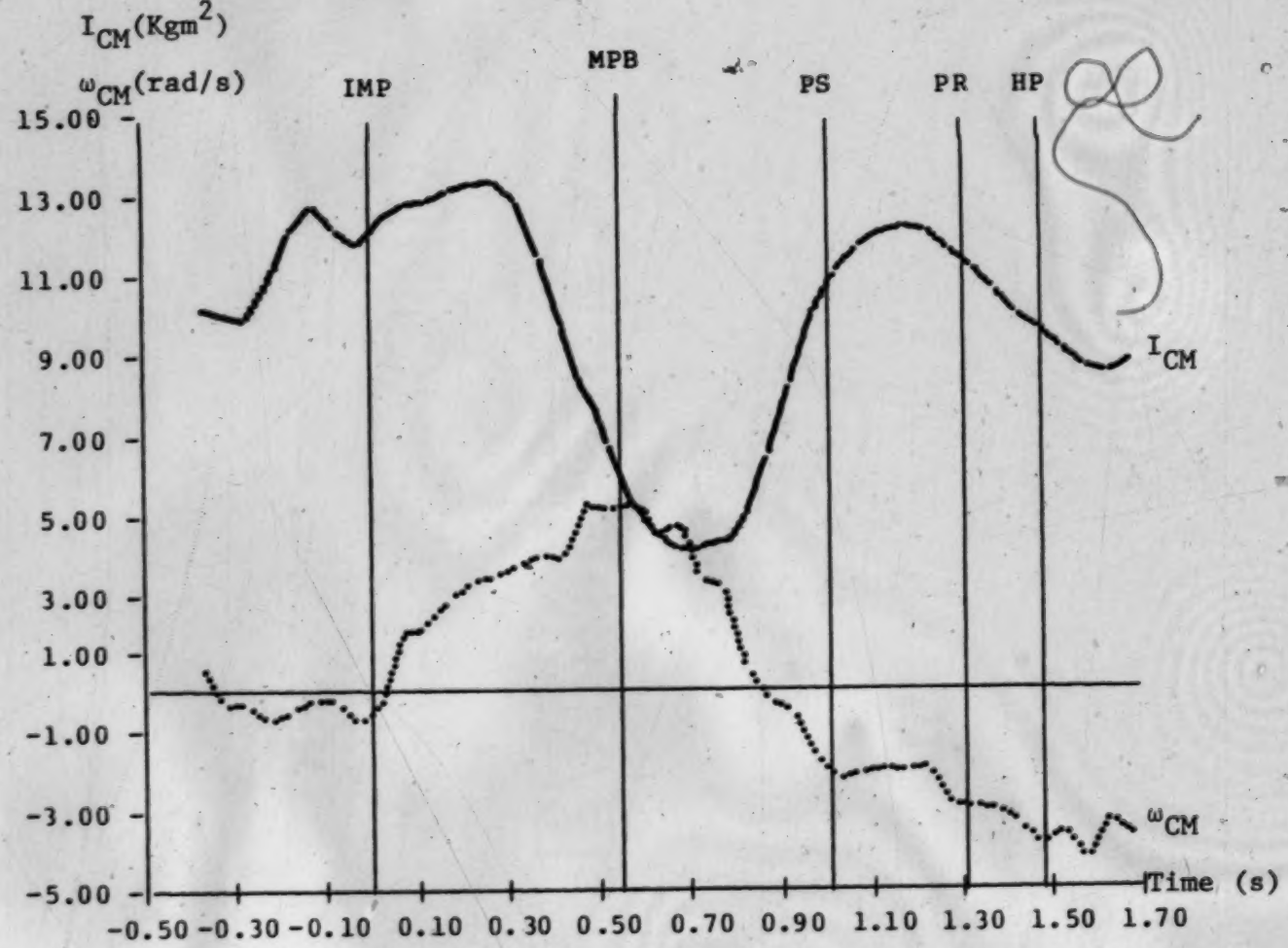

FIGURE 13

MOMENT OF INERTIA (I_{CM}) AND ANGULAR VELOCITY (ω_{CM})

ABOUT THE CENTER OF MASS

as indicated by the smallest moment of inertia value (3.5 Kgm^2), 0.11 seconds after the pole was maximally bent. From this instant on, and until after the pole was released (PR at t=1.31s), an increase in the moment of inertia to 12.1 Kgm^2, which was indicative of full body extension, was observed.

The angular velocity (ω_{CM}) increased from values close to zero radians per second to a relative maximum of 5.3 rad/s between 0.475 and 0.575 seconds (MPB). During the pole uncoiling phase ω_{CM} decreased, reversing to a clockwise rotation at t = 0.85 seconds. Following pole release, the angular velocity about the vaulter's center of mass varied between 3.0 and 4.4 rad/s (clockwise). The reversal of the direction of rotation was caused by gravity. From the time when the pole was straight until the vaulter released the pole the center of mass was not in line with the axis of rotation (the top hand). This caused an early dropping of the legs and resulted in a push-off angle of 127^{o} to the vertical.

The total angular momentum, comprised of the transfer and local terms, showed an increase to a maximum of 48 Kgm^2/s at t = 0.325 seconds followed by a decrease to -25 Kgm^2/s at the instant when the pole was straight. After pole release the angular momentum varied between -28 and -38 Kgm^2/s with a mean of 34 Kgm^2/s and a standard deviation of 3.2.

Comparison of Cinematographic Data to Criterion Direct Force Measurements

In the following section the results of the comparison between data derived from biomechanics cinematography procedures and criterion data obtained from direct force measurements in the vaulting box are reported. Table III summarizes the values of the predicted horizontal

TABLE III

COMPARISON OF HORIZONTAL IMPULSE AS COMPUTED FROM CRITERION FORCE MEASUREMENTS AND BIOMECHANICS CINEMATOGRAPHY

TIME (s)	$\Delta M_{(T)}$ (Ns)	I_h+S (Ns)	E_a (Ns)	E_r %	I_h (Ns)	E_a (Ns)	E_r %
0.05	60	68	8	-11.8	43	-17	39.5
0.10	120	112	-8	7.1	87	-33	37.9
0.15	151	158	7	-4.4	133	-18	13.5
0.20	229	205	-24	11.7	180	-49	27.2
0.25	258	252	-6	2.4	227	-31	13.7
0.30	308	306	-2	0.7	281	-27	9.6
0.35	350	357	7	-2.0	332	-18	5.4
0.40	371	394	23	-5.8	369	-2	0.5
0.45	396	422	26	-6.2	397	1	-0.2
0.50	415	438	23	-5.3	413	-2	0.5
0.55	429	444	15	-3.4	419	-10	2.4
0.60	414	446	32	-7.2	421	7	-1.7
0.65	442	450	8	-1.8	425	-17	4.0
0.70	440	455	15	-3.3	430	-10	2.3
0.75	437	455	18	-4.0	430	-7	1.6
0.80	439	459	20	-4.4	434	-5	1.5
0.85	428	460	32	-7.0	435	7	-1.6
MEAN:			16.1 $\bar{E}_a$	5.2 $\bar{E}_r$		15.4 $\bar{E}_a$	9.5 $\bar{E}_r$

LEGEND: E_a, E_r = absolute and relative error of the cinematographic data;

$\Delta M_{(T)}$ = change in horizontal momentum from time t=0.0s to t as determined from biomechanics cinematography;

I_h = horizontal impulse measured in the vaulting box;

I_h+S = I_h plus the estimated striking impulse of 24.5 Ns.

impulses ($\Delta M_{(T)}$) and the impulses derived from the force measurements with and without consideration of the initial estimated horizontal striking impulse. When the horizontal striking impulse was omitted, the mean absolute difference was 15.4 Ns with a range of -47 to +7 Ns. This corresponded to an average relative error of 9.5%. Adding the estimated horizontal striking impulse of 24.5 Ns yielded an average absolute difference of 16.4 Ns (-24 to +32 Ns); this corresponded to an average relative error of 5.2%. Negative values for the differences in Table III indicate that the measured impulse is smaller than the change in momentum computed through biomechanics cinematography procedures. Figure 14 is a graphical representation of the comparison between predicted and measured impulses. Figure 15 illustrates the influence of the rotational component of the total momentum on the predicted impulse.

Consideration of the striking impulse results in an overall smaller relative error of 5.4% as compared to 9.5%. However the mean absolute error is slightly greater (16.1 as compared to 15.4 Ns). This reflects the fact, that, in the case of the calculations considering the horizontal striking impulse, the larger absolute differences are found in the last part of the considered time interval.

Figures 16 and 17 represent the absolute and relative differences between predicted and measured impulse values. The data suggest that consideration of the striking impulse results in a better approximation for the time interval t = 0.0 to t = 0.3 seconds. Throughout the remainder of the vault the measured impulse minus the estimated horizontal striking impulse differed less from the predicted impulse. This indicates that the initial striking impulse was absorbed through internal friction 0.3 seconds after the pole contacted the vaulting box.

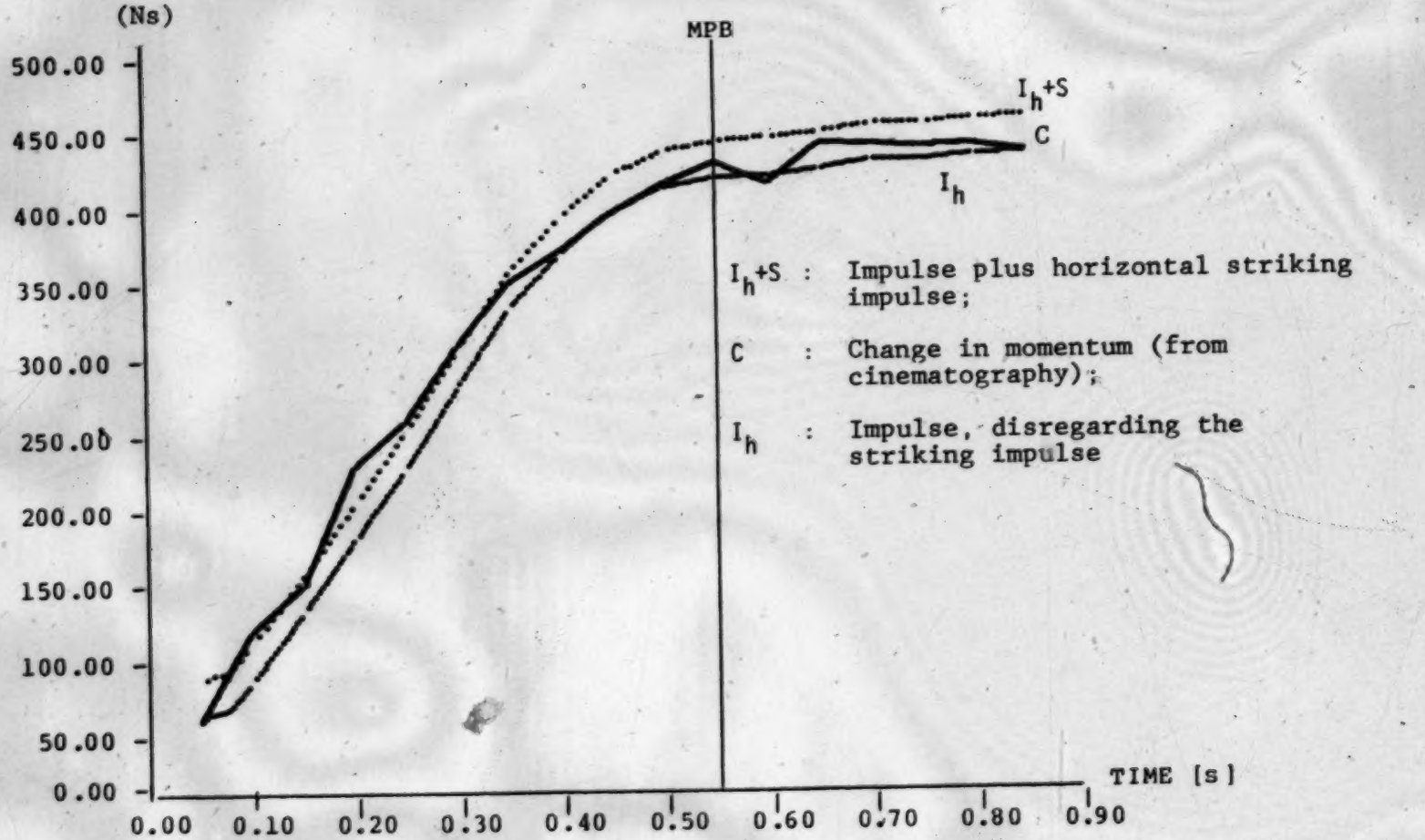

FIGURE 14

COMPARISON OF THE CHANGE IN MOMENTUM OBTAINED FROM BIOMECHANICS CINEMATOGRAPHY AND HORIZONTAL IMPULSE MEASURED IN THE VAULTING BOX

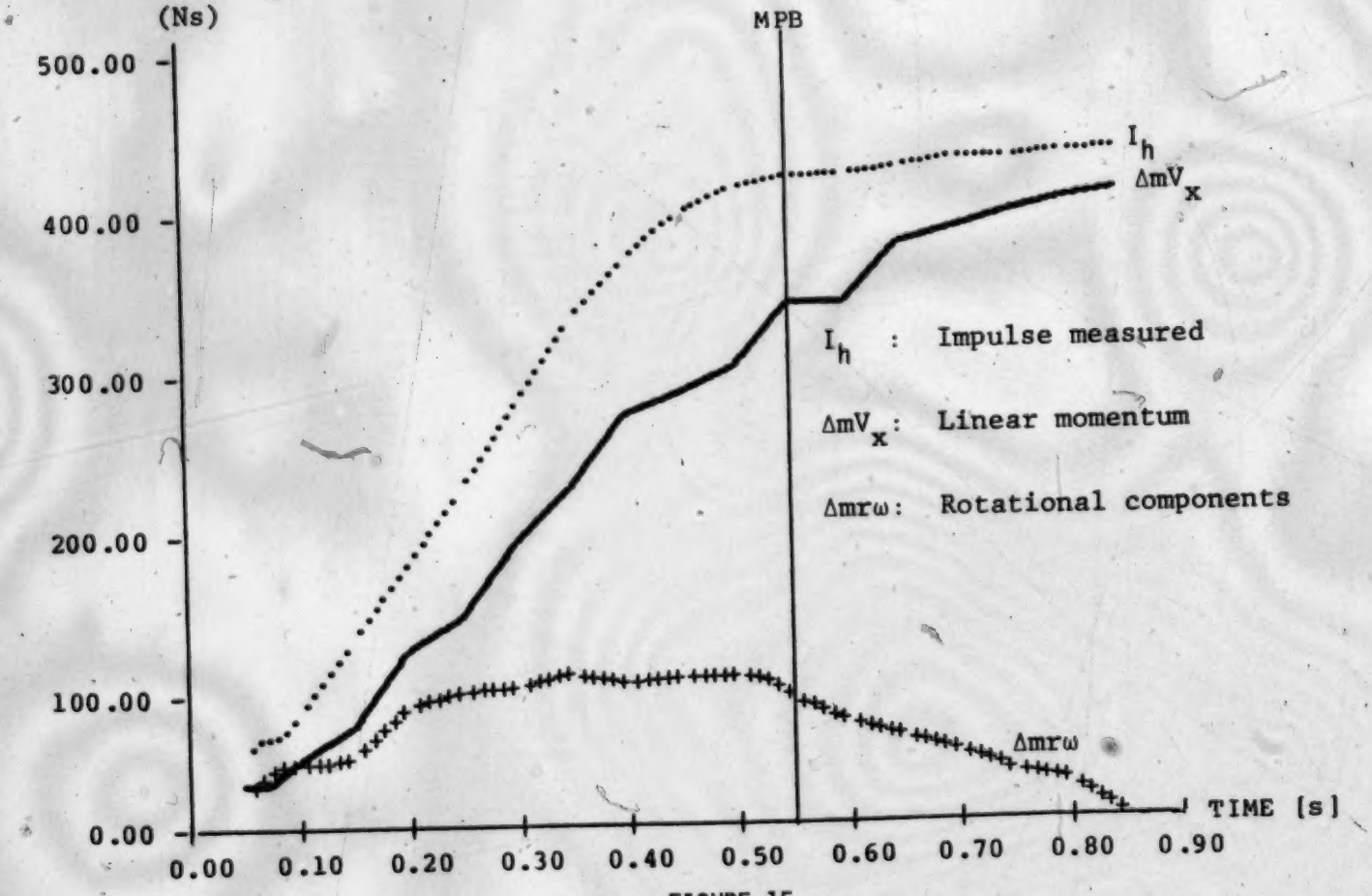

FIGURE 15

INFLUENCE OF THE ROTATIONAL COMPONENT ON THE PREDICTED CHANGE IN MOMENTUM

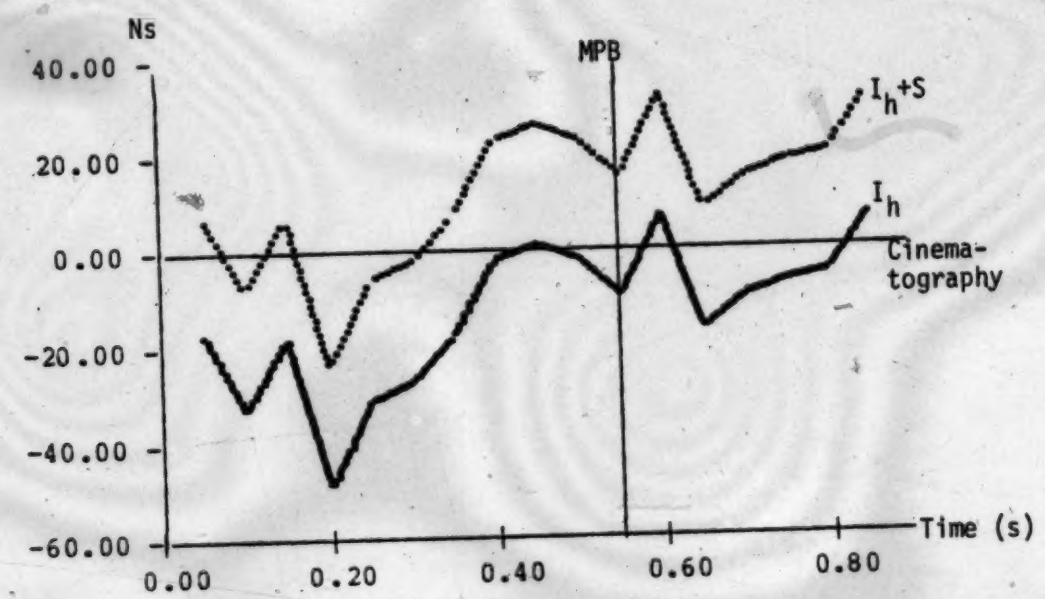

FIGURE 16

ABSOLUTE DIFFERENCE OF CHANGES IN MOMENTUM OBTAINED FROM BIOMECHANICS CINEMATOGRAPHY AND HORIZONTAL IMPULSE MEASURED IN THE VAULTING BOX

(I_h, I_h+S = horizontal impulse and impulse plus estimated striking impulse)

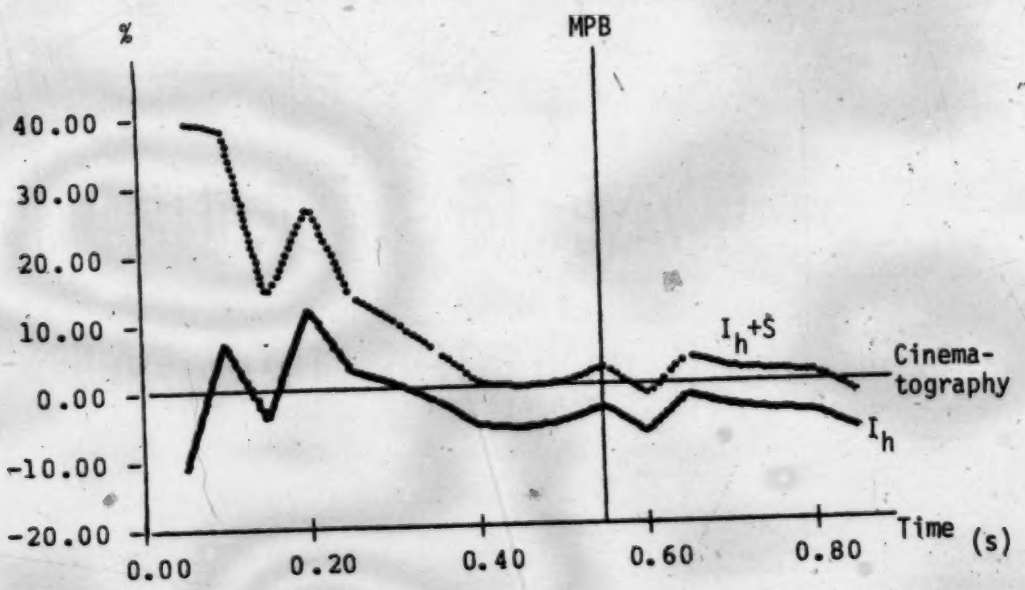

FIGURE 17

RELATIVE DIFFERENCE OF CHANGES IN MOMENTUM OBTAINED FROM BIOMECHANICS CINEMATOGRAPHY AND HORIZONTAL IMPULSE MEASURED IN THE VAULTING BOX

Vertical impulse and predicted change in vertical momentum were compared over the time interval when the vertical force measured exceeded the body weight of the athlete, namely over the interval t = 0.6 to t = 1.0 seconds. Table IV summarizes the results. The computed predicted and measured impulses are plotted in Figure 18; a graphical representation of the relative and absolute differences is given in Figure 19. The mean absolute error of 12.1 Ns, with a range from -3 to +36 Ns, compares favourably with the corresponding error of the predicted horizontal impulse. However, the relative error is considerably larger with a mean of 16.9% due to the smaller absolute values of the considered impulses.

Measurement Error

The static response of the vertical force transducer was tested before, during and after the experiment by recording the weight of the subject hanging on the pole. The measured force of 835 N, in the range 829-838 N, was within 1% of the actual weight of the subject plus pole. The determination of the impact force at t=0.0 seconds had an uncertainty of 200 N or 4.7% of the resultant force. This was caused by the large magnitude (4.2 KN) and short duration ($\Delta t < 0.2s$) of the impact force which caused movement of the analog display during the exposure time of 1/2400s. An indication of the measurement accuracy of the horizontal and vertical force components with respect to each other was obtained from the following computations: At impact the angle of the pole with respect to the horizontal, as determined from cinematography, was 30^{o}. The simultaneously recorded horizontal and vertical force components in the vaulting box were 3734 N and 2021 N respectively. The angle of

TABLE IV

COMPARISON OF VERTICAL IMPULSE AS MEASURED WITH BIOMECHANICS CINEMATOGRAPHY AND FORCE TRANSDUCER

$t_{(sec)}$	ΔmV_y (Ns)	I_v (Ns)	E_a (Ns)	E_r %
0.65	13	10	-3	30.0
0.70	25	24	-1	4.2
0.75	35	43	8	-18.6
0.80	58	67	9	-13.4
0.85	80	89	9	-10.1
0.90	91	108	17	-15.7
0.95	80	116	36	-31.0
1.00	102	116	14	-12.1
MEAN			$\overline{E}_a$=12.1	$\overline{E}_r$=16.9

LEGEND:

ΔmV_y = change in vertical momentum from time t=0.6 seconds to t;

I_v = vertical impulse measured in the vaulting box;

E_a, E_r = absolute and relative errors respectively.

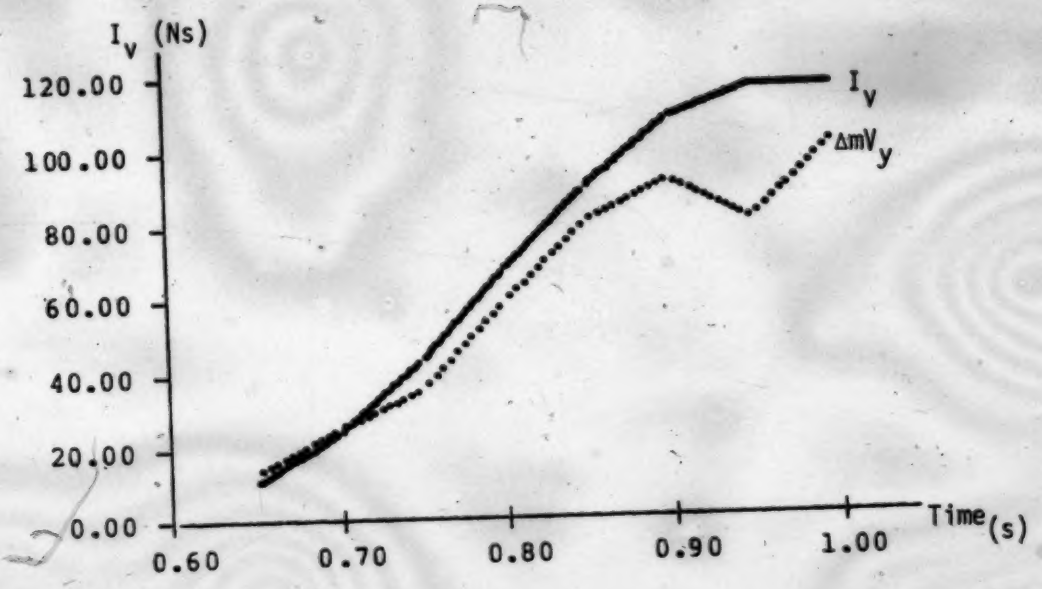

FIGURE 18

COMPARISON OF THE CHANGE IN VERTICAL MOMENTUM OBTAINED FROM BIOMECHANICS CINEMATOGRAPHY AND VERTICAL IMPULSE MEASURED IN THE VAULTING BOX (I_v)

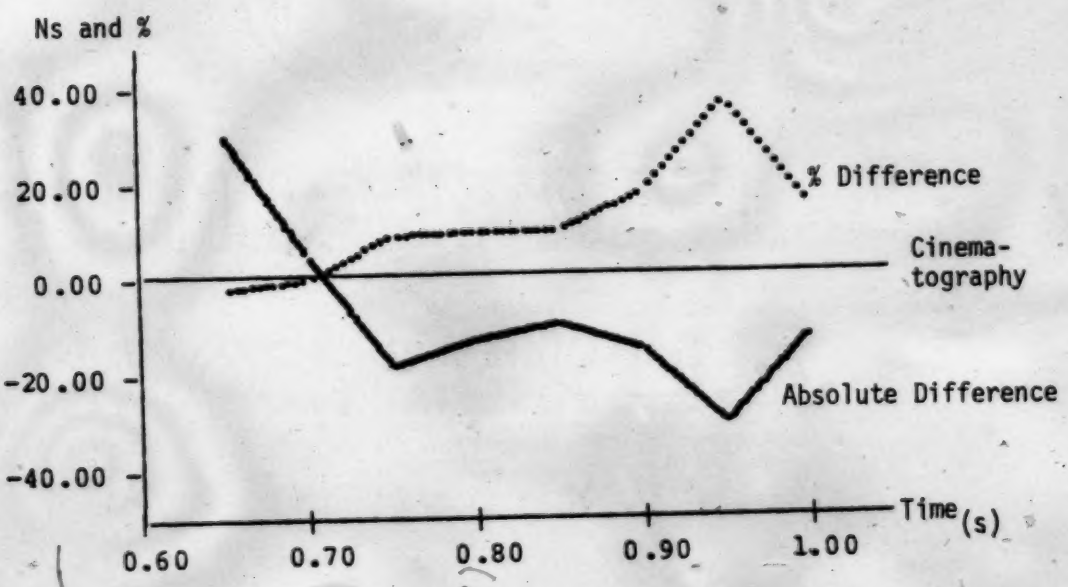

FIGURE 19

ABSOLUTE AND RELATIVE DIFFERENCE BETWEEN FORCE PLATE MEASURED VERTICAL IMPULSE AND CHANGE IN VERTICAL MOMENTUM OBTAINED FROM BIOMECHANICS CINEMATOGRAPHY

the resultant force vector was thus 28.4° to the horizontal. The difference between the direction of the force vector and the long axis of the pole was 1.6° (5.3%). Throughout the remainder of the vault the maximum absolute error associated with the resolution limit, as assessed from repeated measures, did not exceed ±2.5 N. The relative error introduced through the process of converting the analog signal to digital values representing the measured instantaneous forces was a function of the absolute magnitude of the forces. The maximum relative error comprised the measurement error of the transducer (±1%) and the error introduced through the resolution limit of the force data analysis. The maximum relative error exceeded ±5% for forces smaller than 28 N and remained within ±2% for forces greater than 250 N.

The accuracy of the computed horizontal, vertical and linear impulses depended on the magnitude of the absolute force value, the accuracy of the timing light generator (±0.01%) and the numerical integration of the force-time data. The error factor for solutions, computed by the cubic spline program used to obtain the integral, was given as t^4 where t stands for the time interval over which the integration was performed. In the present study this time interval was kept at 0.01 seconds for all force measurements. The error incurred when computing the horizontal striking impulse was influenced by the uncertainty of the force measurements at times t=0.0s and t=0.01s. Furthermore, the sampling rate of 100 Hz was found to be insufficient to determine the precise time interval over which the initial impact occurred. At impact the horizontal force component was 3734 N. The next sampled value (t=0.01s) was 1170 N. The horizontal striking impulse was estimated by assuming a triangular peak on a rectangular base.

For the analysis of the subject film the researcher's precision was operationally defined as the ability to reproduce the coordinates of proximal and distal segmental endpoints. All errors are reported in life size units. Reproducability was checked during the actual analysis by digitizing frames #20 and #39 two times. The maximum error was found to be ±2.3 cm. The mean error was: $\bar{E}_a$ = ±0.65 cm. Since the procedure to compute the total CM of the body tended to average and thereby reduce the effects of random error in the single digitized input point, the X and Y coordinates of the centers of mass in the selected frames were reproduced well within ±1.0 cm (Table V). The effect of smoothing the data through first differences and the cubic spline function was assessed by integrating smoothed velocity-time curves and comparing the results to the raw displacement data of the center of mass. Over the entire vault the difference was less than 1% (Table VI). For time intervals of 0.2 seconds the maximum absolute error in the predicted horizontal displacement was 5.0 cm; the maximum relative error was 8.3% (Table VII). The mean absolute error was 1.4 cm, the mean relative error was 4%.

Discussion

The main findings of the present study are discussed in two parts: the first part deals with the comparison between biomechanics cinematography data and the criterion force (impulse) measurements in the vaulting box, in the second part selected parameters that are relevant for the pole vaulting performance are discussed.

The present study is, to the researcher's knowledge, the first

TABLE V

COMPARISON OF REPEATED MEASUREMENTS AND RESULTING

X,Y COORDINATES OF THE CM (m)

Frame	Measurement 1		Measurement 2		Absolute Difference	
	$X_{CM\ 1}$	$Y_{CM\ 1}$	$X_{CM\ 2}$	$Y_{CM\ 2}$	ΔX_{CM}	ΔY_{CM}
F 20	6.7003	2.2686	6.6931	2.2723	0.0073	0.0036
F 39	8.5313	4.6619	8.5222	4.6556	0.0091	0.0064

TABLE VI

COMPARISON OF INTEGRATED HORIZONTAL AND VERTICAL VELOCITIES OF THE CM

AND RAW DATA X,Y DISPLACEMENTS OF THE CM

OVER THE ENTIRE PERFORMANCE

Initial CM Coordinates	Final CM Coordinates	CM Displacement	Integrated CM Velocities	Absolute Error (m)	% Error
$X_{CM\ 1}$	$X_{CM\ 43}$	ΔX_{CM}	$\int \tilde{V}_x\ (dt)$	$\int \tilde{V}_x\ (dt) - \Delta X_{CM}$	
1.07	8.9	7.83	7.77	0.06	0.77
$Y_{CM\ 1}$	$Y_{CM\ 43}$	ΔY_{CM}	$\int \tilde{V}_y\ (dt)$	$\int \tilde{V}_y\ (dt) - Y_{CM}$	
1.05	4.48	3.43	3.46	0.03	0.87

TABLE VII

COMPARISON OF INTEGRATED HORIZONTAL VELOCITIES AND RAW DISPLACEMENT DATA OF THE CM OVER 2 FRAME INTERVALS (m)

Frame	$\int \tilde{V}_x$ (dt)	dx	$\int \tilde{V}_x$ (dt)-dx
1			
	0.77	0.78	-0.01
3			
	0.79	0.78	0.01
5			
	0.79	0.82	-0.03
7			
	1.08	1.03	0.05*
10			
	0.61	0.60	0.01
12			
	0.52	0.53	-0.01
14			
	0.46	0.43	0.03
16			
	0.37	0.35	0.02
18			
	0.29	0.30	-0.01
20			
	0.24	0.26	-0.02+
22			
	0.21	0.20	0.01
24			
	0.18	0.19	-0.01
26			
	0.20	0.19	0.01
28			
	0.18	0.17	0.01
30			
	0.17	0.17	0.00
32			
	0.18	0.17	0.01
34			
	0.18	0.19	-0.01
36			
	0.19	0.19	0.00
38			
	0.19	0.20	-0.01
40			
	0.20	0.19	0.01
42			

LEGEND:

$\int \tilde{V}_x$(dt) = integrated, smoothed velocity-time data between frames x and x+1;

ds = raw data displacement over the same time interval;

*,+ = maximum absolute (*) and relative (+) errors.

attempt to match data from two independent measurement systems to determine the validity of biomechanics cinematography data collection and analysis procedures through a comparison to direct force measurements in the pole vaulting event. In light of the fact that the changes of momentum of the pole vaulter throughout the vault must be derived through a number of error magnifying computations, the total absolute and relative errors incurred in this study are acceptable to the researcher. On the basis of the reported results and within the limitations of this study it can be stated that careful adherence to the procedures of biomechanics cinematography results in data that compare very well to the criterion force (impulse) measurements. Highly developed data acquisition and analysis instrumentation in biomechanics cinematography enable the researcher to gather comprehensive and relevant data through a non-invasive method in competitive situations. However, biomechanics cinematography procedures are susceptible to various errors which can easily increase to unacceptable orders of magnitude when parameters are derived through single or double differentiation of displacement data. Therefore independent simultaneous measurements of relevant parameters such as forces or accelerations are valuable as an outside criterion to assess the accuracy of the cinematographic analysis.

The stated limitations and delimitations of the present study do not warrant the formulation of generalized statements about the pole vaulting event on different levels of performance. The researcher rather tries to point out how relevant information may be extracted from the presented data.

The initial kinetic energy at take-off, the efficient utilisation of the energy and the work done by the vaulter are important

parameters for a successful vault. For the analysed vault the initial kinetic energy was 2444 J. This value compares unfavourably to the 3240 J measured in a competitive vault (5.5 m) of the same subject and must be considered as a partial explanation for the difference in the achieved height. Dillman (1968) operationally defined two variables that are used as indicators for efficient energy utilisation. The 'predicted height' is the vertical rise of the center of mass based on the assumption that the kinetic energy at take-off is completely converted to potential energy. The 'adjusted predicted height' accounts for the final kinetic energy at the instant when the vaulter has reached the peak of his flight curve. Efficient use of initially available energy thus means that the vaulter must keep the difference between the total energy and the gravitational potential energy at the high point small. This is achieved by reducing the kinetic energy at this time to the smallest possible value required for bar clearance. Data reported by Dillman (1968) and the analysis of a world record performance by the author (Gros, 1981) suggest that a horizontal velocity of approximately 1 m/s is sufficient for bar clearance. In the analysed vault the athlete had a final kinetic energy of 220 J. This is equivalent to a 0.27 m vertical displacement. The subject could gain 0.21 m in height through more efficient energy utilisation. The net work done by the vaulter can be estimated by subtracting the total initial kinetic energy from the total final energy of the system. The net work done by the vaulter in the specific vault under investigation was 621 J which is equivalent to a vertical rise of the center of mass of 0.76 m. All three parameters, the initial kinetic energy, the efficient energy utilisation and the work done by the vaulter combined can be used to evaluate a

vault and detect factors that limit the performance.

The angular momentum of the vaulter about the center of mass and its components, namely moment of inertia and angular velocity, are indicative of the vaulter's behaviour on the pole. Changes in body configuration such as extension or tuck as well as the result of those movements become transparant. In the analysed vault the moment of inertia versus time graph clearly shows the hang phase, the shortening of the pendulum where the upper hand is considered to be the axis of rotation and the body tuck or rock-back position. Since angular momentum data has not been reported in the literature to date, a comparison to other vaults is not possible. The subject of the present study does not reach a fully inverted position which could be caused by a late or insufficient decrease of the moment of inertia, or too early leg extension into the J position after rock-back. The center of mass is not directly in line with the axis of rotation. Thus the legs and upper body drop which finds its ultimate expression in a very low push-off angle of 127 degrees. Bergemann (1978) reported values of 132^{o}, 165^{o} and 164^{o}. The subject of the present study reached 145^{o} in a competitive vault (5.5 m), 150^{o} was measured in a 5.7 m vault (Gros, 1981).

CHAPTER V

SUMMARY AND RECOMMENDATIONS

The purpose of the present study was to investigate the relationship between kinematic and kinetic parameters of the pole vault event determined from biomechanics cinematography procedures and direct measurements of horizontal and vertical force components in the vaulting box. Simultaneous cinematographic records of the movements of the vaulter in the sagittal plane and the analog force signal from two piezoelectric force transducers, integrated in the force summing device in the vaulting box, were obtained. The film of the vaulting performance was used to compute the horizontal, vertical and linear velocities of the vaulter's center of mass, the translational, rotational kinetic and gravitational potential energy and the linear and angular momentum throughout the vault The horizontal, vertical and resultant force components were numerically integrated with respect to time. The resulting horizontal impulse was compared to the change in momentum of the vaulter from the time of impact to the time when the application of the horizontal force ceased. The vertical impulse was compared to the change in vertical momentum over that time interval, where the recorded vertical force exceeded the body weight of the athlete.

When the initial striking impulse was considered, the mean difference between horizontal impulse predicted from biomechanics cine-

matography and the horizontal impulse measured in the vaulting box was 16.1 Ns (5.2%). Omitting the horizontal striking impulse yielded an absolute difference of 15.4 Ns (9.5%). The average deviation for the predicted vertical impulse was 12.1 Ns (16.9%). Within the limitations of the study it was concluded that the use of sophisticated biomechanics cinematography data collection and analysis procedures is a viable and accurate tool for the determination of the parameters discussed in the present study.

The following recommendations are made:

(1) Acknowledging the potential sources of error inherent in cinematographic analysis it may be desirable to employ alternative methods of data collection whenever feasible to check the accuracy of the analysis and, in certain cases, to provide information that cannot be obtained through biomechanics cinematography.

(2) Replication of the present study on a number of vaulters and vaults would assess whether the methods and procedures employed are susceptible to variations in these parameters.

(3) The computational procedures used for the cinematographical analysis of the performance should be applied to several vaults in order to identify characteristics of successful performances and interpret these for coaches and athletes.

BIBLIOGRAPHY

Ariel, G. "The Contribution of the Pole to the Vault." Paper presented at the International Sport Scientific Congress, Munich, 1972.

Ballreich, R. "Eine Mechanische Betrachtung des Stabhochsprungs." Die Lehre der Leichtathletik (1962), 41, pp. 995-98.

Barlow, D.A. Kinematic and Kinetic Factors Involved in Pole Vaulting. Ph.D. Thesis, Indiana University, 1973.

Barlow, D.A. "Kinematic and Kinetic Factors Involved in Pole Vaulting". Track and Field Quarterly Review 79 (1979) 1, pp. 19-21.

Bartholomew, S.K. A Mechanical Analysis of Selected Differentials Between Maximal - and Submaximal - Ability Pole Vaulters. MS Thesis, Washington State University, 1967.

Beckwith, Buck. Mechanical Measurements. Addison-Wesley, 1973.

Bergemann, B.W. "Contribution of Research to the Pole Vault". In: Science in Athletics, J. Terauds (Ed.), Academic Publishers, Del Mar, California, 1978.

Bowers, W. "Review of Modern Pole Vaulting". Track Technique 39 (1970), pp. 1233-34.

Bush, J., Weiskopf, R. "The Pole Vault". The Athletic Journal Vol. 59, #8 (1979), pp. 32-39 and 67-71.

Change, N.D. General Guide to ICP Instrumentation PCB Piezotronics, Buffalo, New York.

Cramer, John. "Fiberglass Pole Vaulting by the Champions", Part 1, Individual Differences. Scholastic Coach Vol. 38, #5 (1969), pp. 14-16 and 74-76.

Cramer, John. "Fiberglass Pole Vaulting by the Champions", Part 2, Techniques. Scholastic Coach Vol 38, #6 (1969), pp. 14-16 and 63-67.

Dapena, Jesus. "A Method to Determine the Angular Momentum of a Human Body about Three Orthogonal Axes Passing Through its Center of Gravity". Journal of Biomechanics Vol. 11 (1978), pp. 251-256.

Diffrient, N. et. al. Humanscale The MIT Press, Cambridge, Massachusetts, 1974.

Dillman, Charles J. Energy Transformations During the Pole Vault with a Fiberglass Pole. MSc. Penn. State, 1966.

Dillman, J.D., Nelson, R.C. "The Mechanical Energy Transformations of Pole Vaulting with a Fiberglass Pole". Journal of Biomechanics Vol. 1 (1978), pp. 175-183.

Ecker, Tom. "The Fiberglass Vault". The Athletic Journal Vol. 45, #8 (1965), pp. 30-33.

Ecker, Tom. "No More Guessing in Fiberglass Vaulting". The Athletic Journal Vol. 45, #7 (1968), p. 36 and 81.

Ecker, Tom. "The 20-Foot Vault is Coming". The Athletic Journal Vol. 51, #6 (1971), pp. 22-23, 60.

Elliott, G.M. "Vaulting with Flexible Poles". Track Technique #26 (1966), pp. 808-810.

Ganslen, Richard V. Mechanics of the Pole Vault. John Swift and Co., St. Louis, No. (1970).

Ganslen, R.V. "Evolution of Modern Vaulting". The Athletic Journal Vol. 51, #7 (1971), pp. 102-113 and 133-138.

General Utilities Routines, Hewlett Packard Part #09825-10001 Revision E.

Greville, T.N.E. (Ed.) Theory and Applications of Spline Functions. Academic Press, N.Y., London (1969), pp. 156-167.

Gros, H.J. "Computerized Analysis of Two World Class Pole Vault Performances" Lab Report, Biomechanics Laboratory, The University of Alberta, March 1981.

Hay, J.G. "Pole Vaulting: A Mechanical Analysis of Factors Influencing Pole-Bend". The Research Quarterly Vol. 38, #1, pp. 34-40.

Hay, J.G. "Mechanical Energy in Pole Vaulting". Track Technique, #38 (1968), pp. 1047-51.

Hay. J.G. "Moment of Inertia of the Human Body". Kinesiology IV, pp. 43-52.

Hay, James G. "Advantages of Fiberglass Poles". Track Technique, #24 (1966), pp. 756-57.

Hay. J.G., Wilson, B.D. "A Computational Technique to Determine the Angular Displacement, Velocity and Momentum of a Human Body". Paper presented at the 22nd Annual ACSM Meeting, New Orleans, Louisiana, May, 1975.

Hoke, R.J. "Development of Fiberglass Vaulting Technique". Track Technique, #42 (1970), pp. 1344-45.

Hopper, B.J. "Rotation - A Vital Factor in Athletic Technique". Track Technique, #14 (1964), pp. 430-33.

Housden, F. "An Approach to Analysis of Fiberglass Pole Vaulting". Track Technique, #13 (1963), pp. 398-99.

Jagodin, V., Maljutin, A. "Pole Vault Run-Up". Modern Athlete and Coach, #14 (1976) 5.6, pp. 42-43.

Jarver, J. "Fiberglass Vaulting Mechanics". Track Technique, #47 (1972), pp. 1483-86.

Jeitner, G. "Fiberglass Vaulting Technique". Track Technique, #19 (1965), pp. 598-99.

Jeitner, G. "Pole Vault Technique". Track Technique, #28 (1967), pp. 886-892.

Kaufmann, D.A. "A Biomechanical Block Diagram of the Pole Vault". Track Technique, #54 (1973), pp. 1732-34.

Keller, P. Biomechanische Untersuchungen im Stabhochsprung, Diplomarbeit ETH Zurich, 1974.

Kruber/Lehnhartz. Der Stabhochsprung. Bartels and Wernitz, (1972), 1.

Letters Re: The Curved Vaulting Pole. Track Technique, #59 (1975), pp. 1892-93.

Lindner, E. "Vaulting with the Fiberglass Pole". Track Technique, #23 (1966), pp. 716-19.

Mansvetov, V. "Contemporary Technique in the Pole Vault". Track and Field Quarterly Review 79 (1979) 1, p. 14. Table of temporal parameters.

Moore, G. "Analysis of the Take-off in Fiberglass Vaulting". In: Science in Athletics, Juris Terauds (Ed.), Academic Publishers, Del Mar, California (1978), p. 111.

Moore, Neil E. "Variables in Pole Vaulting". Track and Field Quarterly Review Vol. 79 (1979) 1. pp. 3-6.

Musgrove, D. "An Overview of the Fiberglass Pole". Modern Athlete and Coach #16 (1978), pp. 37-38.

Oakley, C.O. The Calculus. Barnes and Noble, New York, 1957.

Pikulsky, T. "Fiberglass Pole Vaulting". The Athletic Journal, #44 (1964), p. 16, 18, 92-93.

Ralston, Wilf. Mathematical Methods for Digital Computers, Vol. II, John Wiley and Sons, New York, (1967), pp. 156-158.

Rohrbough, J. "Approach Velocity in Pole Vaulting". Track Technique, #52 (1973), pp. 1663-65.

Simonyi, G. "Vertical Carry in Pole Vaulting". Track Technique, #39 (1970), pp. 1235-37.

Smith, A.J. "The Kinetic Energy of the Human Body". Journal of Human Movement Studies, Vol. 1, #1 (1975).

Steben, R.E. "A Cinematographic Study of Selective Factors in the Pole Vault". The Research Quarterly, Vol. 41, #1, pp. 95-104.

Stepp, R.D. "An Orderly Approach to the Mechanics of the Pole Vault". Modern Athlete and Coach, #15 (2), (1977), pp. 13-17.

Vernon, J.B. "Mathematical Estimation of an Athlete's Pole Vaulting Potential". Track and Field Quarterly, #7A (1974), pp. 165-76.

Vernon, J.B. "Curved Vaulting Pole". Track and Field Quarterly, #74 (1974), pp. 177-79.

Vernon, J.B. "How To Make a Crooked Vaulting Pole". Track Technique, #67 (1977), pp. 2140-43.

Walker, H.S., Kirmser, P.G. "Computer Modeling of Pole Vault". Mechanics and Sports, Bluestein, J.L. (Ed.), ASME, New York, (1973), p. 131.

Whitsett, Charles E. "Some Dynamic Response Characteristics of Weightless Man". AMRL Technical Documentary Report 63-18 Wright Patterson Air Force Base, Ohio, 1963.

Willimczik, A. Grundkurs Datenerhebung 1, Limpert, Frankfurt, (1977), 1.

Wilson, B.D., Hay, J.G. "A Comparison of Three Methods for Determining the Angular Momentum of the Human Body". Paper presented to the Vth ISB Congress, Jyvaskyla, Finland, July, 1975.

Woznik, T., Geese, R. "Modell zur Bestimmung biomechanischer Einflussgroessen der Stabhochsprungleistung und zur Schaetzung ihrer Einflusshoehe". Leistungssport 10 (1980), 4, pp. 315-327.

APPENDICES

APPENDIX A

KINEMATIC DATA

Raw Data

Abbreviations:

TT	: Total time
dT	: Time interval between successive frames
XCM, YCM	: X and Y coordinates of the center of mass
Dh, Dv, DL	: Horizontal, verical and linear displacements (m)
Vh, Vv, VL	: Horizontal, vertical and linear velocities (m/s)

CENTER OF MASS [TII J4 Raw Data]

F#	TT	dT	XCM	YCM	Dh	Dv	DL	Vh	Vv	VL
1	-0.40		1.07	1.05						
		0.05			0.39	0.02	0.39	7.84	0.45	7.85
2	-0.35		1.46	1.07						
		0.05			0.40	-0.02	0.40	7.90	-0.47	7.92
3	-0.30		1.85	1.05						
		0.05			0.37	-0.01	0.37	7.48	-0.27	7.48
4	-0.25		2.23	1.03						
		0.05			0.40	0.03	0.40	8.06	0.54	8.08
5	-0.20		2.63	1.06						
		0.05			0.39	0.03	0.39	7.76	0.65	7.78
6	-0.15		3.02	1.09						
		0.05			0.43	0.02	0.43	8.62	0.30	8.62
7	-0.10		3.45	1.11						
		0.05			0.37	-0.01	0.37	7.38	-0.23	7.38
8	-0.05		3.82	1.09						
		0.05			0.33	0.10	0.35	6.67	1.99	6.96
9	0.00		4.15	1.19						
		0.05			0.33	0.14	0.36	6.60	2.86	7.20
10	0.05		4.48	1.34						
		0.05			0.30	0.10	0.32	6.09	1.97	6.41
11	0.10		4.79	1.44						
		0.05			0.30	0.11	0.31	5.93	2.11	6.30
12	0.15		5.08	1.54						
		0.05			0.27	0.08	0.29	5.46	1.63	5.70
13	0.20		5.36	1.62						
		0.05			0.25	0.11	0.27	5.00	2.14	5.43
14	0.25		5.61	1.73						
		0.05			0.24	0.08	0.25	4.78	1.66	5.06
15	0.30		5.84	1.81						
		0.05			0.20	0.08	0.22	4.01	1.63	4.33
16	0.35		6.04	1.89						
		0.05			0.19	0.08	0.21	3.88	1.69	4.23
17	0.40		6.24	1.98						
		0.05			0.15	0.11	0.19	3.08	2.11	3.73
18	0.45		6.39	2.08						
		0.05			0.17	0.09	0.19	3.46	1.75	3.88
19	0.50		6.57	2.17						
		0.05			0.13	0.10	0.16	2.63	1.92	3.26

CM [TH J4 F9 cont.]

F#	TT	dT	XCM	YCM	Dh	Dv	DL	Vh	Vv	VL
20	0.55		6.69	2.27						
		0.05			0.14	0.12	0.18	2.73	2.33	3.59
21	0.60		6.83	2.39						
		0.05			0.12	0.12	0.17	2.35	2.48	3.42
22	0.65		6.95	2.51						
		0.05			0.10	0.13	0.17	2.09	2.63	3.36
23	0.70		7.05	2.64						
		0.05			0.10	0.14	0.17	2.04	2.76	3.44
24	0.75		7.15	2.78						
		0.05			0.09	0.15	0.17	1.87	2.93	3.47
25	0.80		7.25	2.93						
		0.05			0.09	0.16	0.19	1.84	3.28	3.76
26	0.85		7.34	3.09						
		0.05			0.09	0.17	0.19	1.81	3.42	3.86
27	0.90		7.43	3.26						
		0.05			0.10	0.17	0.20	2.03	3.49	4.04
28	0.95		7.53	3.44						
		0.05			0.08	0.17	0.18	1.59	3.34	3.70
29	1.00		7.61	3.61						
		0.05			0.09	0.20	0.22	1.77	3.94	4.32
30	1.05		7.70	3.80						
		0.05			0.09	0.18	0.20	1.76	3.69	4.09
31	1.10		7.79	3.99						
		0.05			0.08	0.15	0.17	1.63	3.06	3.47
32	1.15		7.87	4.14						
		0.05			0.09	0.13	0.16	1.83	2.68	3.24
33	1.20		7.96	4.27						
		0.05			0.08	0.12	0.14	1.63	2.36	2.87
34	1.25		8.04	4.39						
		0.05			0.10	0.09	0.14	2.08	1.90	2.81
35	1.30		8.15	4.49						
		0.05			0.09	0.07	0.11	1.73	1.45	2.26
36	1.35		8.23	4.56						
		0.05			0.08	0.08	0.12	1.69	1.59	2.32
37	1.40		8.32	4.64						
		0.05			0.10	0.02	0.11	2.08	0.35	2.11
38	1.45		8.42	4.66						
		0.05			0.11	0.01	0.11	2.22	0.12	2.22

CM [TH J4 F12 cont.]

F#	TT	dT	XCM	YCM	Dh	Dv	DL	Vh	Vv	VL
39	1.50		8.52	4.66						
		0.05			0.10	-0.01	0.10	1.91	-0.23	1.92
40	1.55		8.62	4.64						
		0.05			0.10	-0.03	0.10	1.94	-0.62	2.04
41	1.60		8.71	4.61						
		0.05			0.10	-0.06	0.11	1.91	-1.12	2.22
42	1.65		8.81	4.56						
		0.05			0.09	-0.08	0.12	1.85	-1.53	2.41
43	1.70		8.90	4.48						

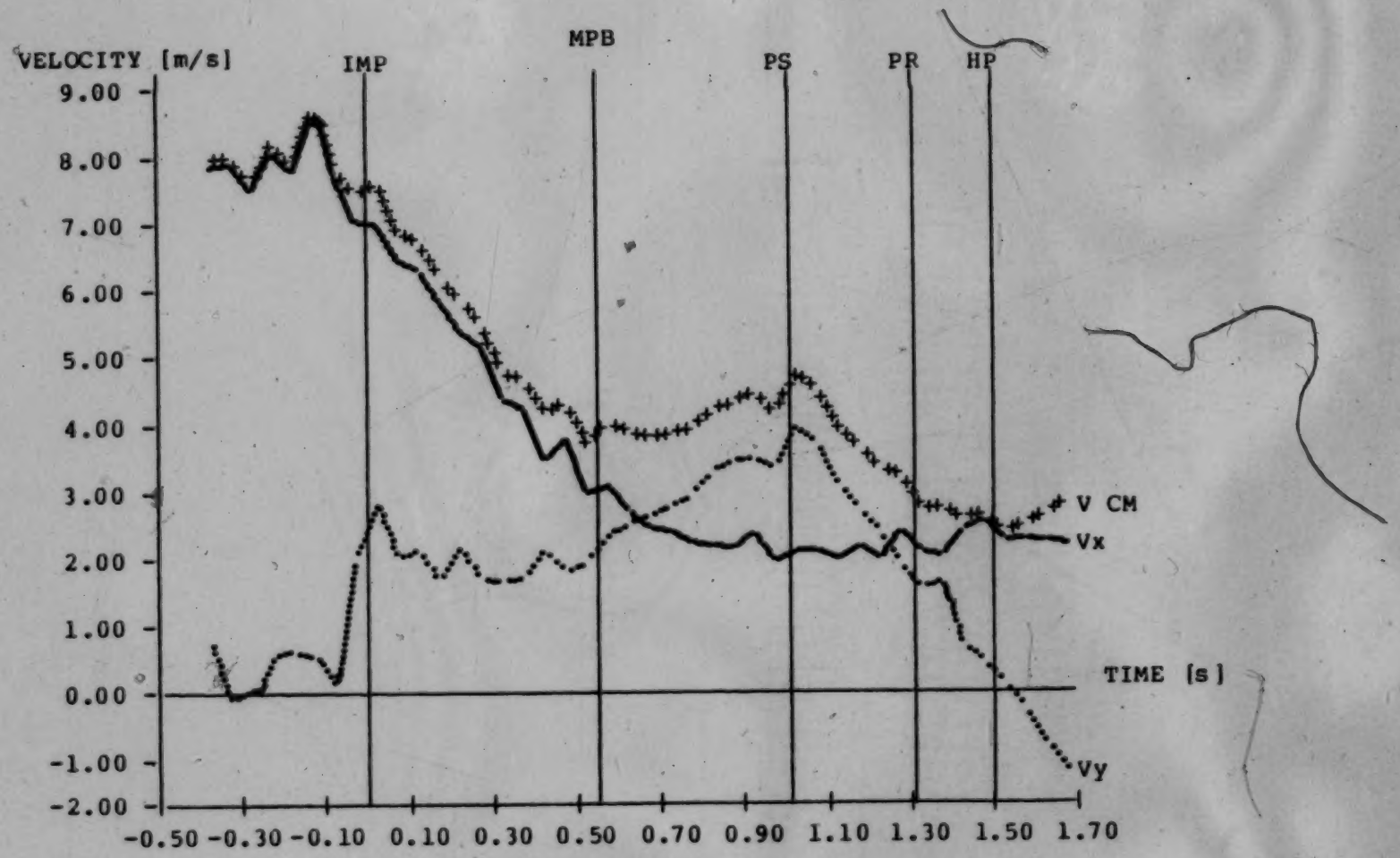

FIGURE A1

HORIZONTAL (V_x), VERTICAL (V_y) AND LINEAR (VCM)
VELOCITIES OF THE CM (RAW DATA)

Finite Differences Data Smoothing

Abbreviations:

TT	: Total time (t=0.0s at impact)
dT	: Time interval between successive frames
XCM, YCM	: X and Y coordinates of the center of mass
V1, V2	: Velocities obtained from first and second finite differences respectively
A1, A2	: Accelerations obtained from first and second finite differences respectively

DATA SMOOTHING USING 1st and 2nd DIFFERENCES

HORIZONTAL VELOCITY OF CM [TH J4 F6,9,12]

TT	dT	XCM	V1	A1	V2	A2
-0.45						
	0.05	1.07	7.80	0.00	7.80	4.00
-0.40						
	0.05	1.46	7.80	0.00	7.90	-16.00
-0.35						
	0.05	1.85	7.70	-4.00	7.67	-5.33
-0.30						
	0.05	2.23	7.80	8.00	7.75	9.00
-0.25						
	0.05	2.63	8.20	8.00	8.27	9.33
-0.20						
	0.05	3.05	8.20	-8.00	8.28	-9.00
-0.15						
	0.05	3.45	7.70	-12.00	7.73	-12.00
-0.10						
	0.05	3.82	7.00	-16.00	6.95	-17.67
-0.05						
	0.05	4.15	6.60	0.00	6.57	2.00
0.00						
	0.05	4.48	6.40	-8.00	6.43	-8.67
0.05						
	0.05	4.79	6.00	-8.00	5.98	-8.33
0.10						
	0.05	5.08	5.70	-4.00	5.72	-3.00
0.15						
	0.05	5.36	5.30	-12.00	5.32	-13.00
0.20						
	0.05	5.61	4.80	-8.00	4.80	-7.33
0.25						
	0.05	5.84	4.30	-12.00	4.27	-13.33
0.30						
	0.05	6.04	4.00	0.00	4.03	2.67
0.35						
	0.05	6.24	3.50	-20.00	3.45	-24.33
0.40						
	0.05	6.39	3.30	12.00	3.30	17.33
0.45						
	0.05	6.57	3.10	-20.00	3.15	-24.33
0.50						
	0.05	6.70	2.60	0.00	2.53	2.00
0.55						
	0.05	6.83	2.50	-4.00	2.53	-4.00

0.60						
	0.05	6.95	2.20	-8.00	2.18	-9.00
0.65						
	0.05	7.05	2.00	0.00	1.97	0.67
0.70						
	0.05	7.15	2.00	0.00	2.02	0.33
0.75						
	0.05	7.25	1.90	-4.00	1.90	-4.67
0.80						
	0.05	7.34	1.80	0.00	1.77	0.00
0.85						
	0.05	7.43	1.90	4.00	1.93	5.33
0.90						
	0.05	7.53	1.80	-8.00	1.80	-10.00
0.95						
	0.05	7.61	1.70	4.00	1.67	5.33
1.00						
	0.05	7.70	1.80	0.00	1.83	0.00
1.05						
	0.05	7.79	1.70	-4.00	1.68	-5.00
1.10						
	0.05	7.87	1.70	4.00	1.70	5.33
1.15						
	0.05	7.96	1.70	-4.00	1.67	-6.00
1.20						
	0.05	8.04	1.90	12.00	1.93	15.33
1.25						
	0.05	8.15	1.90	-12.00	1.93	-15.33
1.30						
	0.05	8.23	1.70	4.00	1.63	5.33
1.35						
	0.05	8.32	1.90	4.00	1.92	4.33
1.40						
	0.05	8.42	2.00	0.00	2.02	-0.33
1.45						
	0.05	8.52	2.00	0.00	2.02	0.33
1.50						
	0.05	8.62	1.90	-4.00	1.88	-5.00
1.55						
	0.05	8.71	1.90	4.00	1.70	-8.00
1.60						
	0.05	8.81	2.00	4.00	2.10	12.00

DATA SMOOTHING USING 1st and 2nd DIFFERENCES

VERTICAL VELOCITY OF CM [TH J4 F6,9,12]

TT	dT	YCM	V1	A1	V2	A2
-0.45						
	0.05	1.05	0.40	-16.00	0.80	-32.00
-0.40						
	0.05	1.07	0.00	-16.00	-0.40	-20.00
-0.35						
	0.05	1.05	-0.40	0.00	-0.55	-0.33
-0.30						
	0.05	1.03	0.10	20.00	0.10	23.33
-0.25						
	0.05	1.06	0.60	0.00	0.70	-1.33
-0.20						
	0.05	1.09	0.50	-4.00	0.57	-3.33
-0.15						
	0.05	1.11	0.00	-16.00	-0.22	-22.33
-0.10						
	0.05	1.09	0.80	48.00	0.65	55.67
-0.05						
	0.05	1.19	2.50	20.00	2.78	21.00
0.00						
	0.05	1.34	2.50	-20.00	2.58	-25.00
0.05						
	0.05	1.44	2.00	0.00	1.95	2.33
0.10						
	0.05	1.54	1.80	-8.00	1.75	-10.33
0.15						
	0.05	1.62	1.90	12.00	1.92	15.67
0.20						
	0.05	1.73	1.90	-12.00	1.95	-15.00
0.25						
	0.05	1.81	1.60	0.00	1.53	0.67
0.30						
	0.05	1.89	1.70	4.00	1.68	4.33
0.35						
	0.05	1.98	1.90	4.00	1.93	4.67
0.40						
	0.05	2.08	1.90	-4.00	1.90	-5.33
0.45						
	0.05	2.17	1.90	4.00	1.85	4.33
0.50						
	0.05	2.27	2.20	8.00	2.22	9.00
0.55						
	0.05	2.39	2.40	0.00	2.42	-1.00

0.60						
	0.05	2.51	2.50	4.00	2.48	4.33
0.65						
	0.05	2.64	2.70	4.00	2.70	4.00
0.70						
	0.05	2.78	2.90	4.00	2.90	4.00
0.75						
	0.05	2.93	3.10	4.00	3.10	4.00
0.80						
	0.05	3.09	3.30	4.00	3.30	4.00
0.85						
	0.05	3.26	3.50	4.00	3.53	4.67
0.90						
	0.05	3.44	3.50	-4.00	3.48	-5.67
0.95						
	0.05	3.61	3.60	8.00	3.58	9.67
1.00						
	0.05	3.80	3.80	0.00	3.90	0.67
1.05						
	0.05	3.99	3.40	-16.00	3.43	-18.00
1.10						
	0.05	4.14	2.80	-8.00	2.75	-7.67
1.15						
	0.05	4.27	2.50	-4.00	2.50	-3.33
1.20						
	0.05	4.39	2.20	-8.00	2.23	-8.00
1.25						
	0.05	4.49	1.70	-12.00	1.65	-13.67
1.30						
	0.05	4.56	1.50	4.00	1.55	7.67
1.35						
	0.05	4.64	1.00	-24.00	1.05	-27.67
1.40						
	0.05	4.66	0.20	-8.00	0.13	-6.67
1.45						
	0.05	4.66	-0.20	-8.00	-0.22	-8.33
1.50						
	0.05	4.64	-0.50	-4.00	-0.50	-3.33
1.55						
	0.05	4.61	-0.80	-8.00	-0.70	0.00
1.60						
	0.05	4.56	-1.00	-8.00	-1.20	-12.00

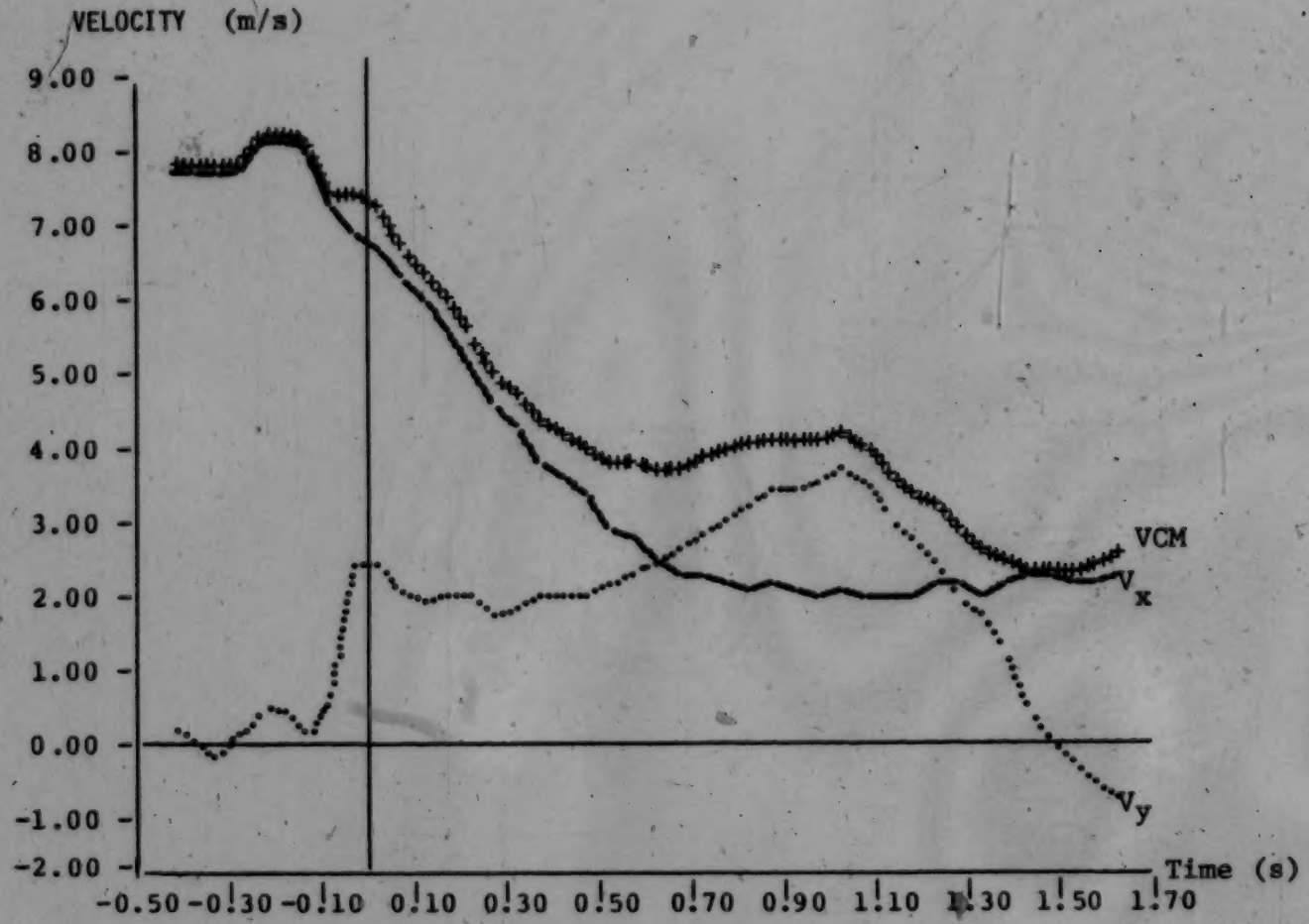

FIGURE A2

VELOCITIES OF CM OBTAINED FROM FIRST DIFFERENCES SMOOTHING

Smoothed, Interpolated and Integrated Center of Mass Velocities

---

HORIZONTAL VELOCITY OF CM [TH J4 F6,9,12 1]

OF INPUT POINTS: 21
USER DEFINED STEPSIZE: 0.0250
EPSILON: 1.00E-06

INTEGRAL -0.425 to 1.625 = 7.7669E 00

* :x = Input X
< :x < Input X < x+1

	Time	Velocity	Acceleration
*	-0.43	7.80	-2.44
	-0.40	7.74	-2.17
	-0.38	7.70	-1.36
	-0.35	7.68	-0.01
*	-0.33	7.70	1.87
	-0.30	7.77	3.43
	-0.28	7.86	3.80
	-0.25	7.95	2.97
*	-0.23	8.00	0.95
	-0.20	7.99	-1.43
	-0.18	7.93	-3.32
	-0.15	7.83	-4.73
*	-0.13	7.70	-5.66
	-0.10	7.55	-6.32
	-0.08	7.38	-6.91
	-0.05	7.21	-7.43
	-0.03	7.01	-7.89
	0.00	6.81	-8.28
*	0.03	6.60	-8.61
	0.05	6.38	-8.87
	0.08	6.16	-9.05
	0.10	5.93	-9.16
*	0.13	5.70	-9.19
	0.15	5.47	-9.15
	0.18	5.24	-9.04
	0.20	5.02	-8.87
*	0.23	4.80	-8.63
	0.25	4.59	-8.34
	0.28	4.38	-8.02
	0.30	4.19	-7.67
*	0.33	4.00	-7.29
	0.35	3.82	-6.98
	0.38	3.65	-6.87
	0.40	3.48	-6.95

	Time	Velocity	Acceleration
*	0.43	3.30	-7.23
	0.45	3.12	-7.41
	0.48	2.93	-7.24
	0.50	2.76	-6.71
*	0.53	2.60	-5.81
	0.55	2.47	-4.80
	0.58	2.36	-3.92
	0.60	2.27	-3.16
*	0.63	2.20	-2.52
	0.65	2.14	-2.07
	0.68	2.09	-1.85
	0.70	2.05	-1.85
*	0.73	2.00	-2.09
	0.75	1.94	-2.29
	0.78	1.89	-2.20
	0.80	1.84	-1.81
*	0.83	1.80	-1.12
	0.85	1.78	-0.39
	0.88	1.78	0.14
	0.90	1.79	0.46
*	0.93	1.80	0.58
	0.95	1.81	0.48
	0.98	1.82	0.15
	1.00	1.82	-0.40
*	1.03	1.80	-1.18
	1.05	1.76	-1.70
	1.08	1.72	-1.49
	1.10	1.69	-0.54
*	1.13	1.70	1.14
	1.15	1.75	2.59
	1.18	1.82	2.81
	1.20	1.88	1.82
*	1.23	1.90	-0.40
	1.25	1.86	-2.46
	1.28	1.79	-3.01
	1.30	1.72	-2.04
*	1.33	1.70	0.45
	1.35	1.75	2.96
	1.38	1.84	3.99
	1.40	1.93	3.54
*	1.43	2.00	1.61
	1.45	2.01	-0.55
	1.48	1.98	-1.68
	1.50	1.94	-1.79
*	1.53	1.90	-0.89
	1.55	1.89	0.35
	1.58	1.91	1.24
	1.60	1.95	1.77
*	1.63	2.00	1.94

VERTICAL VELOCITY OF CM [TH J4 F6,9,12 1]

OF INPUT POINTS: 21
USER DEFINED STEPSIZE: 0.0250
EPSILON: 1.00E-06

INTEGRAL -0.425 to 1.625 = 3.4631E 00

* :x = Input X
< :x < Input X < x+1

	Time	Velocity	Acceleration
*	-0.43	0.40	-14.44
	-0.40	0.05	-13.23
	-0.38	-0.24	-9.61
	-0.35	-0.41	-3.57
*	-0.33	-0.40	4.87
	-0.30	-0.18	11.87
	-0.28	0.15	13.55
	-0.25	0.45	9.90
*	-0.23	0.60	0.94
	-0.20	0.50	-7.62
	-0.18	0.27	-10.07
	-0.15	0.05	-6.42
*	-0.13	0.00	3.35
	-0.10	0.23	14.08
	-0.08	0.67	20.62
	-0.05	1.22	22.96
	-0.03	1.78	21.10
	0.00	2.24	15.06
*	0.03	2.50	4.82
	0.05	2.49	-5.11
	0.08	2.28	-10.21
	0.10	2.02	-10.50
*	0.13	1.80	-5.96
	0.15	1.73	-0.31
	0.18	1.76	2.74
	0.20	1.84	3.18
*	0.23	1.90	1.01
	0.25	1.89	-1.72
	0.28	1.83	-2.98
	0.30	1.75	-2.77
*	0.33	1.70	-1.08
	0.35	1.70	1.01
	0.38	1.75	2.44
	0.40	1.82	3.21

	Time	Velocity	Acceleration
*	0.43	1.90	3.32
	0.45	1.98	3.12
	0.48	2.06	2.97
	0.50	2.13	2.87
*	0.53	2.20	2.82
	0.55	2.27	2.84
	0.58	2.34	2.94
	0.60	2.42	3.13
*	0.63	2.50	3.40
	0.65	2.59	3.71
	0.68	2.69	4.01
	0.70	2.79	4.29
*	0.73	2.90	4.57
	0.75	3.02	4.63
	0.78	3.13	4.28
	0.80	3.23	3.51
*	0.83	3.30	2.33
	0.85	3.34	1.40
	0.88	3.38	1.39
	0.90	3.42	2.29
*	0.93	3.50	4.12
	0.95	3.62	5.33
	0.98	3.75	4.42
	1.00	3.83	1.38
*	1.03	3.80	-3.80
	1.05	3.64	-8.86
	1.08	3.38	-11.57
	1.10	3.08	-11.93
*	1.13	2.80	-9.93
	1.15	2.59	-7.21
	1.18	2.43	-5.40
	1.20	2.31	-4.49
*	1.23	2.20	-4.48
	1.25	2.08	-5.23
	1.28	1.93	-6.59
	1.30	1.74	-8.56
*	1.33	1.50	-11.14
	1.35	1.19	-13.29
	1.38	0.85	-13.97
	1.40	0.51	-13.20
*	1.43	0.20	-10.96
	1.45	-0.04	-8.36
	1.48	-0.22	-6.51
	1.50	-0.37	-5.39
*	1.53	-0.50	-5.01
	1.55	-0.63	-5.00
	1.58	-0.75	-5.00
	1.60	-0.88	-5.00
*	1.63	-1.00	-4.99

LINEAR VELOCITY OF CM [TH J4 F6,9,12 1]

OF INPUT POINTS: 21
USER DEFINED STEPSIZE: 0.0250
EPSILON: 1.00E-06

INTEGRAL -0.425 to 1.625 = 9.3077E 00

* :x = Input X
< :x < Input X < x+1

	Time	Velocity	Acceleration
*	-0.43	7.81	-2.57
	-0.40	7.75	-2.28
	-0.38	7.70	-1.39
	-0.35	7.68	0.08
*	-0.33	7.71	2.15
	-0.30	7.79	3.80
	-0.28	7.89	4.06
	-0.25	7.98	2.91
*	-0.23	8.02	0.36
	-0.20	8.00	-2.35
	-0.18	7.91	-3.96
	-0.15	7.81	-4.47
*	-0.13	7.70	-3.88
	-0.10	7.61	-3.07
	-0.08	7.54	-2.88
	-0.05	7.47	-3.33
	-0.03	7.37	-4.42
	0.00	7.24	-6.13
*	0.03	7.06	-8.48
	0.05	6.82	-10.58
	0.08	6.54	-11.56
	0.10	6.25	-11.40
*	0.13	5.98	-10.10
	0.15	5.75	-8.58
	0.18	5.54	-7.71
	0.20	5.35	-7.50
*	0.23	5.16	-7.96
	0.25	4.96	-8.48
	0.28	4.74	-8.50
	0.30	4.54	-8.01
*	0.33	4.35	-7.01
	0.35	4.19	-5.92
	0.38	4.05	-5.16
	0.40	3.92	-4.74

	Time	Velocity	Acceleration
*	0.43	3.81	-4.64
	0.45	3.69	-4.57
	0.48	3.58	-4.21
	0.50	3.48	-3.57
*	0.53	3.41	-2.64
	0.55	3.35	-1.62
	0.58	3.32	-0.69
	0.60	3.32	0.14
*	0.63	3.33	0.88
	0.65	3.36	1.51
	0.68	3.40	2.01
	0.70	3.46	2.39
*	0.73	3.52	2.64
	0.75	3.59	2.70
	0.78	3.66	2.52
	0.80	3.71	2.10
*	0.83	3.76	1.44
	0.85	3.79	1.01
	0.88	3.82	1.29
	0.90	3.86	2.29
*	0.93	3.94	3.99
	0.95	4.05	5.04
	0.98	4.17	4.05
	1.00	4.24	1.02
*	1.03	4.20	-4.04
	1.05	4.04	-8.82
	1.08	3.79	-11.02
	1.10	3.51	-10.62
*	1.13	3.28	-7.65
	1.15	3.13	-4.23
	1.18	3.05	-2.54
	1.20	2.99	-2.57
*	1.23	2.91	-4.32
	1.25	2.77	-6.34
	1.28	2.60	-7.18
	1.30	2.42	-6.85
*	1.33	2.27	-5.34
	1.35	2.16	-3.52
	1.38	2.09	-2.22
	1.40	2.04	-1.45
*	1.43	2.01	-1.21
	1.45	1.98	-1.09
	1.48	1.96	-0.66
	1.50	1.95	0.08
*	1.53	1.96	1.12
	1.55	2.01	2.17
	1.58	2.07	2.91
	1.60	2.15	3.36
*	1.63	2.24	3.51

APPENDIX B

TRANSLATIONAL/ROTATIONAL KINETIC AND GRAVITATIONAL POTENTIAL ENERGY

Translational and Rotational Kinetic Energy for each Body Segment

Abbreviations:

HN	: Head and neck
T	: Trunk
RUA, LUA	: Right and left upper arm
RLA,LLA	: Right and left lower arm
RH,LH	: Right and left hand
RT,LT	: Right and left thigh
RLL,LLL	: Right and left leg
RF,LF	: Right and left foot
R	: Rotational kinetic energy
T	: Translational kinetic energy

KINETIC ENERGY [TH J4 F6 Raw Data] 84Kg

ENERGY IN JOULE

	HN	T	RUA	RLA	RH	LUA	LLA	LH	RT	RLL	RF	LT	LLL	LF			
1	0.0	0.6	0.8	3.6	0.1	0.1	2.1	0.0	1.6	3.6	0.7	0.6	4.0	0.1	R=	17.9	
	211.2	1087.5	88.4	61.1	24.1	72.2	50.9	23.5	258.1	159.0	102.1	309.4	145.5	57.0	T=	2650.0	SUM= 2667.9
2	0.0	0.4	0.0	0.6	0.0	0.0	0.3	0.1	2.4	0.0	0.0	2.5	1.6	0.0	R=	8.1	
	231.5	1186.1	91.3	63.9	27.3	77.8	49.6	19.5	197.0	73.9	22.4	357.7	210.3	74.3	T=	2682.5	SUM= 2690.6
3	0.0	0.8	3.4	0.0	0.0	0.2	0.0	0.0	1.4	2.5	0.2	4.3	0.2	0.2	R=	13.2	
	203.1	1039.5	93.2	72.8	24.3	63.1	43.5	17.8	151.1	20.3	0.1	437.0	267.5	97.2	T=	2530.5	SUM= 2543.7
4	0.4	0.0	8.6	0.0	0.0	0.0	0.0	0.0	6.8	2.4	0.1	5.7	9.1	0.9	R=	34.1	
	234.8	1279.3	123.7	81.7	27.3	81.4	52.9	19.7	208.8	20.3	1.5	384.9	255.1	131.6	T=	2903.2	SUM= 2937.3
5	0.0	1.4	0.4	0.0	0.0	0.2	0.1	0.0	2.2	0.4	0.7	0.5	3.7	0.2	R=	9.9	
	211.0	1218.3	99.9	61.4	19.5	79.0	48.5	15.1	219.8	59.1	13.5	275.5	185.6	97.3	T=	2603.5	SUM= 2613.3
6	0.2	0.7	0.1	0.0	0.0	0.0	0.0	0.0	0.9	5.0	0.3	1.5	2.4	0.1	R=	11.4	
	335.2	1376.2	104.1	53.9	18.0	80.0	39.6	13.8	388.3	186.2	69.5	275.9	139.3	80.2	T=	3160.1	SUM= 3171.5
7	0.4	0.8	0.2	0.0	0.0	0.0	0.1	0.0	4.9	2.0	0.3	1.7	2.0	0.0	R=	12.4	
	199.0	1037.4	73.3	34.3	11.8	65.5	33.3	10.9	384.2	268.4	112.6	166.6	27.9	1.6	T=	2426.8	SUM= 2439.2
8	0.0	0.1	0.1	0.0	0.0	0.0	0.0	0.0	10.9	2.3	0.3	5.6	0.6	0.0	R=	20.0	
	205.7	956.2	67.8	33.3	11.4	71.7	42.1	14.1	398.1	250.1	63.7	89.6	6.2	0.1	T=	2210.0	SUM= 2230.0
9	0.3	0.4	0.1	0.1	0.0	0.0	0.1	0.0	1.1	5.3	1.3	5.2	0.1	1.1	R=	15.0	
	175.6	1109.9	60.9	25.1	6.6	72.5	34.6	9.9	340.0	157.5	68.5	162.6	42.5	7.6	T=	2273.9	SUM= 2288.8
10	0.0	6.7	0.3	0.1	0.0	0.1	0.1	0.0	0.0	3.7	0.4	0.3	0.8	0.1	R=	12.6	
	147.0	784.6	34.8	10.2	1.7	44.1	18.8	4.6	244.8	136.3	77.8	207.1	64.8	18.3	T=	1795.0	SUM= 1807.6
11	0.4	10.1	0.1	0.0	0.0	0.2	0.0	0.0	0.6	1.8	0.2	0.0	0.0	0.0	R=	13.3	
	86.5	781.3	27.0	11.0	3.2	36.2	18.0	5.6	208.8	110.5	65.8	224.1	104.9	31.9	T=	1714.9	SUM= 1728.3
12	0.1	5.2	0.0	0.0	0.0	0.0	0.0	0.0	0.0	0.6	0.2	0.5	0.0	0.0	R=	6.7	
	65.2	571.2	24.7	14.3	5.3	32.4	20.4	5.7	176.3	99.9	43.7	206.0	101.5	40.3	T=	1406.7	SUM= 1413.4
13	0.0	0.6	0.0	0.0	0.0	0.0	0.0	0.0	2.5	0.0	0.0	2.8	0.9	0.1	R=	7.1	
	82.8	438.7	25.9	18.5	7.2	29.1	18.9	7.9	155.5	97.7	34.2	203.2	148.2	67.0	T=	1334.6	SUM= 1341.7
14	0.1	0.1	0.1	0.0	0.0	0.0	0.0	0.0	3.9	0.1	0.0	3.6	3.7	0.5	R=	12.1	
	60.8	367.8	28.8	22.7	8.6	25.7	18.5	7.3	113.2	84.9	29.4	158.3	173.8	110.2	T=	1209.8	SUM= 1221.9
15	0.0	0.0	0.0	0.0	0.0	0.0	0.0	0.0	4.8	0.6	0.1	7.0	3.2	0.4	R=	16.3	
	62.4	239.1	26.3	19.1	7.0	18.7	12.6	5.6	56.4	59.6	31.2	137.4	181.1	102.9	T=	959.6	SUM= 975.9
16	0.1	0.6	0.0	0.0	0.0	0.0	0.0	0.0	3.5	0.9	0.2	7.7	2.7	0.3	R=	15.8	
	53.7	269.1	26.2	16.3	5.8	23.6	14.5	5.6	44.0	41.5	26.6	137.3	172.1	91.7	T=	927.9	SUM= 943.7
17	0.0	4.6	0.1	0.0	0.0	0.0	0.0	0.0	3.4	1.6	0.1	6.7	1.8	0.4	R=	18.8	
	50.6	218.5	20.5	16.3	6.0	17.7	12.4	4.6	42.4	32.4	22.2	93.7	112.8	60.0	T=	710.3	SUM= 729.1
18	0.0	5.7	0.0	0.0	0.0	0.0	0.0	0.0	4.8	1.3	0.1	8.3	0.7	0.0	R=	20.7	
	48.4	360.6	19.3	13.6	5.3	14.6	9.7	3.5	52.4	17.7	12.7	114.2	73.8	32.9	T=	778.8	SUM= 799.6
19	0.0	8.5	0.0	0.0	0.0	0.3	0.0	0.0	4.1	1.4	0.0	5.9	0.4	0.0	R=	20.7	
	36.3	245.9	18.0	11.8	4.6	15.5	7.2	2.7	50.3	10.1	8.1	67.5	37.4	16.7	T=	532.2	SUM= 552.9
20																	

KINETIC ENERGY [TH J4 F9 Raw Data] 84Kg

ENERGY IN JOULE

	HN	T	RUA	RLA	RH	LUA	LLA	LH	RT	RLL	RF	LT	LLL	LF				
1	0.2	13.4	0.0	0.0	0.0	0.0	0.0	0.0	2.0	1.2	0.2	5.3	0.5	0.0	R=	22.8		
	33.6	332.5	18.5	12.4	4.7	18.4	8.4	2.1	57.9	13.2	8.3	62.2	20.6	10.8	T=	603.7	SUM=	626.6
2	0.6	3.9	0.0	0.0	0.0	0.0	0.0	0.0	0.8	0.8	0.2	1.5	1.9	0.1	R=	9.8		
	39.7	260.9	20.6	11.9	4.3	11.7	5.1	1.2	65.9	17.5	6.8	54.8	11.2	7.2	T=	518.8	SUM=	528.7
3	0.0	9.9	0.0	0.0	0.2	0.3	0.3	0.0	0.1	0.9	0.1	2.2	0.2	0.0	R=	14.3		
	35.3	263.6	18.2	13.1	4.8	9.4	5.1	2.6	67.6	25.8	8.9	40.6	12.4	7.9	T=	515.0	SUM=	529.3
4	0.1	6.6	0.0	0.0	0.2	0.1	0.0	0.0	0.8	1.6	0.0	0.6	0.8	0.0	R=	10.9		
	46.3	216.6	15.5	9.8	4.1	12.1	7.8	2.3	71.2	35.6	11.6	62.5	31.9	9.2	T=	536.4	SUM=	547.3
5	0.0	6.3	0.0	0.0	0.0	0.0	0.1	0.0	0.4	0.5	0.0	0.3	0.4	0.0	R=	8.2		
	33.1	199.1	14.5	7.4	2.4	10.8	4.5	0.5	91.9	36.6	9.4	82.2	35.7	9.4	T=	537.6	SUM=	545.8
6	0.0	14.0	0.0	0.0	0.0	2.4	1.9	0.0	0.5	0.2	0.1	0.7	0.0	0.0	R=	19.9		
	33.8	229.8	16.8	11.6	3.6	8.1	1.8	1.2	93.2	57.8	25.5	91.0	48.4	16.8	T=	639.4	SUM=	659.4
7	0.0	10.6	0.0	0.0	0.0	0.1	3.1	0.1	2.5	0.3	0.1	0.8	0.2	0.2	R=	17.9		
	30.7	243.4	12.9	7.3	2.6	9.9	2.2	1.1	90.9	65.2	28.3	105.2	63.0	22.5	T=	685.1	SUM=	703.0
8	0.3	7.2	0.1	3.4	0.0	0.0	0.8	0.1	2.9	0.6	0.1	0.7	0.3	0.0	R=	16.6		
	32.4	270.8	14.3	8.8	3.2	12.8	4.4	0.8	104.1	67.0	28.9	95.2	64.5	28.7	T=	735.9	SUM=	752.5
9	0.2	0.4	0.0	3.6	0.0	0.5	0.0	0.0	2.2	0.5	0.0	0.8	0.7	0.0	R=	9.1		
	37.5	211.5	17.8	8.2	2.2	12.9	5.8	2.9	83.9	51.9	22.5	78.2	53.2	26.7	T=	615.4	SUM=	624.5
10	0.1	0.1	0.0	0.0	0.2	1.6	0.2	0.0	1.0	0.5	0.2	0.7	1.1	0.2	R=	6.0		
	67.8	380.5	18.0	7.2	1.8	20.3	3.6	0.6	98.4	53.6	21.1	95.6	42.7	18.4	T=	829.6	SUM=	835.7
11	0.0	0.0	0.3	1.3	0.0	0.1	0.1	0.0	1.7	0.2	0.1	1.0	0.3	0.1	R=	5.5		
	61.8	390.2	14.5	2.3	0.0	14.3	3.4	0.4	80.9	44.1	12.4	72.1	44.9	12.6	T=	754.0	SUM=	759.4
12	0.1	0.1	9.4	0.0	0.0	0.0	0.3	0.0	0.7	0.2	0.0	2.3	0.0	0.0	R=	13.1		
	59.4	302.3	9.6	1.8	0.2	21.0	5.6	0.4	63.0	16.2	3.9	42.8	29.6	16.6	T=	572.3	SUM=	585.4
13	0.0	1.4	2.8	0.8	0.0	0.1	0.0	0.0	0.7	0.1	0.3	2.0	0.3	0.3	R=	8.8		
	44.3	223.8	9.7	2.2	0.0	23.9	16.5	5.7	65.8	29.3	12.5	40.5	17.5	5.7	T=	497.2	SUM=	506.1
14	0.0	0.6	0.0	0.1	0.0	0.2	0.0	0.0	0.6	0.3	0.1	2.2	0.4	0.2	R=	4.9		
	42.6	192.6	6.1	1.1	0.0	20.2	18.4	7.8	39.4	10.0	5.6	33.1	15.0	4.6	T=	396.5	SUM=	401.4
15	0.1	2.3	1.5	1.2	0.0	0.0	0.1	0.0	0.2	0.3	0.0	2.6	0.1	0.2	R=	8.6		
	46.0	194.8	9.4	1.5	0.4	17.2	13.2	6.6	47.5	19.7	3.6	19.3	7.9	3.7	T=	390.9	SUM=	399.5
16	0.0	5.2	0.0	0.0	0.0	0.0	0.1	0.0	0.0	0.1	0.0	4.3	0.1	0.1	R=	10.0		
	35.7	126.0	4.3	0.7	0.1	13.8	9.5	4.0	38.9	10.4	2.0	13.5	8.7	5.5	T=	273.1	SUM=	283.1
17	0.0	1.8	0.1	0.0	0.0	0.0	0.1	0.0	0.5	1.0	0.0	2.6	1.5	0.2	R=	7.9		
	36.9	176.7	9.1	4.1	0.8	10.2	6.2	2.5	26.6	4.8	1.8	7.0	4.6	9.1	T=	300.4	SUM=	308.3
18	0.2	5.1	0.0	0.0	0.0	0.0	0.0	0.0	0.2	4.1	0.1	2.4	2.2	0.1	R=	14.3		
	24.8	115.3	6.6	5.6	2.4	9.1	5.1	2.0	37.9	9.0	3.4	19.7	16.7	13.9	T=	271.3	SUM=	285.6
19	0.1	12.4	0.0	0.0	0.0	0.0	0.2	0.0	0.7	1.7	0.3	1.8	1.6	0.1	R=	19.0		
	20.5	161.3	16.9	8.1	2.7	6.8	3.9	1.3	40.1	6.5	2.0	14.2	11.1	10.9	T=	306.2	SUM=	325.2
20																		

KINETIC ENERGY [TH J4 F12 Raw Data] 84Kg

ENERGY IN JOULE

	HN	T	RUA	RLA	RH	LUA	LLA	LH	RT	RLL	RF	LT	LIL	LF				
1	0.0	11.9	0.0	0.1	0.0	0.0	0.2	0.0	0.1	0.2	0.2	0.3	0.9	0.0	R=	14.1		
	25.9	86.6	12.7	7.4	2.9	9.6	3.7	0.9	26.6	6.7	0.2	18.4	4.2	3.6	T=	209.5	SUM=	223.6
2	0.3	19.2	0.2	0.2	0.1	0.0	0.1	0.0	0.9	0.0	0.0	0.1	0.2	0.0	R=	21.3		
	26.3	103.1	7.7	6.7	2.3	5.3	3.2	1.0	39.1	22.0	6.1	16.1	5.3	1.0	T=	245.2	SUM=	266.5
3	0.2	5.3	0.0	0.1	0.0	0.0	0.0	-1.0	2.6	2.5	0.2	0.0	0.1	0.0	R=	10.0		
	22.4	80.2	13.6	8.8	3.0	7.6	3.2	1.2	30.0	38.1	28.7	20.4	10.4	5.7	T=	273.3	SUM=	283.3
4	0.0	15.3	0.9	0.0	0.0	0.0	0.0	0.0	3.6	4.6	0.9	0.1	0.5	0.1	R=	25.9		
	24.5	54.8	18.1	15.9	3.8	7.0	3.9	1.1	48.1	70.1	67.8	28.6	21.0	9.7	T=	374.4	SUM=	400.3
5	0.2	14.5	0.0	0.0	0.0	0.1	0.0	0.0	0.0	7.8	0.8	0.0	1.6	0.0	R=	25.2		
	23.5	38.8	9.3	5.7	1.8	5.7	2.8	0.9	5.3	31.3	54.1	5.6	7.4	11.3	T=	203.5	SUM=	228.7
6																		

RAW DATA GRAVITATIONAL POTENTIAL ENERGY (mgh)

Time	mgh	Time	mgh
-.375	866.59	.725	2223.07
-.325	866.13	.775	2339.62
-.275	850.91	.825	2466.64
-.225	856.42	.875	2603.65
-.175	880.73	.925	2745.13
-.125	900.09	.975	2885.02
-.075	901.55	1.025	3034.00
-.025	937.63	1.075	3190.22
.025	1037.07	1.125	3328.42
.075	1136.14	1.175	3445.86
.125	1219.67	1.225	3549.06
.175	1296.11	1.275	3636.32
.225	1373.23	1.325	3704.95
.275	1450.92	1.375	3767.27
.325	1518.20	1.425	3806.98
.375	1586.22	1.475	3816.47
.425	1664.06	1.525	3808.56
.475	1743.16	1.575	3791.24
.525	1818.33	1.625	3755.72
.575	1909.23	1.675	3701.42
.625	2007.75	1.725	3660.15
.675	2112.54		

Kinetic Energy as Computed by Cubic Spline Approximation

KINETIC ENERGY [Translation][TH J4 F6,9,12]

OF INPUT POINTS: 28
USER DEFINED STEPSIZE: 0.0250
EPSILON: 1.00E-06

INTEGRAL -0.375 to 1.675 = 2.2467E 03

* :x = Input X
< :x < Input X < x+1

	Time	Energy
*	-0.38	2650.00
	-0.35	2650.10
*	-0.33	2682.50
	-0.30	2765.78
	-0.28	2863.66
	-0.25	2926.14
*	-0.23	2903.20
	-0.20	2770.15
*	-0.18	2603.50
	-0.15	2486.15
	-0.13	2425.36
	-0.10	2409.46
*	-0.08	2426.80
	-0.05	2460.67
	-0.03	2474.25
	0.00	2425.65
*	0.03	2273.00
	0.05	2012.80
*	0.08	1795.00
	0.10	1742.31
*	0.13	1714.90
	0.15	1568.89
*	0.18	1406.70
	0.20	1347.92
*	0.23	1334.60
	0.25	1286.24
*	0.28	1209.80
	0.30	1129.83
	0.33	1053.95
	0.35	985.51
*	0.38	927.90
	0.40	883.00
	0.43	846.83
	0.45	813.92

Time	Energy
0.48	778.80
0.50	737.52
0.53	692.18
0.55	646.37
0.58	603.70
0.60	567.44
0.63	539.51
0.65	521.50
0.68	515.00
0.70	520.78
0.73	536.40
0.75	558.72
0.78	585.04
0.80	612.80
0.83	639.40
0.85	663.06
0.88	685.10
0.90	708.03
0.93	735.90
0.95	770.72
0.98	804.73
1.00	827.75
1.03	829.60
1.05	803.21
1.08	754.00
1.10	690.48
1.13	620.98
1.15	553.79
1.18	497.20
1.20	457.13
1.23	430.01
1.25	409.91
1.28	390.90
1.30	368.50
1.33	344.07
1.35	320.43
1.38	300.40
1.40	285.41
1.43	271.30
1.45	254.05
1.48	235.66
1.50	219.64
1.53	209.50
1.55	208.37
1.58	217.84
1.60	239.08
1.63	273.30
1.65	320.31
1.68	374.40

ROT. KIN. ENERCY. [TH J4 F6,9,12]

OF INPUT POINTS: 41
USER DEFINED STEPSIZE: 0.0125
EPSILON: 1.00E-06

INTEGRAL -0.375 to 1.675 = 2.7466E 01

* :x = Input X
< :x < Input X < x+1

	Time	Energy
*	-0.38	17.90
	-0.36	14.99
	-0.35	12.27
	-0.34	9.91
*	-0.33	8.10
	-0.31	7.07
	-0.30	7.25
	-0.29	9.14
*	-0.28	13.20
	-0.26	19.51
	-0.25	26.44
	-0.24	31.95
*	-0.23	34.00
	-0.21	31.22
	-0.20	24.96
	-0.19	17.21
*	-0.18	10.00
	-0.16	4.94
	-0.15	2.08
	-0.14	1.09
	-0.13	1.61
	-0.11	3.30
	-0.10	5.83
	-0.09	8.84
*	-0.08	12.00
	-0.06	14.97
	-0.05	17.48
	-0.04	19.25
*	-0.03	20.00
	-0.01	19.59
	0.00	18.33
	0.01	16.65
*	0.03	15.00
	0.04	13.73

	Time	Energy
	0.05	12.91
	0.06	12.54
*	0.08	12.60
	0.09	13.03
	0.10	13.53
	0.11	13.74
*	0.13	13.30
	0.14	12.00
	0.15	10.15
	0.16	8.23
*	0.18	6.70
	0.19	5.92
	0.20	5.83
	0.21	6.28
*	0.23	7.10
	0.24	8.15
	0.25	9.37
	0.26	10.70
*	0.28	12.10
	0.29	13.49
	0.30	14.76
	0.31	15.74
*	0.33	16.30
	0.34	16.36
	0.35	16.11
	0.36	15.84
*	0.38	15.80
	0.39	16.20
	0.40	16.93
	0.41	17.86
*	0.43	18.80
	0.44	19.62
	0.45	20.25
	0.46	20.62
*	0.48	20.70
	0.49	20.48
	0.50	20.20
	0.51	20.18
*	0.53	20.70
	0.54	21.89
	0.55	23.16
	0.56	23.72
*	0.58	22.80
	0.59	19.94
	0.60	16.02
	0.61	12.24
*	0.63	9.80
	0.64	9.54
	0.65	10.85
	0.66	12.76
*	0.68	14.30
	0.69	14.71
	0.70	14.08

	Time	Energy
	0.71	12.74
*	0.73	11.00
	0.74	9.21
	0.75	7.82
	0.76	7.32
*	0.78	8.20
	0.79	10.71
	0.80	14.13
	0.81	17.51
*	0.83	19.90
	0.84	20.61
	0.85	20.06
	0.86	18.93
*	0.88	17.90
	0.89	17.48
	0.90	17.41
	0.91	17.27
*	0.93	16.60
	0.94	15.12
	0.95	13.10
	0.96	10.95
*	0.98	9.10
	0.99	7.85
	1.00	7.07
	1.01	6.53
*	1.03	6.00
	1.04	5.34
	1.05	4.80
	1.06	4.73
*	1.08	5.50
	1.09	7.28
	1.10	9.58
	1.11	11.74
*	1.13	13.10
	1.14	13.17
	1.15	12.19
	1.16	10.60
*	1.18	8.80
	1.19	7.18
	1.20	5.90
	1.21	5.10
*	1.23	4.90
	1.24	5.36
	1.25	6.30
	1.26	7.46
*	1.28	8.60
	1.29	9.50
	1.30	10.07
	1.31	10.25
*	1.33	10.00
	1.34	9.33
	1.35	8.51
	1.36	7.92

	Time	Energy
*	1.38	7.90
	1.39	8.71
	1.40	10.20
	1.41	12.15
*	1.43	14.30
	1.44	16.41
	1.45	18.13
	1.46	19.11
*	1.48	19.00
	1.49	17.65
	1.50	15.77
	1.51	14.28
*	1.53	14.10
	1.54	15.77
	1.55	18.36
	1.56	20.54
*	1.58	21.00
	1.59	18.91
	1.60	15.34
	1.61	11.85
*	1.63	10.00
	1.64	10.95
	1.65	14.30
	1.66	19.25
*	1.68	25.00

APPENDIX C

MOMENTUM

Angular Momentum About the Top Hand and the Center of Mass (Raw Data)

Abbreviations:

LOC	: Local angular momentum
Hh	: Angular momentum about the top hand
Wh	: Angular velocity about the top hand
Ih	: Moment of inertia about the top hand
Hcm	: Angular momentum about the center of mass
Wcm	: Angular velocity about the center of mass
Icm	: Moment of inertia about the center of mass

ANGULAR MOMENTUM [TH J4 F6 Raw Data] 83.5 Kg

		LOC	Hh	Wh	Ih	Hcm	Wcm	Icm
1	-0.40	1.73	-98.42	-4.22	23.34	6.87	0.68	10.16
2	-0.35	-1.36	-138.62	-5.52	25.09	-3.90	-0.39	9.98
3	-0.30	2.06	-130.42	-3.95	33.04	-3.23	-0.33	9.87
4	-0.25	0.34	-118.70	-2.64	44.92	-8.74	-0.81	10.80
5	-0.20	2.23	-43.77	-0.75	58.25	-5.87	-0.49	12.07
6	-0.15	-1.70	24.84	0.35	71.54	-3.04	-0.24	12.78
7	-0.10	-1.78	45.53	0.53	85.50	-3.16	-0.26	12.12
8	-0.05	0.31	22.61	0.24	92.65	-10.58	-0.90	11.70
9	0.00	1.38	187.17	2.04	91.84	-3.08	-0.25	12.41
10	0.05	4.48	353.22	3.91	90.43	20.21	1.58	12.77
11	0.10	5.49	266.70	2.92	91.32	29.95	2.33	12.83
12	0.15	4.47	134.68	1.41	95.24	37.80	2.89	13.07
13	0.20	2.98	62.27	0.63	98.81	43.87	3.31	13.24
14	0.25	2.91	-1.84	-0.02	99.86	45.64	3.44	13.28
15	0.30	3.17	-11.01	-0.11	98.03	47.57	3.72	12.80
16	0.35	1.82	24.13	0.26	93.66	46.08	4.05	11.38
17	0.40	6.32	-6.91	-0.08	83.29	37.56	3.88	9.67
18	0.45	6.75	15.61	0.22	71.65	41.40	5.32	7.78
19	0.50	7.29	-17.02	-0.27	62.19	28.69	4.70	6.11

ANGULAR MOMENTUM [TH J4 F9 Raw Data] 83.5 Kg

		LOC	Ih	Wh	Ih	Hcm	Wcm	Icm
20	0.55	8.29	-8.82	-0.17	52.37	24.72	5.32	4.65
21	0.60	5.10	-30.19	-0.66	46.00	14.70	3.76	3.91
22	0.65	6.47	-43.51	-1.09	40.01	15.83	4.54	3.49
23	0.70	3.90	-32.45	-0.93	34.75	9.67	2.75	3.52
24	0.75	4.02	-0.56	-0.02	28.01	10.37	2.58	4.02
25	0.80	4.78	6.12	0.25	24.61	2.51	0.51	4.96
26	0.85	3.49	4.97	0.20	24.30	-1.95	-0.30	6.44
27	0.90	3.11	5.84	0.25	22.95	-4.54	-0.55	8.23
28	0.95	-0.43	-6.30	-0.29	21.99	-16.36	-1.64	9.95
29	1.00	-1.26	16.53	0.82	20.08	-25.37	-2.30	11.01
30	1.05	-1.31	77.94	4.30	18.11	-24.21	-2.08	11.65
31	1.10	-0.00	52.68	2.36	22.29	-23.99	-2.00	12.02
32	1.15	-3.38	60.33	1.92	31.50	-24.97	-2.06	12.14
33	1.20	-2.72	37.03	0.87	42.47	-23.49	-1.95	12.05
34	1.25	-3.83	39.29	0.72	54.45	-33.19	-2.87	11.57
35	1.30	-4.91	-43.29	-0.64	67.56	-33.18	-2.98	11.15
36	1.35	-3.52	-68.76	-0.89	77.67	-31.79	-3.01	10.57
37	1.40	-4.52	-137.50	-1.79	76.77	-33.63	-3.38	9.95
38	1.45	-6.73	-145.10	-2.12	68.50	-38.38	-4.01	9.57

ANGULAR MOMENTUM [TH J4 F12 Raw Data] 83.5 Kg

		LOC	Ilh	Wh	Ih	Ilcm	Wcm	Icm
39	1.50	-6.24	-158.11	-2.72	58.08	-32.02	-3.51	9.12
40	1.55	-7.87	-138.81	-2.77	50.13	-38.11	-4.40	8.67
41	1.60	-5.01	-104.77	-2.47	42.37	-27.88	-3.29	8.46
42	1.65	-7.41	-66.45	-1.94	34.30	-32.51	-3.72	8.75
43	1.70	-6.92	-63.21	-2.25	28.15	-34.53	-3.70	9.34

Cubic Spline Approximations

(Linear and Angular Momentum)

---

mVx

OF INPUT POINTS: 28
USER DEFINED STEPSIZE: 0.0250
EPSILON: 1.00E-06

INTEGRAL -0.025 to 1.325 = 3.5171E 02

* :x = Input X
< :x < Input X < x+1

	Time	Horizontal Momentum
*	-0.03	557.15
	0.00	558.93
*	0.03	551.42
	0.05	530.02
*	0.08	508.90
	0.10	500.97
*	0.13	495.43
	0.15	479.49
*	0.18	456.21
	0.20	432.81
*	0.23	417.20
	0.25	412.18
*	0.28	399.40
	0.30	365.09
*	0.33	334.86
	0.35	331.04
*	0.38	323.58
	0.40	285.84
*	0.43	257.25
	0.45	273.42
*	0.48	288.58
	0.50	257.66
*	0.53	219.80
	0.55	218.18
*	0.58	227.95
	0.60	217.54
*	0.63	196.56
	0.65	181.38
*	0.68	174.20
	0.70	172.71
*	0.73	170.66
	0.75	163.33
*	0.78	156.16
	0.80	154.55

Time	Horizontal Momentum
0.83	153.69
0.85	149.45
0.88	150.80
0.90	163.70
0.93	169.10
0.95	151.25
0.98	132.51
1.00	135.80
1.03	148.14
1.05	151.91
1.08	146.91
1.10	138.46
1.13	136.48
1.15	146.64
1.18	152.89
1.20	142.32
1.23	136.44
1.25	154.63
1.28	173.46
1.30	167.26
1.33	144.31

---

mVy

OF INPUT POINTS: 20
USER DEFINED STEPSIZE: 0.0250
EPSILON: 1.00E-06

INTEGRAL 0.575 to 1.525 = 1.9440E 02

* :x = Input X
< :x < Input X < x+1

	Time	Vertical Momentum
*	0.58	194.28
	0.60	200.90
*	0.63	207.42
	0.65	213.76
*	0.68	219.87
	0.70	225.67
*	0.73	230.81
	0.75	235.76
*	0.78	244.43
	0.80	259.28
*	0.83	273.47
	0.85	280.57
*	0.88	285.20
	0.90	291.63
*	0.93	291.68
	0.95	280.48
*	0.98	278.73
	1.00	303.11
*	1.03	328.74
	1.05	328.53
*	1.08	308.26
	1.10	280.90
*	1.13	255.25
	1.15	237.00
*	1.18	223.61
	1.20	210.99
*	1.23	197.20
	1.25	180.59
*	1.28	158.62
	1.30	132.74
*	1.33	121.22
	1.35	134.25
*	1.38	132.89
	1.40	84.27

	Time	Vertical Momentum
*	1.43	29.00
	1.45	10.47
*	1.48	9.70
	1.50	-0.70
*	1.53	-19.50

ANGULAR MOMENTUM (CM) [TH J4 F6,9,12]

OF INPUT POINTS: 43
USER DEFINED STEPSIZE: 0.0100
EPSILON: 1.00E-06

INTEGRAL -0.375 to 1.725 = -2.2823E 00

* :x = Input X
< :x < Input X < x+1

	Time	Angular Momentum
*	-0.38	6.87
	-0.37	4.01
	-0.36	1.33
	-0.35	-1.00
	-0.34	-2.80
*	-0.33	-3.90
	-0.32	-4.20
	-0.31	-3.95
	-0.30	-3.49
	-0.29	-3.14
*	-0.28	-3.23
	-0.27	-4.00
	-0.26	-5.23
	-0.25	-6.64
	-0.24	-7.91
*	-0.23	-8.74
	-0.22	-8.90
	-0.21	-8.51
	-0.20	-7.75
	-0.19	-6.80
*	-0.18	-5.87
	-0.17	-5.09
	-0.16	-4.47
	-0.15	-3.95
	-0.14	-3.49
*	-0.13	-3.04
	-0.12	-2.59
	-0.11	-2.24
	-0.10	-2.13
	-0.09	-2.39
*	-0.08	-3.16
	-0.07	-4.51
	-0.06	-6.21
	-0.05	-7.99

	Time	Angular Momentum
	-0.04	-9.54
*	-0.03	-10.58
	-0.02	-10.86
	-0.01	-10.30
	0.01	-8.84
	0.02	-6.45
*	0.03	-3.08
	0.04	1.24
	0.05	6.16
	0.06	11.24
	0.07	16.07
*	0.08	20.21
	0.09	23.35
	0.10	25.63
	0.11	27.32
	0.12	28.67
*	0.13	29.95
	0.14	31.37
	0.15	32.91
	0.16	34.54
	0.17	36.19
*	0.18	37.80
	0.19	39.33
	0.20	40.73
	0.21	41.98
	0.22	43.04
*	0.23	43.87
	0.24	44.46
	0.25	44.87
	0.26	45.16
	0.27	45.39
*	0.28	45.64
	0.29	45.96
	0.30	46.33
	0.31	46.74
	0.32	47.16
*	0.33	47.57
	0.34	47.92
	0.35	48.08
	0.36	47.92
	0.37	47.30
*	0.38	46.08
	0.39	44.20
	0.40	42.00
	0.41	39.88
	0.42	38.26
*	0.43	37.56
	0.44	38.02
	0.45	39.23
	0.46	40.59
	0.47	41.51
*	0.48	41.40
	0.49	39.87

Time	Angular Momentum
0.50	37.27
0.51	34.18
0.52	31.13
0.53	28.69
0.54	27.25
0.55	26.55
0.56	26.18
0.57	25.71
0.58	24.72
0.59	22.93
0.60	20.62
0.61	18.20
0.62	16.09
0.63	14.70
0.64	14.31
0.65	14.64
0.66	15.28
0.67	15.82
0.68	15.83
0.69	15.04
0.70	13.67
0.71	12.08
0.72	10.63
0.73	9.67
0.74	9.44
0.75	9.73
0.76	10.21
0.77	10.53
0.78	10.37
0.79	9.49
0.80	8.02
0.81	6.22
0.82	4.30
0.83	2.51
0.84	1.04
0.85	-0.11
0.86	-0.97
0.87	-1.57
0.88	-1.95
0.89	-2.17
0.90	-2.38
0.91	-2.73
0.92	-3.40
0.93	-4.54
0.94	-6.27
0.95	-8.49
0.96	-11.01
0.97	-13.69
0.98	-16.36
0.99	-18.86
1.00	-21.10
1.01	-22.99
1.02	-24.44

Time	Angular Momentum
1.03	-25.37
1.04	-25.73
1.05	-25.64
1.06	-25.25
1.07	-24.72
1.08	-24.21
1.09	-23.85
1.10	-23.65
1.11	-23.62
1.12	-23.73
1.13	-23.99
1.14	-24.37
1.15	-24.77
1.16	-25.08
1.17	-25.18
1.18	-24.97
1.19	-24.40
1.20	-23.67
1.21	-23.09
1.22	-22.94
1.23	-23.49
1.24	-24.93
1.25	-26.99
1.26	-29.30
1.27	-31.49
1.28	-33.19
1.29	-34.13
1.30	-34.40
1.31	-34.20
1.32	-33.73
1.33	-33.18
1.34	-32.72
1.35	-32.36
1.36	-32.10
1.37	-31.91
1.38	-31.79
1.39	-31.74
1.40	-31.82
1.41	-32.11
1.42	-32.68
1.43	-33.63
1.44	-34.96
1.45	-36.41
1.46	-37.68
1.47	-38.44
1.48	-38.38
1.49	-37.31
1.50	-35.62
1.51	-33.83
1.52	-32.46
1.53	-32.02
1.54	-32.85
1.55	-34.51

	Time	Angular Momentum
	1.56	-36.36
	1.57	-37.77
*	1.58	-38.11
	1.59	-36.95
	1.60	-34.72
	1.61	-32.04
	1.62	-29.55
*	1.63	-27.88
	1.64	-27.48
	1.65	-28.14
	1.66	-29.46
	1.67	-31.05
*	1.68	-32.51
	1.69	-33.54
	1.70	-34.15
	1.71	-34.45
	1.72	-34.54
*	1.73	-34.53

APPENDIX D

FORCE AND IMPULSE

HORIZONTAL FORCE

OF INPUT POINTS: 33
USER DEFINED STEPSIZE: 0.0100
EPSILON: 1.00E-06

INTEGRAL 0.020 to 0.980 = 4.3598E 02

* :x = Input X
< :x < Input X < x+1

	Time	Force	Impulse
*	0.02	520.40	0.00
	0.03	630.83	6.48
	0.04	721.64	13.12
*	0.05	773.20	20.06
	0.06	775.74	27.41
	0.07	758.85	35.12
*	0.08	762.00	43.09
	0.09	811.90	51.25
	0.10	884.37	59.69
*	0.11	942.50	68.56
	0.12	958.98	77.90
	0.13	944.86	87.48
*	0.14	920.80	96.97
	0.15	904.00	106.14
	0.16	897.80	115.11
*	0.17	902.10	124.07
	0.18	915.52	133.19
	0.19	931.57	142.44
*	0.20	942.50	151.77
	0.21	943.21	161.12
	0.22	939.19	170.52
*	0.23	938.60	180.00
	0.24	946.25	189.56
	0.25	953.68	199.09
*	0.26	949.10	208.45
	0.27	928.10	217.58
	0.28	915.87	226.75
*	0.29	945.00	236.30
	0.30	1033.41	246.52
	0.31	1140.42	257.39
*	0.32	1210.70	268.84
	0.33	1203.76	280.70
	0.34	1138.38	292.50
*	0.35	1048.20	303.66

	Time	Force	Impulse
	0.36	961.93	313.77
	0.37	888.70	322.97
*	0.38	832.70	331.53
	0.39	795.73	339.68
	0.40	769.91	347.52
*	0.41	744.90	355.06
	0.42	712.43	362.34
	0.43	672.31	369.27
*	0.44	626.40	375.78
	0.45	576.79	381.78
	0.46	526.58	387.29
*	0.47	479.10	392.34
	0.48	436.32	396.95
	0.49	394.67	401.11
*	0.50	349.20	404.79
	0.51	297.09	407.97
	0.52	243.97	410.67
*	0.53	197.60	412.93
	0.54	163.30	414.79
	0.55	136.73	416.29
*	0.56	111.10	417.47
	0.57	82.00	418.37
	0.58	54.44	419.04
*	0.59	35.80	419.55
	0.60	31.03	419.94
	0.61	35.41	420.27
*	0.62	41.80	420.59
	0.63	45.28	420.95
	0.64	49.87	421.41
*	0.65	61.80	422.05
	0.66	83.50	422.91
	0.67	102.18	[illegible]
*	0.68	101.20	424.75
	0.69	70.84	425.46
	0.70	28.88	425.95
*	0.71	0.00	426.25
	0.72	1.97	426.38
	0.73	25.00	426.49
*	0.74	52.40	426.75
	0.75	70.97	427.30
	0.76	81.47	428.08
*	0.77	88.10	428.99
	0.78	93.96	429.94
	0.79	97.55	430.89
*	0.80	96.20	431.84
	0.81	87.98	432.75
	0.62	73.78	433.57
*	0.83	55.20	434.22
	0.84	34.32	434.65
	0.85	15.20	434.89
*	0.86	2.40	435.00
	0.87	-1.07	435.03
	0.88	1.71	435.03

	Time	Force	Impulse
*	0.89	6.10	435.04
	0.90	8.52	435.09
	0.91	9.51	435.18
*	0.92	10.60	435.30
	0.93	12.81	435.44
	0.94	14.90	435.58
*	0.95	15.10	435.71
	0.96	12.11	435.82
	0.97	6.67	435.90
*	0.98	0.00	435.98

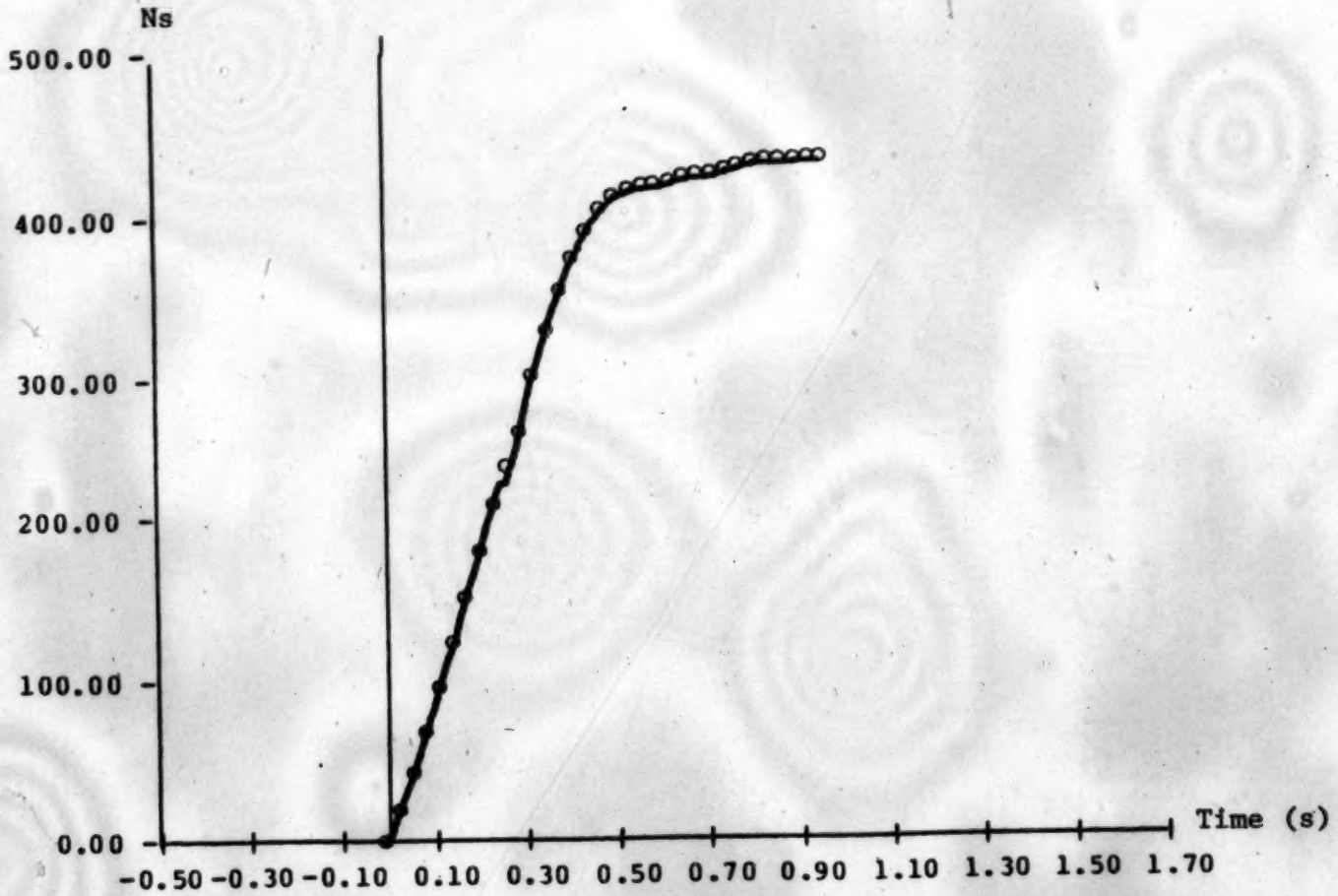

FIGURE D1

HORIZONTAL IMPULSE

VERTICAL FORCE

OF INPUT POINTS: 44
USER DEFINED STEPSIZE: 0.0100
EPSILON: 1.00E-06

INTEGRAL 0.020 to 1.310 = 6.9598E 02

* :x = Input X
< :x < Input X < x+1

	Time	Force	Impulse
*	0.02	395.50	0.00
	0.03	345.43	3.52
	0.04	296.51	6.81
*	0.05	249.90	9.64
	0.06	208.75	11.88
	0.07	184.18	13.79
*	0.08	189.30	15.71
	0.09	230.69	17.93
	0.10	288.73	20.53
*	0.11	337.30	23.53
	0.12	356.81	26.90
	0.13	353.99	30.49
*	0.14	342.10	34.07
	0.15	332.14	37.49
	0.16	325.85	40.77
*	0.17	322.70	43.97
	0.18	322.80	47.16
	0.19	328.95	50.41
*	0.20	344.60	53.80
	0.21	371.86	57.40
	0.22	407.39	61.30
*	0.23	446.50	65.54
	0.24	485.31	70.19
	0.25	523.24	75.24
*	0.26	560.50	80.66
	0.27	597.39	86.43
	0.28	634.40	92.58
*	0.29	672.10	99.14
	0.30	708.74	106.11
	0.31	733.39	113.34
*	0.32	732.80	120.63
	0.33	697.39	127.76
	0.34	632.19	134.45
*	0.35	545.90	140.38

Time	Force	Impulse
0.36	448.20	145.31
0.37	352.75	149.30
0.38	274.20	152.47
0.39	223.70	154.98
0.40	198.33	157.06
0.41	191.70	158.96
0.42	197.59	160.90
0.43	210.65	162.95
0.44	225.70	165.12
0.45	238.92	167.44
0.46	251.73	169.89
0.47	266.90	172.49
0.48	287.18	175.24
0.49	315.38	178.23
0.50	354.30	181.60
0.51	404.76	185.44
0.52	459.58	189.76
0.53	509.60	194.56
0.54	548.51	199.82
0.55	581.42	205.48
0.56	616.30	211.49
0.57	660.32	217.84
0.58	717.49	224.69
0.59	791.00	232.27
0.60	880.33	240.72
0.61	970.02	249.99
0.62	1040.90	259.96
0.63	1079.26	270.49
0.64	1093.32	281.38
0.65	1096.80	292.42
0.66	1101.18	303.44
0.67	1109.11	314.47
0.68	1121.00	325.60
0.69	1136.81	336.90
0.70	1154.62	348.36
0.71	1172.00	359.98
0.72	1187.68	371.74
0.73	1204.84	383.69
0.74	1227.80	395.89
0.75	1258.48	408.38
0.76	1289.29	421.13
0.77	1310.30	434.07
0.78	1314.53	447.15
0.79	1307.00	460.27
0.80	1295.70	473.34
0.81	1286.88	486.29
0.82	1279.68	499.11
0.83	1271.50	511.84
0.84	1260.37	524.48
0.85	1246.96	537.02
0.86	1232.60	549.43
0.87	1217.87	561.69
0.88	1200.33	573.78

	Time	Force	Impulse
*	0.89	1176.80	585.67
	0.90	1143.83	597.31
	0.91	1096.89	608.54
*	0.92	1031.20	619.16
	0.93	944.69	629.01
	0.94	846.20	637.97
*	0.95	747.30	645.98
	0.96	657.91	652.99
	0.97	581.36	659.16
*	0.98	519.30	664.67
	0.99	470.71	669.68
	1.00	423.78	674.16
*	1.01	364.00	678.00
	1.02	282.38	681.14
	1.03	192.03	683.54
*	1.04	111.60	685.17
	1.05	55.60	686.06
	1.06	22.07	686.41
*	1.07	4.90	686.48
	1.08	-1.66	686.48
	1.09	-1.95	686.46
*	1.10	0.00	686.46
	1.11	0.96	686.48
	1.12	0.76	686.50
*	1.13	0.00	686.47
	1.14	0.52	686.39
	1.15	9.16	686.41
*	1.16	34.00	686.71
	1.17	77.99	687.41
	1.18	123.56	688.44
*	1.19	148.00	689.66
	1.20	136.04	690.95
	1.21	102.07	692.16
*	1.22	67.90	693.15
	1.23	50.21	693.83
	1.24	45.14	694.28
*	1.25	43.70	694.64
	1.26	38.77	695.02
	1.27	30.73	695.38
*	1.28	21.80	695.67
	1.29	13.78	695.85
	1.30	6.66	695.94
*	1.31	0.00	695.98

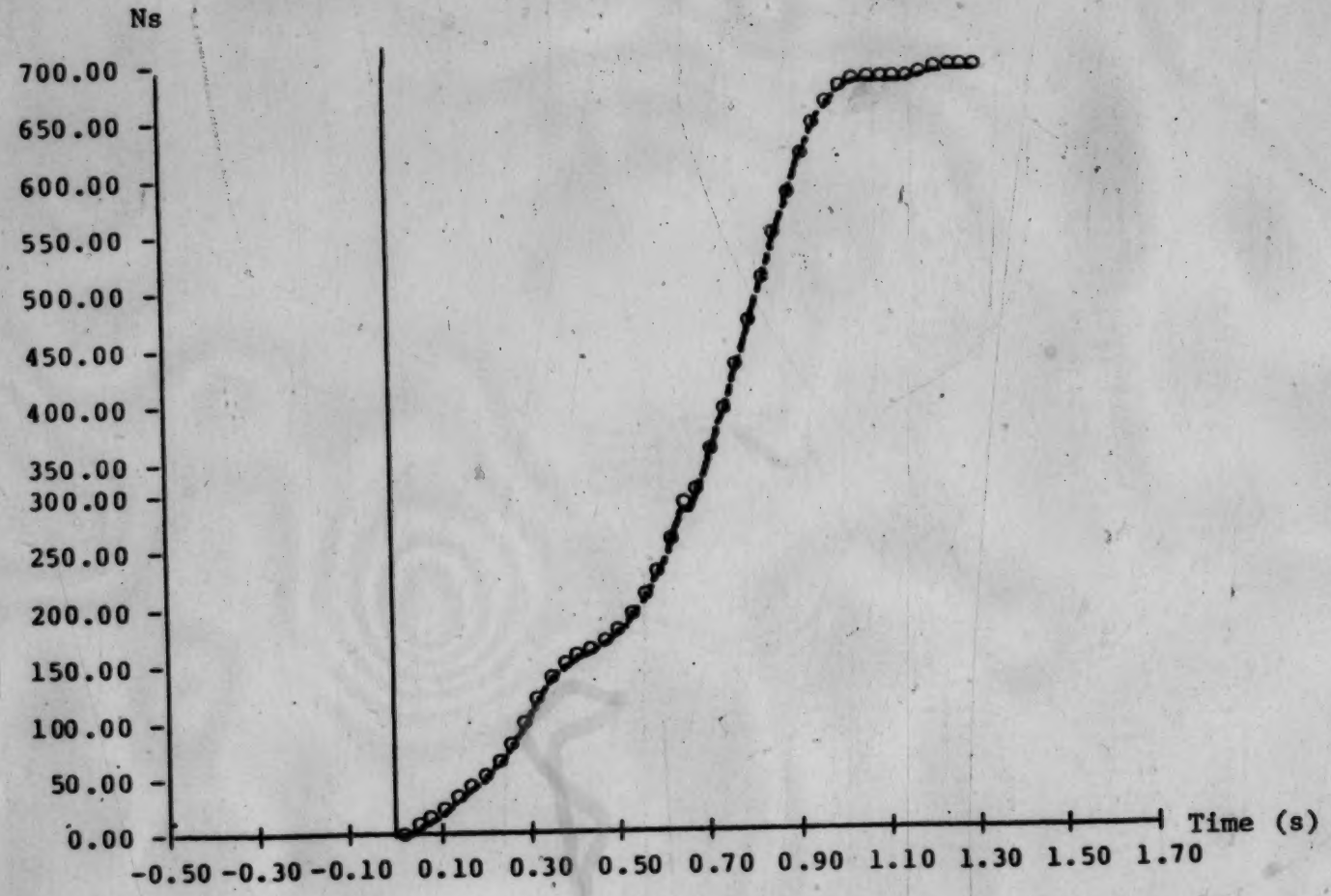

FIGURE D2

VERTICAL IMPULSE

VERTICAL FORCE [0=mg]

OF INPUT POINTS: 18
USER DEFINED STEPSIZE: 0.0100
EPSILON: 1.00E-06

INTEGRAL 0.600 to 0.940 = 1.1599E 02

* :x = Input X
< :x < Input X < x+1

	Time	Force	Impulse
*	0.60	41.00	0.00
	0.61	143.35	1.19
*	0.62	216.00	2.77
	0.63	240.08	4.98
*	0.64	240.00	7.49
	0.65	244.59	9.94
*	0.66	257.00	12.41
	0.67	274.42	15.05
*	0.68	296.00	17.91
	0.69	320.06	21.01
*	0.70	339.70	24.30
	0.71	350.00	27.73
*	0.72	359.10	31.29
	0.73	376.36	34.97
*	0.74	402.80	38.85
	0.75	436.04	43.04
*	0.76	468.30	47.57
	0.77	490.97	52.39
*	0.78	497.40	57.33
	0.79	485.66	62.23
*	0.80	470.70	67.03
	0.81	465.83	71.74
*	0.82	461.00	76.35
	0.83	445.21	80.87
*	0.84	427.00	85.25
	0.85	416.11	89.47
*	0.86	407.60	93.58
	0.87	394.16	97.59
*	0.88	373.70	101.44
	0.89	345.71	105.02
*	0.90	310.60	108.33
	0.91	267.11	111.29
*	0.92	206.20	113.61
	0.93	121.10	115.05
*	0.94	21.80	115.99

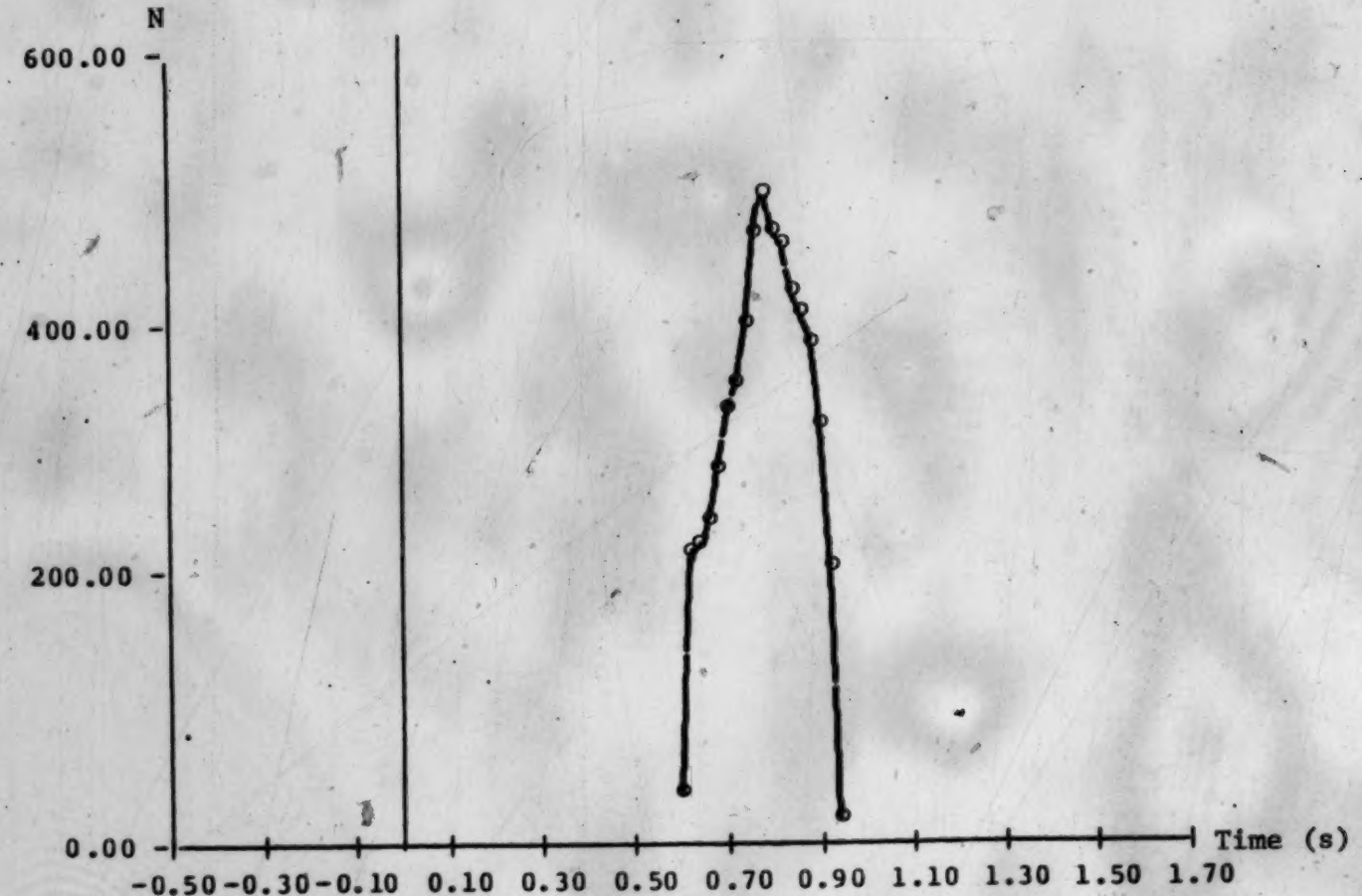

FIGURE D3

VERTICAL FORCE ADJUSTED TO 0 = BODY WEIGHT

RESULTANT FORCE

OF INPUT POINTS: 44
USER DEFINED STEPSIZE: 0.0100
EPSILON: 3.00E-06

INTEGRAL 0.020 to 1.310 = 9.6499E 02

* :x = Input X
< :x < Input X < x+1

	Time	Force	Impulse
*	0.02	653.70	0.00
	0.03	727.93	7.45
	0.04	786.21	14.95
*	0.05	812.60	22.53
	0.06	800.20	30.24
	0.07	778.29	38.14
*	0.08	785.20	46.28
	0.09	845.89	54.73
	0.10	931.80	63.60
*	0.11	1001.00	72.98
	0.12	1022.41	82.92
	0.13	1008.43	93.13
*	0.14	982.30	103.26
	0.15	963.37	113.05
	0.16	955.36	122.61
*	0.17	958.10	132.13
	0.18	970.47	141.79
	0.19	987.55	151.59
*	0.20	1003.50	161.51
	0.21	1014.43	171.54
	0.22	1024.39	181.72
*	0.23	1039.40	192.11
	0.24	1062.79	202.74
	0.25	1087.14	213.52
*	0.26	1102.30	224.33
	0.27	1104.39	235.14
	0.28	1114.41	246.18
*	0.29	1159.60	257.77
	0.30	1253.74	270.15
	0.31	1356.77	283.21
*	0.32	1415.20	296.79
	0.33	1390.11	310.63
	0.34	1300.98	324.17
*	0.35	1181.90	336.81

	Time	Force	Impulse
	0.36	1062.90	348.07
	0.37	957.88	358.11
*	0.38	876.70	367.26
	0.39	825.30	375.80
	0.40	794.00	383.89
*	0.41	769.20	391.65
	0.42	739.81	399.17
	0.43	704.84	406.40
*	0.44	665.80	413.28
	0.45	624.54	419.74
	0.46	584.24	425.78
*	0.47	548.40	431.44
	0.48	520.34	436.76
	0.49	502.57	441.86
*	0.50	497.40	446.86
	0.51	505.89	451.90
	0.52	524.02	457.04
*	[illegible]	546.50	462.37
	0.54	569.50	467.94
	0.55	594.94	473.76
*	0.56	626.20	479.86
	0.57	666.77	486.28
	0.58	720.62	493.18
*	0.59	791.80	500.79
	0.60	880.39	509.25
	0.61	970.39	518.52
*	0.62	1041.80	528.48
	0.63	1080.33	539.01
	0.64	1094.48	549.92
*	0.65	1098.50	560.98
	0.66	1104.14	572.03
	0.67	1113.35	583.10
*	0.68	1125.60	594.27
	0.69	1140.26	605.60
	0.70	1156.15	617.09
*	0.71	1172.00	628.72
	0.72	1187.34	640.48
	0.73	1205.07	652.43
*	0.74	1228.90	664.63
	0.75	1260.31	677.12
	0.76	1291.69	689.88
*	0.77	1313.20	702.88
	0.78	1317.91	716.05
	0.79	1310.68	729.23
*	0.80	1299.30	742.25
	0.81	1289.87	755.01
	0.82	1281.77	767.75
*	0.83	1272.70	780.82
	0.84	1260.93	794.29
	0.85	1247.15	807.23
*	0.86	1232.60	818.43
	0.87	1217.81	827.29
	0.88	1200.28	835.58

	Time	Force	Impulse
*	0.89	1176.80	845.67
	0.90	1143.86	859.11
	0.91	1096.96	874.13
*	0.92	1031.30	888.16
	0.93	944.84	899.22
	0.94	846.39	907.80
*	0.95	747.50	914.98
	0.96	658.06	921.66
	0.97	581.42	927.94
*	0.98	519.30	933.68
	0.99	470.69	938.80
	1.00	423.77	943.26
*	1.01	364.00	947.05
	1.02	282.38	950.15
	1.03	192.03	952.54
*	1.04	111.60	954.17
	1.05	55.60	955.06
	1.06	22.07	955.41
*	1.07	4.90	955.48
	1.08	-1.65	955.48
	1.09	-1.95	955.46
*	1.10	0.00	955.46
	1.11	0.96	955.48
	1.12	0.76	955.51
*	1.13	0.00	955.48
	1.14	0.52	955.41
	1.15	9.16	955.42
*	1.16	34.00	955.72
	1.17	77.99	956.42
	1.18	123.56	957.45
*	1.19	148.00	958.67
	1.20	136.04	959.96
	1.21	102.07	961.17
*	1.22	67.90	962.16
	1.23	50.21	962.84
	1.24	45.14	963.29
*	1.25	43.70	963.65
	1.26	38.77	964.02
	1.27	30.73	964.38
* *	1.28	21.80	964.67
	1.29	13.78	964.85
	1.30	6.66	964.94
*	1.31	0.00	964.99